ADDIS ABABA UNIVERSITY

SCHOOL OF GRADUATE STUDIES

FACULTY OF TECHNOLOGY
DEPARTMENT OF CIVIL ENGINEERING

RESPONSE OF MASONRY INFILLED RC FRAME UNDER HORIZONTAL SEISMIC FORCE

A thesis submitted to the school of Graduate Studies in Partial fulfillment of the Requirements for the Degree of Master of Science in Civil Engineering (Structures)

By
Mekonnen Degefa

Advisor: **Dr.-Ing. Adil Zekaria**

July 2005

ADDIS ABABA UNIVERSITY

SCHOOL OF GRADUATE STUDIES

FACULTY OF TECHNOLOGY

DEPARTMENT OF CIVIL ENGINEERING

RESPONSE OF MASONRY INFILLED RC FRAME UNDER HORIZONTAL SEISMIC FORCE

By

Mekonnen Degefa

July 2005

Approved by Board of Examiners

Dr.-Ing. Adil Zekaria	_____	_____
Advisor	Signature	Date
Dr. Shiferaw Taye	_____	_____
External Examiner	Signature	Date
Prof. Alemayehu Tefera	_____	_____
Internal Examiner	Signature	Date
Ato Fekadu Melese	_____	_____
Chairman	Signature	Date

ACKNOWLEDGEMENT

I thank the almighty God who always runs before my path to pave it for a comfortable stride. In Him I thrust and get unstinted support to reach my destination.

My great pleasure is in my advisor, Dr.-Ing. Adil Zekaria. I am grateful of him for his encouragement from the very beginning, valuable suggestions and inspiration in guidance and continuous supervisions. His door was always open to provide me with necessary publications relevant to this work.

I also extend my gratitude towards my friends who in one way or the other helped me in accomplishing this study. In particular, I am very much thankful of Ato Abebe Sine and Ato Tilahun Derib who were not hesitant in lending me their computers at the critical moment. A friend in need is a friend indeed.

Last but not least I would like to thank my wife, Mizan Tafesse, who always stand on my side and pray for successful completion of the work.

TABLE OF CONTENTS

ACKNOWLEDGEMENT i
ABSTRACT ii
LIST OF FIGURES v
LIST OF TABLES viii
LIST OF NOTATIONS ix
1 INTRODUCTION 1
1.1 Background 1
1.2 Objectives 2
1.3 Methodology 2
2 MODEL DEVELOPMENT OF MASONRY INFILL AND BEHAVIOR MODES 5
2.1 General 5
2.2 Historical Perspective 6
2.3 Components of Infilled Wall 7
2.4 Masonry Infilled Frames and Seismic Behavior of Structures 8
2.5 Behavior Modes 9
2.6 Modeling of Masonry Infilled Walls 12
3 LOAD EFFECTS ON MASONRY WALLS AND FRAMES 15
3.1 Strength of Masonry Units 15
3.2 Stress Strain Behavior of Masonry Prisms 15
3.3. Load Effects on Seismic Behavior - Frame Elements 18
3.4. Out-of-Plane and In-Plane Loadings – Masonry Walls 22
3.5. Energy Path in a Masonry Building 23
4. LATERAL RESISTANCE OF MASONRY INFILLED FRAMES 25
4.1. Stiffness of Frame 25
4.2 Stiffness of Masonry Infill 27
4.2.1 Equivalent Width of Infill Strut 27
4.2.2 Sliding Shear Failure 28
4.2.3 Compression Failure 29
4.2.4 Analytical Modeling of Masonry Infill Panel 29
4.2.5 Energy Dissipation Model for Hysteretic Damping 33
4.2.6 Assessment of Nonlinear Response of Masonry Infill Panel in MDOF System 36

5 ANALYSIS FOR THE EVALUATION OF INTERACTION BETWEEN MASONRY INFILLS AND FRAMES 39
5.1 The Synthetic Record of Earthquake as an Exciting Acceleration 39
5.2 Determination of Masses at the Story Levels 41
5.3 Determination of Stiffnesses 42
5.3 Degradation Behavior of Masonry Infill Panel 44
5.4 Comparison of Columns Shear in Bare Frame and Infilled Frame 48
5.5 EBCS-8 and Column Shear 57
5.5.1 Infilled Frames 57
5.5.2 Bare Frames 61
6 CONCLUSIONS AND RECOMMENDATIONS 67
6.1 Conclusions 67
6.2 Future Recommendations 68
REFERENCES 70
APPENDIX-A The Program ASSDMI 73
APPENDIX-B Degradation of Infill Panel 87
APPENDIX-C Tabulated Calculations 99

LIST OF FIGURES

Fig. 2.5.1 Knee-braced frame model for sliding shear failure of masonry infill 10
Fig. 2.5.2 Masonry failure with X-shaped cracks due to the R/C frame inter-storey drift 11
Fig. 3.2.1 Stress-strain behavior of masonry prism 15
Fig. 3.2.2 Failure mechanism for masonry prisms 16
Fig. 3.2.3 Mohr's failure criterion for a masonry unit 17
Fig. 3.2.4 Transverse equilibrium of masonry unit and mortar in prism 17
Fig. 3.3.1 Gravity Load Effects on Seismic Behavior of Components 19
Fig. 3.3.2 Effects of lateral forces on a building 20
Fig. 3.3.3 Generalized Load-Deformation Relations for Non-degrading Components. 20
Fig. 3.3.4 Idealized Flexural Mechanisms in Multi-story Frames 21
Fig. 3.4.1 Response of a masonry wall to biaxial excitation. 22
Fig. 3.4.2 Wall out-of-plane mode shapes and periods of a three-story masonry. 23
Fig. 3.5.1 Seismic response of unreinforced masonry building. 24
Fig. 4.1.1 Action effects of shear frames under lateral loading 26
Fig. 4.2.1.1 Masonry Infilled Frame. 27
Fig. 4.2.2.1 Infill masonry walls and equivalent diagonal compression action parameters. 28
Fig. 4.2.4.1 Compression Strut Analogy (a) Concentric Struts (b) Eccentric Struts. 30
Fig. 4.2.4.2 Damaged CB wall and column. 30
Fig. 4.2.4.3 Shear failures extending from the infills right across the column. 31
Fig. 4.2.4.4 Full-scale wall test. 31
Fig. 4.2.4.5 Strength Envelope for Masonry Infill Panel. 32
Fig. 4.2.5.1 Typical Hysteretic Loop. 33
Fig. 4.2.5.2 Qualitative view of effects of degradations on hysteretic Behavior 35
Fig. 4.2.6.1 Notation for linearly interpolated excitation. 36
Fig. 5.1.1 Normalized elastic design spectrum of EBCS-8 39
Fig. 5.1.2 Synthetic record of earthquake derived from elastic design spectrum curve of EBCS-8. 40
Fig. 5.1.3 Elastic design spectrum curve of EBCS-8 - verified using SAP2000 40
Fig. E5.2.1 3-D view of FRAME-3 with elements tributary to a floor mass 41
Fig. E5.2.2 Tributary columns and walls 41
Fig. E5.2.3 Tributary beams and floors. 42
Fig. 5.3.1 FRAME-1 Single bay frame. 45

Fig. 5.3.2 FRAME-2 Double bay frame. 45
Fig. 5.3.3 FRAME-3 Triple bay frame. 45
Fig. 5.3.4 FRAME-4 Quadruple bay frame. 45
Fig. 5.3.5 Infill shear vs. inter-story drift at different story levels – FRAME-2 with aspect ratio = 2.5 46
Fig. 5.3.6 Infill shear vs. inter-story drift of different frames at the first story level – Aspect ratio = 2.0 47
Fig. 5.4.1 Time history of column shears at the left end of FRAME-1 – aspect ratio = 1.0 .. 49
Fig. 5.4.2 Time history of column shears at the left end of FRAME-2 – aspect ratio = 1.0 .. 49
Fig. 5.4.3 Time history of column shears at the left end of FRAME-3 – aspect ratio = 1.0 .. 50
Fig. 5.4.4 Time history of column shears at the left end of FRAME-4 – aspect ratio = 1.0 . 50
Fig. 5.4.5 Column shears at the left end of frames – aspect ratio = 1.0..... 51
Fig. 5.4.6 Column shears at the left end of frames – aspect ratio = 1.5..... 52
Fig. 5.4.7 Column shears at the left end of frames – aspect ratio = 2.0..... 53
Fig. 5.4.8 Column shears at the left end of frames – aspect ratio = 2.5..... 54
Fig. 5.4.9 Column shears at the left end of frames – aspect ratio = 3.0..... 55
Fig. 5.4.10 First story column shears at the left end of frames vs aspect ratio..... 56
Fig. 5.5.1.1 Modification of column shears based on EBCS-8 for FRAME-1..... 60
Fig. 5.5.2.1Comparison of static and dynamic analyses for the frames with aspect ratio = 2.0 64
Fig. 5.5.2.2 Comparison of static and dynamic analyses for the frames with aspect ratio = 3.0 65
Fig. B.1 Infill shear vs. inter-story drift at different story levels – FRAME-1 with aspect ratio = 1.5. 87
Fig. B.2 Infill shear vs. inter-story drift at different story levels – FRAME-1 with aspect ratio = 2.0 88
Fig. B.3 Infill shear vs. inter-story drift at different story levels – FRAME-1 with aspect ratio = 2.5 89
Fig. B.4 Infill shear vs. inter-story drift at different story levels – FRAME-2 with aspect ratio = 1.5 90
Fig. B.5 Infill shear vs. inter-story drift at different story levels – FRAME-2 with aspect ratio = 2.0 91
Fig. B.6 Infill shear vs. inter-story drift at different story levels – FRAME-2 with aspect ratio = 2.5 92

Fig. B.7 Infill shear vs. inter-story drift at different story levels – FRAME-3 with aspect ratio = 1.5 93
Fig. B.8 Infill shear vs. inter-story drift at different story levels – FRAME-3 with aspect ratio = 2.0 94
Fig. B.9 Infill shear vs. inter-story drift at different story levels – FRAME-3 with aspect ratio = 2.5 95
Fig. B.10 Infill shear vs. inter-story drift at different story levels – FRAME-4 with aspect ratio = 1.5 96
Fig. B.11 Infill shear vs. inter-story drift at different story levels – FRAME-4 with aspect ratio = 2.0 97
Fig. B.12 Infill shear vs. inter-story drift at different story levels – FRAME-4 with aspect ratio = 2.5 98

LIST OF TABLES

Table 2.5.1 Behavior Modes for Solid Infilled Panel Components 12

Table 4.1.1 Initial effective moment of inertia of concrete members. 25

Table 5.5.1.1 Determination of modification factor for bare frame in account of infill 59

Table C-1 Lumped mass at floor level of each story 99

Table C-2 Stiffness calculation for masonry infill 101

LIST OF NOTATIONS

A = constant that controls the shape of the generated hysteretic loops.

a = constant defined as the slip length.

A_g = gross area of a section.

A_s = control parameter to vary the slip length

a_{45} = maximum out-of-plane response acceleration at mid height of the fourth story.

B = width of the building in m in the direction considered.

DI = damage index

d_m = diagonal length of infill panel, cm.

E_f = modulus of elasticity of frame material.

E_m = modulus of elasticity masonry

f_b = lateral tensile stress developed in the masonry unit.

f'_{cb} = uniaxial compressive strength of masonry unit.

f'_{cj} = compressive strength of confined mortar.

f'_j = compressive strength of mortar bed

f_l = lateral compressive stress developed in the mortar.

f'_m = compressive strength of masonry

f'_p = longitudinal stress in masonry prism.

f'_{tb} = biaxial tensile strength of masonry unit.

f_x = lateral tensile stress at failure.

f_y = axial compressive stress at failure.

H = height of the building in m.

h = column height between centerlines of beams, cm.

H_i = horizontal inertia force at storey level i.

h_i = height of a story level above the base.

h_m = height of masonry infill panel, cm.

h_u = height of the masonry unit.

I_{col} = moment of inertia of a columns.

I_{ex} = moment of inertia of exterior columns.

I_g = moment of inertia of gross section, neglecting the reinforcement.

I_{in} = moment of inertia of interior columns.

m = wall mass per unit area.

M_{45} = out-of-plane moment at mid height of the fourth story.

N = vertical load in infill walls.

n = number of stories.

P = axial forces.

P_i = step seismic force at time t_i.

q_i = modal coordinate at time t_i.

r = the inter-story drift angle.

R_c = vertical component of the diagonal compression force.

s_k = V_y multiplier to define the pivot for stiffness deterioration branches.

s_{p1} = parameter controlling the rate of deterioration.

t_m = thickness of infill panel and equivalent strut.

T_{1b} = first mode period of the bare structure without taking into account any stiffness of the infills.

T_{1i} = first mode period of the structure taking into account the infills as structural elements.

u_i = inter-storey drift at the story level i.

U_i = instantaneous displacement at time t_i.

U_m = maximum displacement.

U_p = post-peak residual displacement.

U_u = stress non-uniformity coefficient.

U_y = displacement at yielding.

V_{ij} = shear in column j at storey level i.

V_c = shear at the compression failure of equivalent diagonal strut.

V_f = maximum horizontal shear force due to sliding failure.

V_i = instantaneous shear force at time t_i.

V_m = maximum shear force.

V_p = post-peak residual shear force.

V_y = shear force at yielding.

V_y^0 = original value of shear force at yielding before strength degradation.

W_i = Seismic dead load at the story level i.

Z = width of equivalent diagonal compression strut of infill panel.

Z_i = hysteretic component

α = the ratio of the post-yield stiffness to the pre-yield stiffness.

β = constant that controls the shape of the generated hysteretic loops.

$\varepsilon_m^{'}$ = masonry compression strain at the maximum compression stress.

ϕ_i = mode shape at time t_i.

γ = constant that controls the shape of the generated hysteretic loops.

η_i = parameter controlling the stiffness decay.

λ_1 = coefficient used to determine equivalent width of infill strut.

μ = sliding friction coefficient along the bed joint.

μ_c = monotonic ductility capacity.

μ_i = instantaneous ductility at time t_i.

μ_{max} = maximum attained ductility.

μ_r = ductility attained at the load reversal.

θ = angle whose tangent is the infill height-to-length aspect ratio, radians.

σ_N = vertical compression stress in the infill walls.

τ_f = maximum shear strength

τ_o = cohesive capacity of the mortar bed.

ω_D = the natural circular frequency of a damped vibration of a system.

ω_n = the natural circular frequency of a system.

ξ = viscous damping.

ABSTRACT

Equivalent strut approach coupled with modified Bouc-Wen model for hysteretic behavior has been adapted for the analysis of masonry infilled RC frame. Modification of Bouc-Wen model includes stiffness and strength degradations as well as pinching in the infill panel. Default values for some of the parameters involved in the hysteretic model are adopted from the manual of IDARC-2D version 6.0. A simplified program developed in substitute of IDARC-2D is the backbone of this paper. The program assumes the beams as rigid elements embodied in the floor slabs and the deformation of columns in linearly elastic behavior.

Four frames having the same number of stories but different number of bays are analyzed using the program. Only the first bay, whose aspect ratio (L/H) subject to variation from 1.0 to 3.0, has been infilled with masonry. Comparative analysis of shear in the left end column is performed for the infilled frame and corresponding bare frame. Static analysis using fundamental period and response spectrum curve based on EBCS-8 is carried out to compare the results of analysis of the program.

Key words: Infill; Macro-model; Hysteretic; Degradation; Aspect ratio.

1 INTRODUCTION

1.1 Background

The construction of high rise buildings is basically associated with infilled frames. In most constructions the infill is masonry covering a very wide range of materials such as adobe, brick, stone and concrete blocks. Masonries are easier, faster and even cheaper than other materials in construction of infill walls.

The infill panels were solely considered to be non-structural as they were means of providing enclosure and internal partition to the building. This fact is far from reality as the infill panel will definitely interact with the enclosing frame especially under seismic forces. It is observed in common practice of construction that specific construction measure is not taken to account for the interaction of panels and frames in spite of high seismicity in some regions. Failures that can be ascribed to the behavioral change of frames due to tight infill panel are common reports over all the worlds of catastrophic seismic regions.

It is a common misconception that masonry infill in structural steel or reinforced concrete frames can only increase the overall lateral load capacity. Earthquake damage can be traced to structural modification of the basic frame by so-called nonstructural masonry partitions and infill panels. Masonry infill can drastically alter the intended structural response, attracting forces to parts of the structure that have not been designed to resist them. The high shear forces generated in the infilled frames are transmitted primarily by shear stresses in the panels. Shear failure commonly results, with shedding of masonry into streets below, or into stairwells, with great hazard to life.

As the consequence of the reasons mentioned so far, this paper aims at disclosing the facts related to seismic design of infilled frames which otherwise been considered insignificant from the practitioners point of view in our country.

The analytical models adopted so far can be categorized into two main groups:

1. Micro-modeling: the masonry units, the mortar, and the masonry unit / mortar interface, are modeled separately.

2. Macro-modeling: the masonry is a homogeneous continuum with no distinction between the individual units and joints.

Researches are being carried out in the concerned regions of the world to clearly arrive at a consensus by disclosing the complex behavior of interaction between panels and frames. From time to time laboratory tests are being conducted and mathematical models are being developed that can best simulate the behavior of infilled frames.

1.2 Objectives

The research aims at evaluating the potentially higher shear induced at columns neighboring to the infilled frame. It quantitatively compares the peak shears in a column neighborhood of infilled frame and a corresponding column of a bare frame. The higher shears attracted towards the infilled portions of the frame that are not designed to resist them will be distinguished. The misconception that always the infill is in favor of the frame will be unraveled at this point as higher shears are transmitted to columns in infilled frames compared to columns in bare frames. Such concepts are input to the designers in their effort toward achieving better seismic resistant designs.

The research makes it possible to predict which aspect ratio of the panel is sensitive in magnifying the infill-frame interaction as various aspect ratios of the panel are to be considered. In addition how the shear is distributed at different level of stories is evaluated for the generalized prediction of shear transmitted to columns at these levels.

Last but not least is the assessment to solid infill paves a way to the evaluation of shear in partially infilled frames. Wall perforations and partial infill are very common practical features due to windows, doors and other provisions in walls. The basic concepts for estimations of behaviors in such walls root at the solid infill walls.

1.3 Methodology

The resource for the thesis work is completely dependant on literatures. Therefore chapters 2 through chapter 4 are adopted from literatures to clarify the analysis carried out in chapter 5.

Chapter 2 mainly deals with the history of development of masonry infill model and their failure modes. Chapter 3 is concerned with the explanation of effect of seismic load as revealed through story shears and story moments. Lateral load resistance evaluated by stiffness of the frame elements has been expounded in chapter 4. Here, how masonry infill is contributing resistance to lateral load has been observed. As frames are to be subjected to time history analysis the stiffness and strength degradations through each cycle of loading is also a subject matter of chapter 4. Extracting the ideas of the chapters mentioned, chapter 5 takes the duty of analyzing selected infilled frames using the assumptions and methods stated below.

For the solid infill masonry walls the frame and the wall connection is assumed to be tight in order to include masonry elements in the model of the physical structure. The beam plus the slab system are assumed to form rigid horizontal elements so that it can be modeled as shear frame for simplified analysis. Moreover the column is designed with such adequate overstrength that its response throughout the seismic time history is linearly elastic. The gravity load simultaneously acting with the lateral load and out of plane actions due to lateral load are omitted.

The following parameters are constant for any frame adopted in the analysis:

- The cross section of the columns, 40 X 40 cm.
- The cross section of the beams, 30 X 40 cm.
- The height of the columns, 3 m.
- The width of non-infilled bay(s) in a multi-bay frame system, 6 m.
- The number of stories is always five and the single infilled bay is located at the left end for all frames.
- The material used for the panel is brick with a single wythe.
- The in-plane lateral EQ force is the one artificially generated from response spectrum curve of EBCS-8 of soil type A and factored by 0.3g for moderate seismicity.

Four frames with the number of bays from one to four are center of attention of the analysis. The aspect-ratio of the infilled bay varies from 1:1 to 3:1 for every 0.5 m change in the width of the infilled bay.

A modified Boc-Wen model for hysteretic damping of masonry panel including the degradation of stiffness and strength for the cyclic loading has been used. The developed program **ASSDMI** carries out the time history analysis for the time step of 0.01sec. based on the interpolation of the excitation. At each time step change in stiffness of the panel, which is modeled as compression strut, is taken including account of nonlinearity in the Bouc-Wen hysteretic loop. Effect of all modes on the five story frames was estimated from the modal superposition for the viscous damping of 5%.

Finally the shears of a bare frame and a corresponding frame, whose first bay is infilled, were calculated for the purpose of comparison. The shears of the panel and the column neighboring to the infill are added directly. The value obtained is conservatively high, as the horizontal component of the compression in a strut doesn't account for the friction between the panel and the frame, and it can safely forecast the uncertainties in the infill panel interaction.

2 MODEL DEVELOPMENT OF MASONRY INFILL AND BEHAVIOR MODES

2.1 General

Masonry is a term covering a very wide range of materials such as adobe, brick, stone and concrete blocks; and each of these materials in turn varies widely in form and mechanical properties. It is a non-homogenous and anisotropic composite structural material. Masonry may also be used with or without reinforcement or in conjunction with other materials. In addition to its use for primary structure, masonry is used for infill panels creating partitions or cladding walls. Various construction forms include from unmortared stacked stone blocks, where resistance to lateral forces is provided solely by gravity stability and friction, to carefully mortared and reinforced masonry walls designed for ductile response under seismic attack.

Masonry structures of substantial size can be designed to perform adequately under major earthquakes, provided that careful design and detailing requirements are followed. By virtue of the form of construction masonry has large number of potential weak links than other materials. As masonry is a comparatively brittle material, it is generally necessary to design for higher seismic forces than that required for other materials. Its behavior is not perfectly elastic even in the range of small deformations. Even when lateral deformation of the wall is kept constant during a given time interval, changes in resistance and crack distribution can be observed during the test in the non linear range, which indicates the sensitivity of test results to the time history of lateral loads used for the simulation of seismic loads.

Behavior of infilled frame systems subjected to in-plane lateral forces is influenced by mechanical properties of the frame and infill materials, stress or lateral deformation levels, existence of openings in the infill, and the geometrical proportions of the system. Existence of an initial gap between the frame members and the infill also influences the behavior of the system. It has been usual in several countries to consider that the total vertical and horizontal loading is carried by the frame only. The infills do not participate as part of the primary structure on the assumption that precautions are taken to avoid load being transferred to them. It is evident from the frequently observed diagonal cracking of such infill walls that the

approach is not always valid. Hence such cases require incorporation of modified mode of behavior for the frame and design of walls.

2.2 Historical Perspective

Infilled frame construction has been in use for more than 200 years. Infilled frames are basically associated with the construction of high rise buildings with the frames carrying the gravity loads and the infill is means of providing enclosure and internal partitioning to the building. The infill panels were invariably considered to be 'non-structural'. A pioneering work on the investigation of the interaction between the infill panels and frames began in 1950s in Russia (Polyakov, 1956). In the United States Benjamin and Williams in 1958 (Benjamin et al, 1958) reported the first investigation on the lateral load behavior of infilled frames. Early studies were mostly concerned with the monotonic lateral-strength capacity of infilled frame systems.

Masonry analysis has developed into a mature analytical field in the last half century as the guide rules are replaced by modern standards that are based on a mixture of proven empirical rules, extensive numerical and experimental research, and finite element based analysis (Nichols, 2000). Following the advent of experimental investigations, several different methods of analysis were proposed for determining the composite strength of an infilled frame system (Maghaddam et al, 1987). These include elasticity solution based on the *Airy stress function, the finite-difference method, the finite-element method, and plastic methods of analysis.* These methods are successful in predicting the strength capacity of infilled-frame system. But it is difficult to extend the findings to inelastic behavior as each method has its roots in elasticity or rigid plasticity, especially if cyclic loading is to be considered (FEMA 306, 1998). Hence the equivalent-strut method of analysis has become the most popular approach for analyzing infill frame systems.

Early equivalent-strut methods, starting with Stafford-Smith (1966), used single strut to represent infill behavior. Several multiple strut methods of analysis have been proposed (Chrysostomon et al., 1988 ; Thiruvengadam, 1985; Mander et al., 1994) for more accurate modeling of frame/panel interaction. As there is still drawback in modeling force transfer-slip at the frame panel interfaces (Gergely et al., 1994), non-linear finite element analysis can be

used (Shing et al., 1994; Mosalan et al., 1994). Computational limitations, on analyzing more than one panel at a time are difficulties with the later method. The general consensus is that two struts per panel for reversed cyclic loading analysis, one across each diagonal may be used for design and evaluation studies of infilled frame systems.

There are impediments to reliable modeling. The first being discontinuities of infill, resulting from soft stories or checkered patterns. The second is the large variation in construction practice over different geographic regions and changes of materials over time. Early construction generally consisted of clay brick (or sometimes stone masonry) with iron/steel frames. With time, concrete frames became popular and concrete block units were used for the infill panels.

Ali and Dhanasekar (Ali, 1987 ; Dhanasekar, 1985) researched on further aspects of the static analysis of masonry. Their work has been instrumental in the development of the current code provisions related to the design of masonry structures for bi-axial loading, concentrated loads, and in plane loading of masonry. Early research mostly focused on developing improved seismically resistant design, analysis and construction techniques for new structures. Little research was done to investigate the seismic performance of existing structures with non-ductile detailing. Only a limited amount of research has been undertaken on infilled frames with openings.

2.3 Components of Infilled Wall

Infilled frame elements are made up of infilled-panel and frame components. Infilled panels are categorized according to the material and geometric configuration. Clay brick is the most common and traditional type of infill. Most often it is unreinforced except in modern buildings where it may be reinforced, grouted-cavity wall construction (FEMA 306,1998). At still a relatively modern form of unreinforced masonry infill construction hollow clay tile (HCT) is used. Concrete masonry unit (CMU) is also the commonest form using hollow concrete blocks laid up with mortar. CMU may be left hollow or filled with grout. Concrete with usual minimal reinforcement is also used as infill.

Infills have a wide variety of geometric configurations. Aspect ratios (length/height) for infilled panels usually vary from approximately 1:1 to 3:1 with most ranging from 1.5:1 to 2.5:1. For the sake of partition and/or facade suiting, infills can be configured in varied forms. There may be eccentricity between the frame components and infill axes. Based on geometric configuration there are two categories for infilled panel components - solid panels and panels with openings. Doors and windows are the two most prevalent opening types.

The frame components are categorized primarily by material. Steel frames are popular for modern high rise buildings and low-rise, light-weight, commercial, building constructions. Most often I-sections or wide flange sections are used. Many of the steel frame elements are enclosed by concrete. Because of the relatively high shear capacity of steel columns, the fully restrained mode of behavior may be dominant.

Concrete frames are also common forms of construction: they may be classified as either ductile or non-ductile. Ductile detailing requires closely spaced transverse hoops in the beams, columns and connections. When infills are present, shear force demands are considerably higher leaving the beam or column vulnerable to shear failure. Precast, prestressed, concrete frames are also commonly encountered with infilled panels.

2.4 Masonry Infilled Frames and Seismic Behavior of Structures

The presence of masonry infill affects the seismic behavior of buildings in the following ways (Penelis and Kappos, 1997).

- As a consequence of increase in stiffness of buildings, the fundamental period is decreased and the base shear is increased.
- The lateral stiffness in plan and elevation is modified.
- The structural system is relieved of seismic action as part of the load is carried by the infills.
- Energy dissipation capacity of the building is substantially increased.

The more flexible the structural system, the greater the above effects of the infills.

It is a common misconception that masonry infill in structural steel or reinforced concrete frames can only increase the overall lateral load capacity. Earthquake damage can be traced to structural modification of the basic frame by so-called nonstructural masonry partitions and infill panels. Masonry infill can drastically alter the intended structural response, attracting forces to parts of the structure that have not been designed to resist them (Paulay and Priestley, 1992).

The high degree of uncertainties on the analysis of buildings due to effects of infill includes:

- The variability of their mechanical properties, and hence the low reliability in their strength and stiffness.
- Tightness when connected to the surrounding frame (wedging condition)
- The potential modification of their integrity during the use of the building.
- The non-uniform degree of their damage during the earthquake.

Thus the safety of the structure cannot rely, not even partly, upon the infills and only their probable negative influence is taken into account (Penelis and Kappos, 1997) .

2.5 Behavior Modes

Behavior of infilled frame systems subjected to in-plane lateral forces is influenced by mechanical properties of the frame and infill materials, stress or lateral deformation levels, existence of openings in the infill, and the geometrical proportions of the system. Existence of an initial gap between the frame members and the infill also influences the behavior of the system.

Under small deformations the stiffness behavior is dominated by the panel stiffness characteristics (FEMA 306, 1998). Hence, the events that define the shape of the force deformation curve are bed-joint sliding, diagonal tension, corner crushing, general shear failure, and out-of-plane failure. As the deformation increases the panel characteristics will be a function of its element properties. Stair-stepped pattern of cracks through head and bed joints will result when the masonry units are strong relative to the mortar. When the mortar is stronger than the units, rather a rare case, cracks will develop through the units as well as the mortar.

With the stair-stepped cracks, shear can continue to be resisted after cracking by the development of a compressive stress normal to the bed joints, characterized as a compression strut. If the mortar is weak relative to the units, an infill panel may crack along the bed joints instead of along the diagonal. When the infill panel is sufficiently strong in shear, the compressive stress at the compression corners will fail in crushing. The large forces generated in this mode will be distributed to the beam and column members, and may result in either column or beam shear failures. The following are failure modes recognized in masonry infilled frames

***i). Bed-Joint Sliding*:** Bed-joint sliding is likely to occur when the bounding frame is strong and flexible (such as steel frames). If the mortar beds are relatively weak compared to the adjacent masonry units (especially bricks), a plane of weakness forms, usually near the mid-height level of the infill panel. There is really no limit to the displacement capacity of this behavior mode.

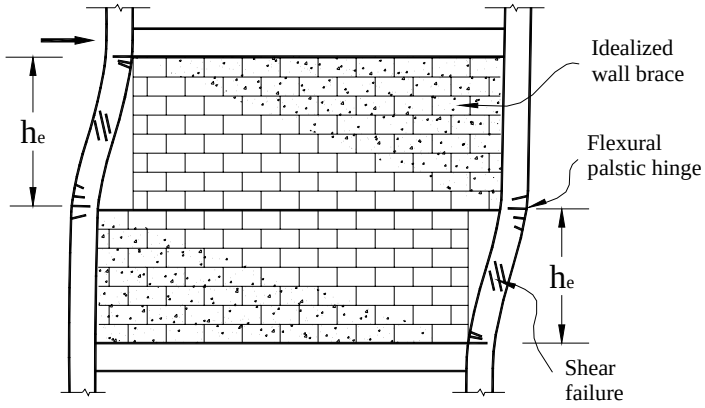

(Paulay and Priestley, 1992)

Fig. 2.5.1 Knee-braced frame model for sliding shear failure of masonry infill

(ii). Diagonal Cracking: Transverse to the principal compression formed across the diagonal of an infill strains are tension strains. Diagonal cracks are formed as a result of the tensile strain exceeding the cracking strain of the infill panel material. These cracks commence in the center of the infill and run parallel to the compression diagonal. The cracks tend to propagate until they extend from one corner to the diagonally opposite corner. Diagonal cracking behavior usually signals the formation of a new diagonal strut behavior mode.

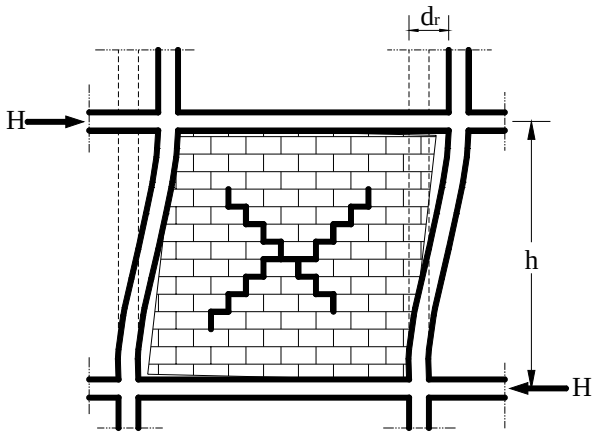

(Penelis and Kappos, 1997)

Fig. 2.5.2 Masonry failure with X-shaped cracks due to the R/C frame inter-storey drift

(iii). Corner Compression: This is because of the high stress concentrations at each corner of the compression diagonal. Corner crushing is located over a relatively small region for strong/stiff columns and beams; whereas for weaker frames, especially concrete frames, corner crushing is more extensive and the damage extends into the concrete frame itself.

(iv). Out-of-Plane Failure: The failure is due to ground shaking transverse to the plane of a wall. Out-of-plane failure may occur in the upper stories of high-rise buildings, where the floor accelerations are basically resonance amplifications of prominent sinusoidal ground motion input. In lower stories, when out-of-plane shear is combined with high in-plane story shears, infill panels tend to progressively "walkout" of the frame enclosure.

(v). Premature Failure of Frame Elements or Connections: Failures of columns, beams, and connections due to compressive "strut" reactions imparted to them by the masonry infill. Another mode of failure of frame elements is the failure of the tension or compression chords of the infill frame acting as a monolithic flexural element. The latter is predominant in cases of slender infilled frame and a single bay infilled in a multibayed multistory building.

(vi). Failure of the Frame: The response of the frame with the infill missing should be assessed, keeping in mind the likelihood that a soft story configuration or stiffness eccentricity may have resulted.

Table 2.5.1 Behavior Modes for Solid Infilled Panel Components
(FEMA 306, 1998)

Behavior Mode	Description/Likelihood of Occurrence	Ductility
Bed-joint sliding	Occurs in brick masonry, particularly when length of panel is large relative to height. Aspect ratio is large and mortar strength is low	High
Diagonal cracking	Likely to occur in some form	Moderate
Corner compression	Crushing generally occurs with stiff columns	Moderate
Out-of-plane failure	More likely to occur in upper stories of buildings. However, out-of-plane "walking" is likely to occur in the bottom stories, due to concurrent in-plane loading.	Low

2.6 Modeling of Masonry Infilled Walls

Unless masonry infill walls are adequately isolated from the concrete frame members and the floor above, masonry elements shall be included in the model of the physical structure. The mathematical model of the physical structure shall represent the spatial distribution of mass and stiffness of the structure to an extent which is adequate for the calculation of the significant features of its dynamic response.

Masonry exhibits distinct directional properties, due to the influence of mortar joints acting as planes of weakness. Depending upon the orientation of the joints to the stress directions, failure can occur in the joints alone or simultaneously in the joints and blocks. The great number of the influencing factors, such as dimension and anisotropy of the bricks, joint width and arrangement of bed and head joints, material properties of both brick and mortar, and quality of workmanship, make the simulation of plain brick masonry extremely difficult.

The following two levels of refinement for masonry models can summarize the analytical procedures (Asteris et al, 2003):

- **Micro-modeling (masonry as a multi-phase material):** According to this procedure the masonry units, the mortar, and the unit/mortar interface, are modeled separately. While this leads to more accurate results, the level of refinement means that any analysis will be computationally intensive, and so will limit its application to small laboratory specimens and structural details.

- ***Macro-modeling (masonry as one-phase material):*** According to this procedure no distinction between the individual masonry units and joints is made, and masonry is considered as a homogeneous, isotropic or anisotropic continuum. While this procedure may be preferred for the analysis of large masonry structures, it is not suitable for the detailed stress analysis of a small panel, due to the fact that it is difficult to capture all its failure mechanisms. The influence of the mortar joints acting as planes of weakness cannot be addressed.

  The macro-model of an infilled frame structure shall include the stiffness effects of the infill as a pair of diagonals in the bays of the frame. The diagonals shall be considered as resisting only compression axial loads. Their lines of action shall intersect the beam-column joints. The secant stiffness of the force-displacement relationship shall be used to determine the effective area of the diagonals.

The load resisting mechanism of infilled frames was idealized as a combination of a moment resisting frame system formed by the frame and a pin-jointed truss system formed by the infill panel. The infill panel was modeled as a combination of three nonparallel struts (one diagonal and two off-diagonal) in each direction of loading (Chrysotomou et al, 1992). The analysis requires the determination of the geometry and hysteretic rule parameters from theoretical or empirical models.

The method developed by Saneinejad and Hobbs (1995) takes into account the elastoplastic behavior of infilled frames considering the limited ductility of infill materials. Various governing factors such as the infill aspect ratio, the shear stresses at the infill-frame interface, and relative beam and column strengths are accounted for in this development. However, the formulation furnishes only extreme or boundary values for design purposes.

The control parameters to calibrate a macro-model are obtained using experimental data or micro-models which would simulate real behavior. For the analysis where the emphasis is on evaluating the overall structural response, macro-models can be substituted for micro-models without substantial loss in accuracy and with significant gains in computational efficiency.

3 LOAD EFFECTS ON MASONRY WALLS AND FRAMES

3.1 Strength of Masonry Units

It is less easy to predict the compressive strength of masonry as it depends on the properties of the masonry units, the mortar and the grout. As a consequence, most masonry design codes specify low design values for compressive strength $f_m^{'}$ unless prism tests are carried out to confirm higher values.

The compressive strength of the masonry units may vary from as low as 5 MPa for low quality limestone blocks to over 100 MPa for high-fired ceramic clay units. A minimum strength of about 12.5 MPa is typically required by design codes (Paulay and Priestley, 1992). The strength of mortar test specimens bears little relationship to mortar strength in the wall, because of absorption of moisture from the mortar by the masonry units.

3.2 Stress Strain Behavior of Masonry Prisms

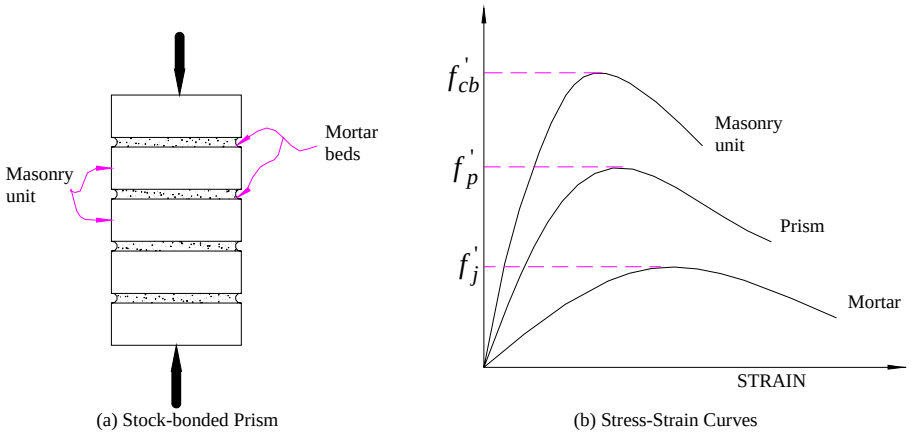

(a) Stock-bonded Prism (b) Stress-Strain Curves

(Paulay and Priestley , 1992)

Fig. 3.2.1 Stress-strain behavior of masonry prism

The combined effects of lower modulus of elasticity and higher Poisson's ratio result in a tendency for lateral mortar tensile strains to greatly exceed the lateral masonry unit strains. Friction and adhesion at the mortar masonry interface constrains the lateral strains of

mortar and masonry unit to be equal. Hence, there will be set up of self-equilibrating lateral forces between compression in the mortar and tension in the masonry unit (Fig. 3.2.2).

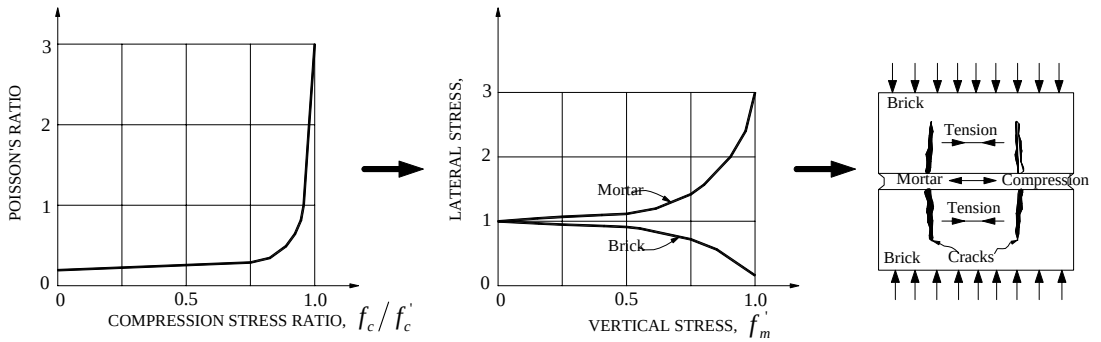

(a) Variation of Mortar Poisson's Ratio with Compressive Stress

(b) Lateral Stress vs Vertical Stress

(c) Tension Cracking of Masonry Unit

(Paulay and Priestley, 1992)

Fig. 3.2.2 Failure mechanism for masonry prisms

The resulting tri-axial compressive stress state in the mortar enhances its crushing strength, while the combination of longitudinal compression and lateral biaxial tension in the masonry unit reduces its crushing strength and induces tendency for vertical splitting.

Strength of the confined mortar may be approximated by (Paulay and Priestley, 1992),

$$f_{cj}' = f_{cb}' + 4.1 f_l \qquad \text{---------- (3.2.1)}$$

f_{cj}' - Compressive strength of confined mortar.

f_{cb}' - Uniaxial compressive strength of masonry unit.

f_l - Lateral compressive stress developed in the mortar.

Linear failure criterion (after Hilsdorf,1969)

For the masonry unit:

$$\frac{f_x}{f_{tb}'} + \frac{f_y}{f_{cb}'} = 1 \qquad \text{---------- (3.2.2)}$$

f_{tb}' - Biaxial tensile strength of masonry unit.

f_x - Lateral tensile stress at failure.

f_y - Axial compressive stress at failure.

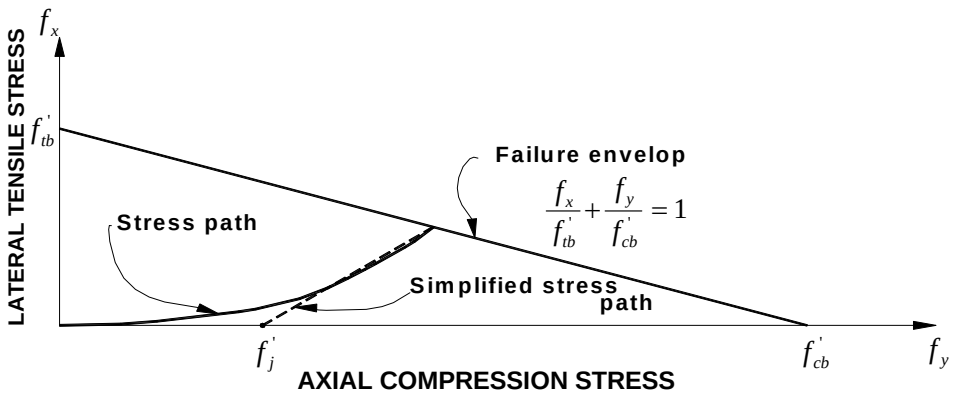

(Paulay and Priestley, 1992)

Fig. 3.2.3 Mohr's failure criterion for a masonry unit

By considering the transverse equilibrium requirements of a mortar joint of thickness j_t, and a tributary height of masonry unit equal to one-half a masonry unit above and below the joint in conjunction with equations (3.2.1) and (3.2.2), the longitudinal stress f'_p that causes failure is found to be,

$$f'_p = f_y = \frac{f'_{cb}\left(f'_{tb} + \alpha f'_j\right)}{U_u\left(f'_{tb} + \alpha f'_{cb}\right)} \qquad \text{---------- (3.2.3)}$$

$$\alpha = \frac{j_t}{4.1 h_u}$$

f'_j - compression strength of mortar bed

h_u - height of the masonry unit

U_u - Stress non-uniformity coefficient (U_u = 1.5 ; Hilsdorf ,1969)

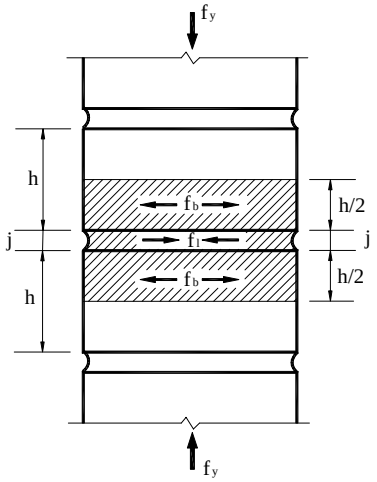

(Paulay and Priestley, 1992)

Fig. 3.2.4 Transverse equilibrium of masonry unit and mortar in prism

It is advisable to adopt conservatively high value for the modulus of elasticity, E_m, to ensure seismic lateral design forces are not underestimated, the following values are recommended (Paulay and Priestley, 1992):

Clay brick masonry: $E_m = 750\, f_m^{'}$

Where: $f_m^{'}$ - compression strength of masonry

3.3. Load Effects on Seismic Behavior - Frame Elements

The analysis of a structure should include the simultaneous effects of gravity and lateral loads. Gravity loads should include dead loads and likely live loads. The nonlinear response of a structure to lateral loads depends (in a nonlinear way) on the gravity loads present at the time of lateral loading. Considering a beam (Figure 3.3.1a), the effect of light gravity load is to reduce the reserve moment and shear strengths at the right end and increase the reserve strengths at the left end (reserve strength is defined as the difference between the total strength and the resistance used up by gravity load). Therefore, for a given lateral drift, the gravity load will increase the inelastic rotation demands at the right end of the beam and decrease them at the left end. For larger gravity loads, the effects are increased, and the inelastic mechanism may shift from beam hinging at the ends to hinging along the beam span. In the case of column (Figure 3.3.1b), variations in gravity load produce variations in column axial force, with consequent changes in both column strength and deformability. Increases in axial load invariably decrease flexural deformability. Increases in moment strength result in increased shear demands and may result in shear failure that would not be expected at lower axial loads.

In general, because of the nonlinear nature of the interactions, it is not appropriate to carry out the gravity load analysis and lateral load analysis separately and then superimpose their results. Instead, the gravity loads should be applied to the numerical model and should be maintained as the lateral deformations are imposed.

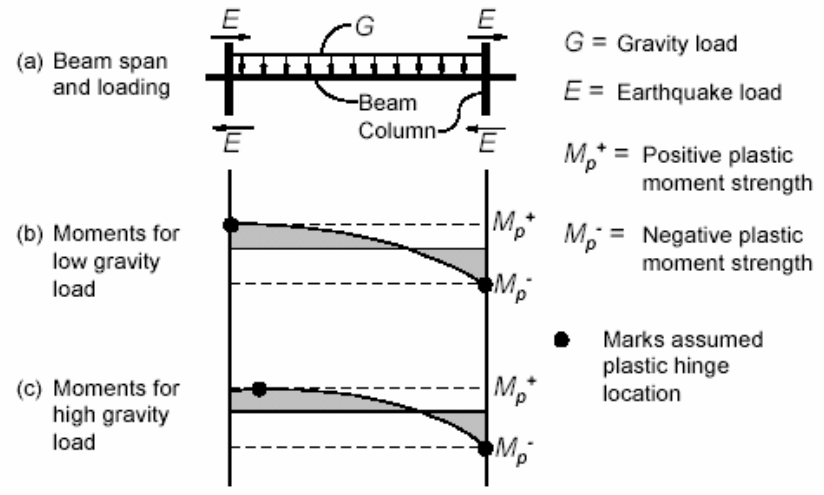

(a)

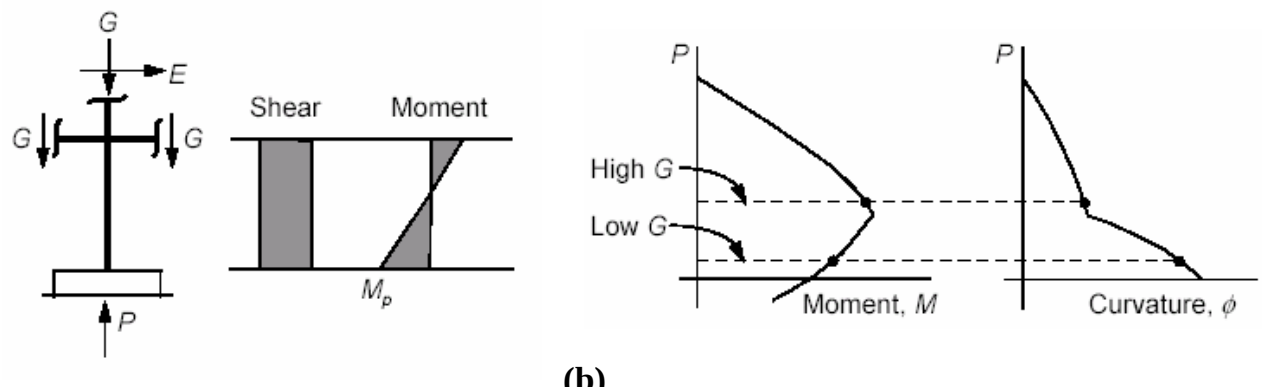

(b)

(ATC-40, 1996)

Fig. 3.3.1 Gravity Load Effects on Seismic Behavior of Components
(a) Beam Elements (b) Column Elements

During an earthquake, acceleration-induced inertia forces will be generated at each floor level, where the mass of an entire story may be assumed to be concentrated. Hence the location of a force at a particular level will be determined by the center of the accelerated mass at that level. The summation of all the floor forces, F_i (Fig. 3.3.2), above a given story will then locate the position of the resultant force V_i within that story.

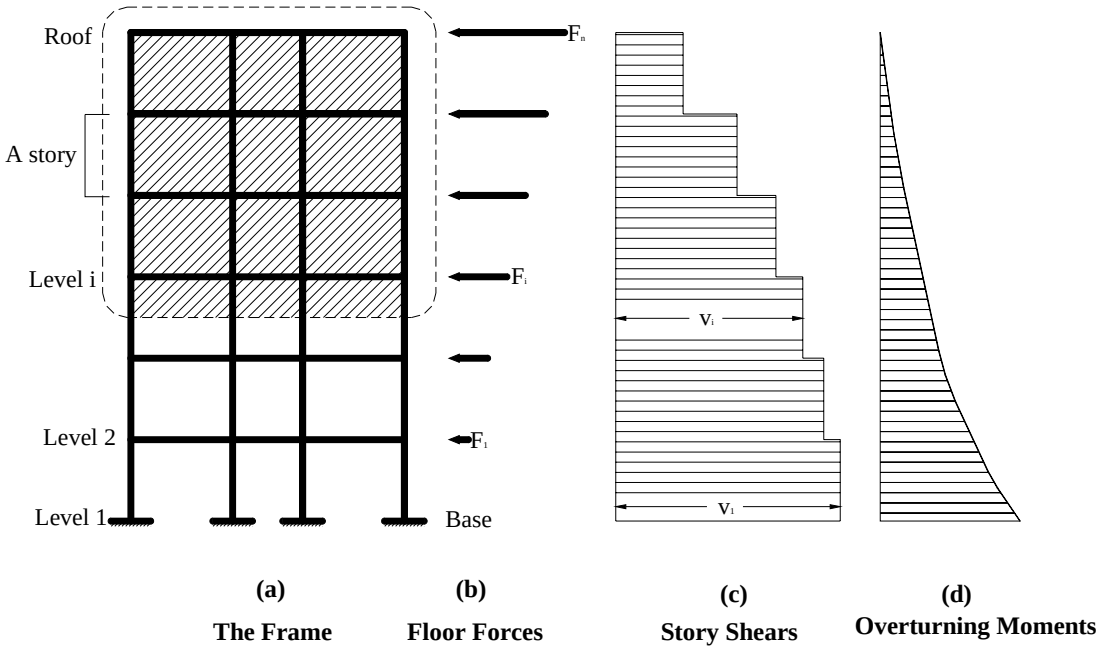

(Paulay and Priestley, 1992)

Fig. 3.3.2 Effects of lateral forces on a building

Figure 3.3.3 illustrates a generalized load-deformation relation appropriate for most concrete components. The relation is described by linear response from A (unloaded component) to an effective yield point B, linear response at reduced stiffness from B to C, sudden reduction in lateral load resistance to D, response at reduced resistance to E, and final loss of resistance thereafter (Fig. 3.3.3a). Deformations beyond point E are not permitted because gravity load can no longer be sustained (Fig. 3.3.3b). In some cases, initial failure at C will result in loss of gravity load resistance, in which case E is a point having deformation equal to that at C and zero resistance (ATC-40, 1996). The above main points are shown on the load-deformation relation of figure 3.3.3.

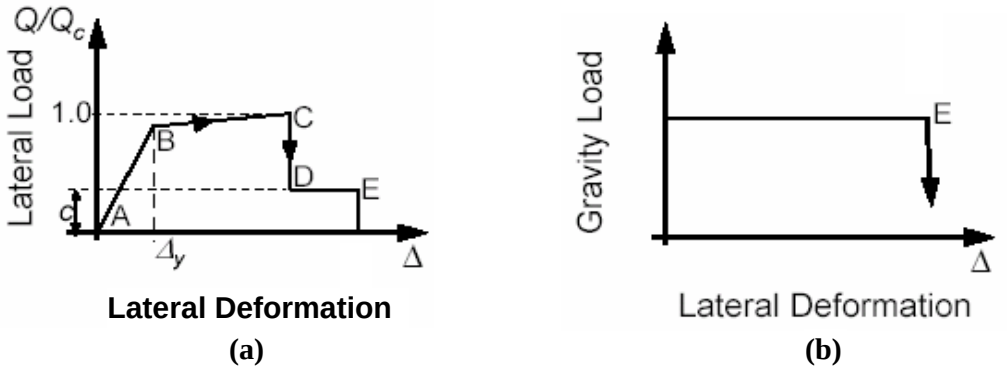

(ATC-40, 1996)

Fig. 3.3.3 Generalized Load-Deformation Relations for Non-degrading Components.

Where, Q_c - refers to the strength of the component.

Q - refers to the demand imposed by the earthquake.

Lateral loads should be applied in predetermined patterns that represent predominant distributions of lateral inertial loads during critical earthquake response. Lateral loads commonly may be lumped at floor levels if the floor diaphragms are sufficiently rigid in their plane. The taller a building, the more significant the effect of lateral forces will be. As a structure is displaced laterally, its lateral load stiffness usually decreases with increasing lateral displacement.

For the same maximum displacement at roof level, the overall ductility demand in terms of the large deflection is much more readily achieved when plastic hinges develop in all the beams (Fig. 3.3.4b) instead of only in the soft-story column (Fig. 3.3.4c). The column sway mechanism, also referred to as a soft-story, may impose plastic hinge rotations, which even with good detailing of affected regions, would be difficult to accommodate (Paulay and Priestley, 1992).

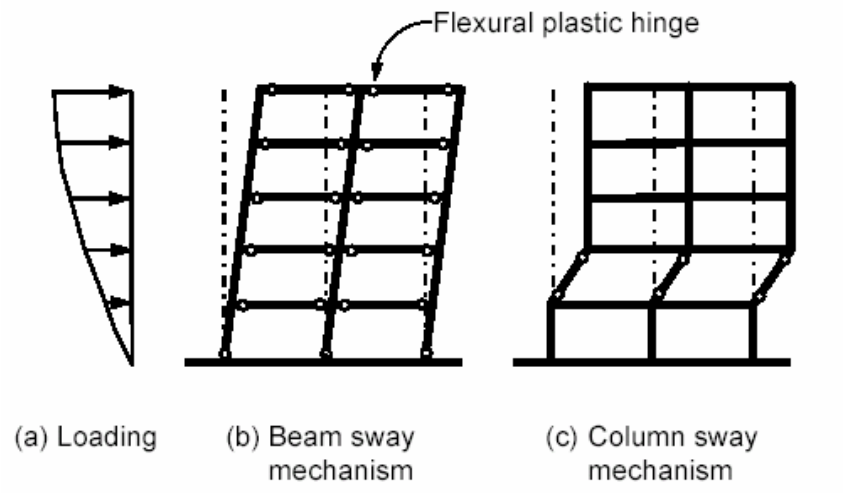

(ATC-40, 1996)

Fig. 3.3.4 Idealized Flexural Mechanisms in Multi-story Frames

It is important to recall the reader at last that the above detail of the effect of loads on the frames is to show the actual behaviors during devastating earthquake but this thesis work has already simplified such complex situations by considering moderate seismic forces and hence omitting the possibility of formation of hinges neither in the beams nor in the columns.

3.4. Out-of-Plane and In-Plane Loadings – Masonry Walls

Walls will be subjected to simultaneous vertical, in plane, and out of plane (face) load, because of the multiaxial nature of ground shaking under seismic forces.

The in-plane response will primarily be a result of the resistance of the wall to inertia forces from other parts of the structure, such as floor masses. The-out-of-plane response will be due to the inertia mass of the walls themselves responding to the floor-level excitation.

The design envelope of in-plane moments exceeds those resulting from the code distribution of forces at levels above the base due to higher-mode effects (Paulay and Priestley, 1992). Magnitude of out-of-plane moments will be larger in the upper than in the lower stories.

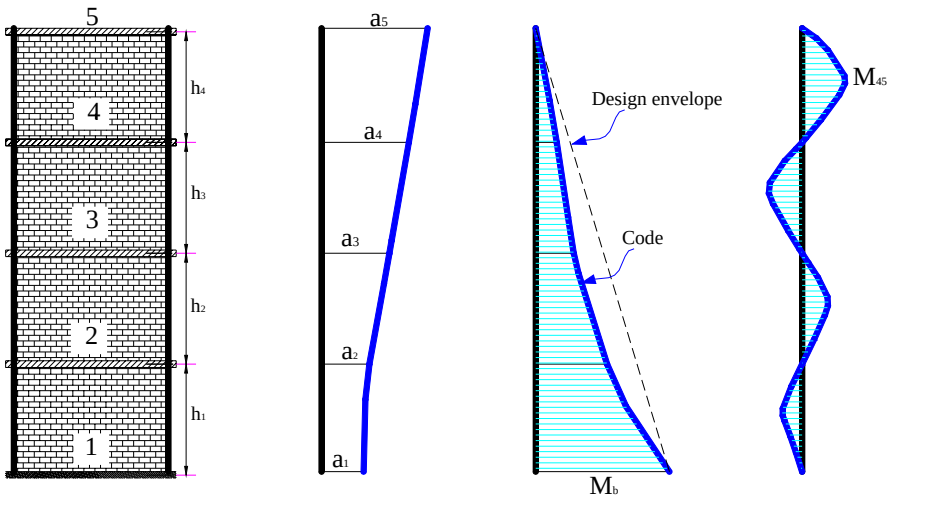

(Paulay and Priestley, 1992)

Fig. 3.4.1 Response of a masonry wall to biaxial excitation.

The first out-of-plane mode of the wall with cotraflexure points at the floor level is more conservative than assuming excitation of any higher mode, which would result in lower maximum bending moments. Due to in-plane action, tension cracking will reduce the ability of the walls to provide restraining moments at floor levels. It should be noted that maximum in-plane moments occur at the base of wall, while maximum out-of-plane moments occur in the top story, where in plane moments are low.

For the wall of fig. 3.4.1, the maximum out-of-plane moment M_{45} will be approximately (Paulay and Priestley, 1992):

$$M_{45} = 0.1ma_{45}h_4^2 \quad \text{- for unit horizontal length of wall}$$

m - Wall mass per unit area.

a_{45} - Maximum response acceleration at mid height of the fourth story.

At mid-height of the story there is possibility of resonant response as a result of near coincidence of natural periods of out-of-plane response of the wall, T_w, and transverse in-plane response of the structure as a whole, T_s.

Fig.3.4.2 shows the first four out-of-plane mode shapes and periods for a three story masonry wall. The modes include the effect of the transverse structural stiffness, and hence are not symmetrical.

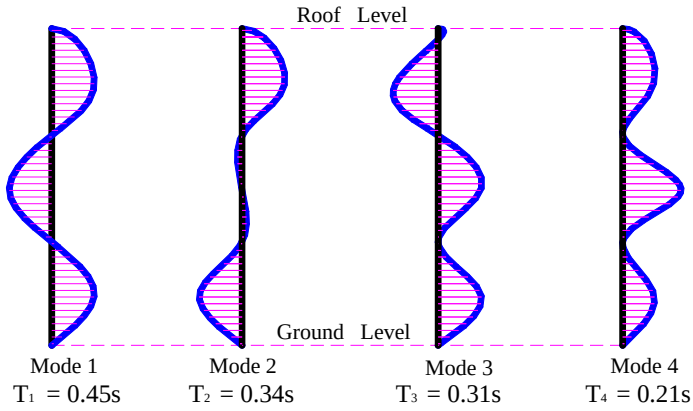

(Paulay and Priestley, 1992)

Fig. 3.4.2 Wall out-of-plane mode shapes and periods of a three-story masonry.

It is extremely likely that some degree of resonance will occur between out-of-plane and transverse structure response. Typical dynamic inelastic time-history analysis has resulted in amplification factors of 1.5 to 2.5.

3.5. Energy Path in a Masonry Building

In a masonry building the wall response accelerations, at a given height, act as input accelerations to the floor diaphragm. If the floor is rigid the floor displacements and accelerations at all points along the floor is the same as the displacements and accelerations

of end wall, or else, if the floor is flexible these responses at the floor level will be modified from the end wall responses. The ground acceleration is modified by two actions: that of the end structural walls and that of the floor diaphragms, before acting as an input acceleration to the face-loaded wall. Input accelerations to the face-loading wall at different floor levels will be of different magnitude, and may be out of phase or have significantly different frequency composition.

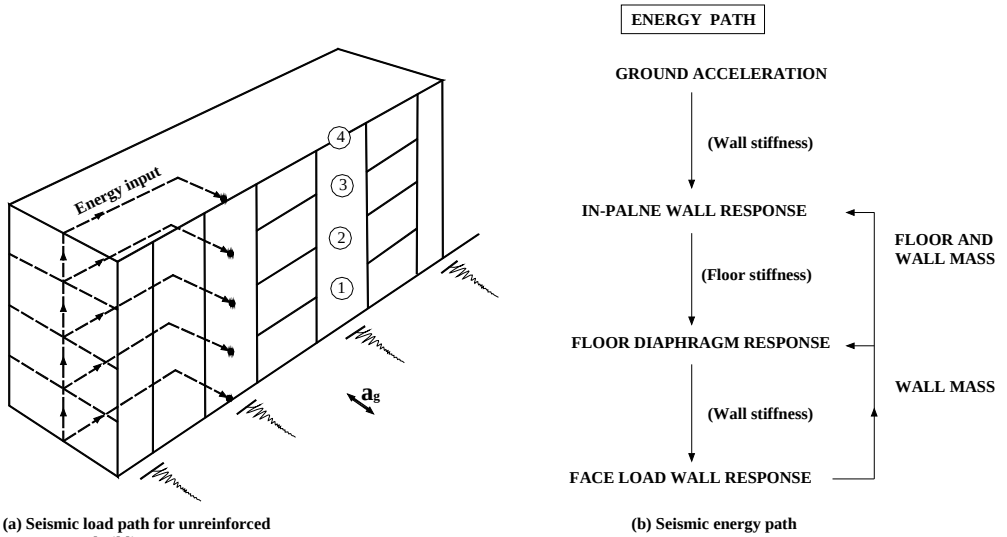

(a) Seismic load path for unreinforced masonry building

(b) Seismic energy path

(Paulay and Priestley, 1992)

Fig. 3.5.1 Seismic response of unreinforced masonry building.

4. LATERAL RESISTANCE OF MASONRY INFILLED FRAMES

4.1. Stiffness of Frame

In order to ensure that the hierarchy of member yield conforms to assumed distribution, and that the member ductilities are reasonably uniformly distributed throughout the frame, it is important that the distribution of member forces be based the realistic stiffness values applying at close to member yield forces.

At any section the moment of inertia will be influenced by the magnitude and sign of the moment, and the amount of flexural reinforcement, as well as by the section geometry and the axial load. Diagonal cracking of a member due to shear, intensity and direction of axial load, and reversed cyclic loading are additional phenomena affecting member stiffness.

In terms of design effort, it is impractical to evaluate the properties of several cross sections in each member of a multistory frame, and a reasonable average effective moment of inertia should be adopted in order to compensate for the cracks formed under reversal cyclic loading (Table 4.1.1).

Table 4.1.1 Initial effective moment of inertia of concrete members.

(Paulay and Priestley, 1992)

Member	Range	Recommended Value
Rectangular Beams	0.30 – 0.5 $\mathbf{I_g}$	0.40$\mathbf{I_g}$
T & L shaped beams	0.25 – 0.45 $\mathbf{I_g}$	0.35$\mathbf{I_g}$
Columns $P > 0.5f_c'A_g$	0.7 – 0.9 $\mathbf{I_g}$	0.80$\mathbf{I_g}$
Columns $P = 0.2f_c'A_g$	0.5 – 0.7 $\mathbf{I_g}$	0.60$\mathbf{I_g}$
Columns $P = -0.05f_c'A_g$	0.3 – 0.5 $\mathbf{I_g}$	0.40$\mathbf{I_g}$

Where: A_g - Gross area of section.

I_g - Moment of inertia of gross section, neglecting the reinforcement.

P - Axial force.

Frames with rigid girders subjected to lateral forces (Figure 4.1.1) exhibit zero moments at the mid-height of the columns, shear distribution proportional to the moments of inertia of the columns and relative displacements (or inter-storey drifts) proportional to the shear forces:

$$u_i = \left[\sum_j V_{ij}\right] \frac{h^3}{12E_f \sum_j I_{col}} = \left[\sum_{i=i}^{i=n} H_i\right] \frac{h^3}{12E_f \sum_j I_{col}}$$

$$V_{ij} = \left(\sum_{i=i}^{i=n} H_i\right) \frac{I_{col}}{\sum_j I_{col}}$$

Where: u_i - Inter-storey drift at the story level i.

V_{ij} - Shear in column j at storey level i.

H_i - Horizontal inertia force at storey level i.

h - Story height.

I_{col} - Moment of inertia of column.

E_f – Modulus of elasticity of frame material.

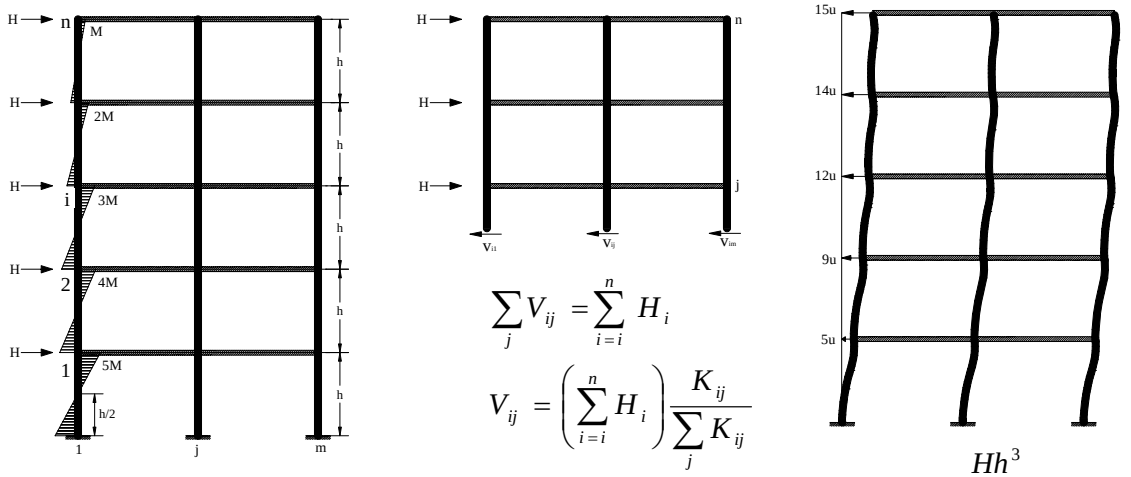

$$M_{ij} = V_{ij} \frac{h}{2}$$

$$\sum_j V_{ij} = \sum_{i=i}^{n} H_i$$

$$V_{ij} = \left(\sum_{i=i}^{n} H_i\right) \frac{K_{ij}}{\sum_j K_{ij}}$$

$$u = \frac{Hh^3}{12E\sum_j K_{ij}}$$

(a) **(b)** **(c)**

Fig. 4.1.1 Action effects of shear frames under lateral loading (Penelis and Kappos, 1997)

(a) M-diagram; (b) Equilibrium between shear and horizontal loads; (c) Storey displacements.

As the relative displacements are proportional to the shear forces these system are called ‘shear systems’. The deformation of these systems is such that they present a concave form on the side of the loading. In real frames, the girders due to their T-section exhibit in general much larger stiffness compared to that of the columns. Therefore their behavior is very similar to the behavior of shear systems.

4.2 Stiffness of Masonry Infill

4.2.1 Equivalent Width of Infill Strut

Prior to cracking the elastic in-plane stiffness of a solid unreinforced masonry infill panel shall be represented with an equivalent diagonal compression strut of width, *Z*, as in equation (4.2.1.1). The thickness and modulus of elasticity of the equivalent strut shall be the same as the infill panel (FEMA 306, 1998).

$$Z = 0.175(\lambda_I h)^{-0.4} d_m \quad \text{---------- (4.2.1.1)}$$

Where: $\lambda_I = \left[\dfrac{E_m t_m \sin 2\theta}{4E_f I_{col} h_m}\right]^{\frac{1}{4}}$

h = column height between centerlines of beams, cm.

h_m = height of masonry infill panel, cm.

E_f = modulus of elasticity of frame material, MPa

E_m = modulus of elasticity of infill material, MPa

I_{col} = moment of inertia of column, cm^4.

l_m = length of infill panel, cm.

d_m = diagonal length of infill panel, cm.

t_m = thickness of infill panel and equivalent strut, cm.

θ = angle whose tangent is the infill height-to-length aspect ratio, radians

λ_I = Coefficient used to determine equivalent width of infill strut.

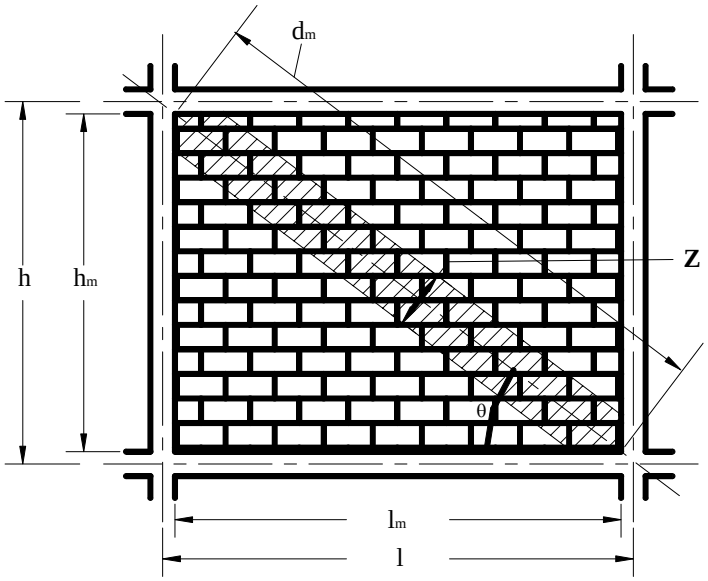

Fig. 4.2.1.1 Masonry Infilled Frame.

4.2.2 Sliding Shear Failure

Maximum shear strength from Mohr-Coulomb failure criteria:

$$\tau_f = \tau_0 + \mu\sigma_N$$

Where: τ_o – Cohesive capacity of the mortar bed.

μ - Sliding friction coefficient along the bed joint.

σ_N - Vertical compression stress in the infill walls.

Maximum horizontal shear force V_f :

$$V_f = \tau_0 t_m l_m + \mu N$$

Where: t_m - Infill wall thickness.

l_m - Length of infill panel.

N - Vertical load in infill walls.

N is caused by vertical shortening strain in the panel due to the lateral drifts.

$$N = l_m t_m E_m r^2$$

Where: r – The inter-story drift angle.

N may be estimated as the sum of applied vertical load on the panel and the vertical component of the diagonal compression force R_c. Usually the former is zero.

$$\therefore \quad N = R_c \sin\theta$$

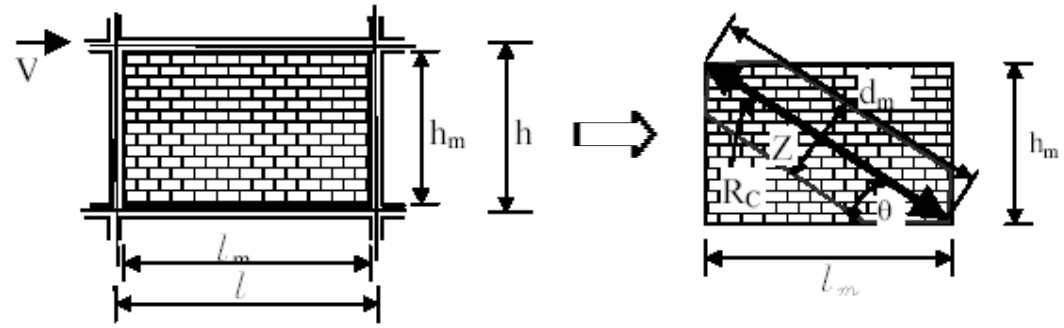

(Mostafaei et al, 2003)

Fig. 4.2.2.1 Infill masonry walls and equivalent diagonal compression action parameters.

Therefore, the maximum shear force is:

$$V_f = \tau_0 t_m l_m + \mu R_c \sin\theta$$

$$V_f = R_c \cos\theta \quad - \quad \textit{Horizontal component of strut}$$

$$R_c \cos\theta = \tau_0 t_m l_m + \mu R_c \sin\theta \;\Rightarrow\; R_c = \frac{\tau_0 t_m l_m / \cos\theta}{1 - \mu \tan\theta}$$

$$\therefore\ V_f = \tau_0 t_m l_m \left[1 + \frac{\mu \tan\theta}{1 - \mu \tan\theta}\right] = \frac{\tau_0 t_m l_m}{1 - \mu \tan\theta}$$

τ_0 is within the range $0.1 \le \tau_0 \le 1.5 MPa$.

For the purpose of analysis, $\tau_0 = 0.04 f_m^{'}$, $\mu = 0.5$ (Paulay and Priestley, 1992)

4.2.3 Compression Failure

Compression failure of infill walls is based on the compression failure of the equivalent diagonal strut. Based on FEMA 306 (1998) recommendations:

$$V_c = Z t_m f_m^{'} \cos\theta$$

Where: V_c - shear at the compression failure of equivalent diagonal strut.

Z - width of equivalent diagonal compression strut of infill panel

t_m - thickness of infill panel and equivalent strut.

$f_m^{'}$ - compressive strength of masonry

θ - angle whose tangent is the infill height-to-length aspect ratio, radians.

4.2.4 Analytical Modeling of Masonry Infill Panel

According to A. Madan (1997) a panel system is replaced by two diagonal masonry compression struts. For global building analysis purposes, these struts may be placed concentrically across the diagonals of the frame, effectively forming a concentrically braced frame system (Fig. 4.2.4.1a). In this configuration, however, the forces imposed on columns (and beams) of the frame by the infill are not represented. To account for these effects, compression struts may be placed eccentrically within the frames as shown in figure 4.2.4.1b (FEMA 356, 2000). If the analytical models incorporate eccentrically located compression struts, the results should yield infill effects on columns directly. Alternatively, global analyses may be performed using concentric braced frame models, and the infill effects on columns (or beams) may be evaluated at a local level by applying the strut loads onto the columns (or beams).

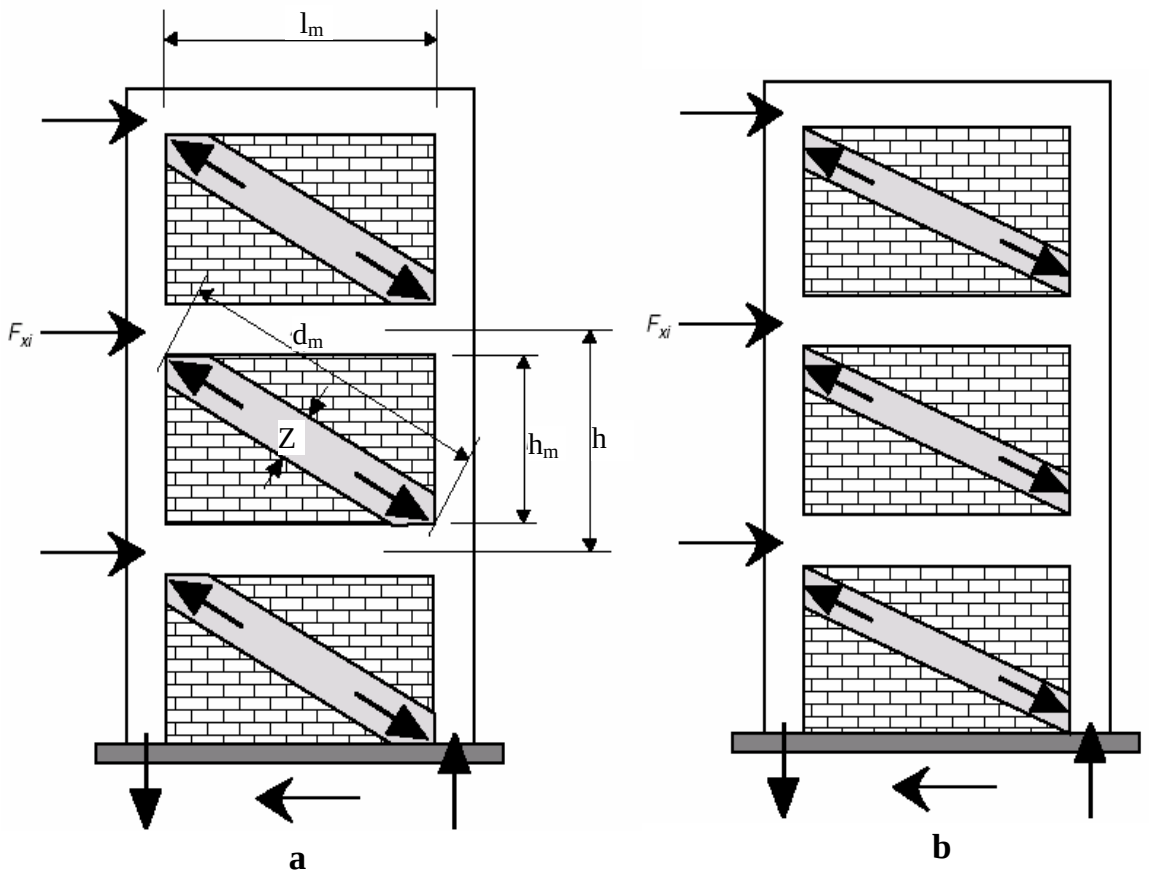

Fig. 4.2.4.1 Compression Strut Analogy (a) Concentric Struts (b) Eccentric Struts.

The following wall cracks are evidences of formation of diagonal struts:

Fig. 4.2.4.2 Damaged CB wall and column.
(Atico Earthquake - Peru 2001)

Fig. 4.2.4.3 Shear failures extending from the infills right across the column. (Bingol Earthquake - Turkey 2001)

Fig. 4.2.4.4 Full-scale wall test. (Research in Peru 2002)

The lateral force-deformation relationship for the structural masonry infill is assumed to be a smooth curve bounded be a bilinear strength envelope with an initial elastic stiffness until the yield force V_y and there on a post yield degraded stiffness until the maximum force V_m is reached after which the post-peak residual shear force V_p will ensue (Fig. 4.2.4.5).

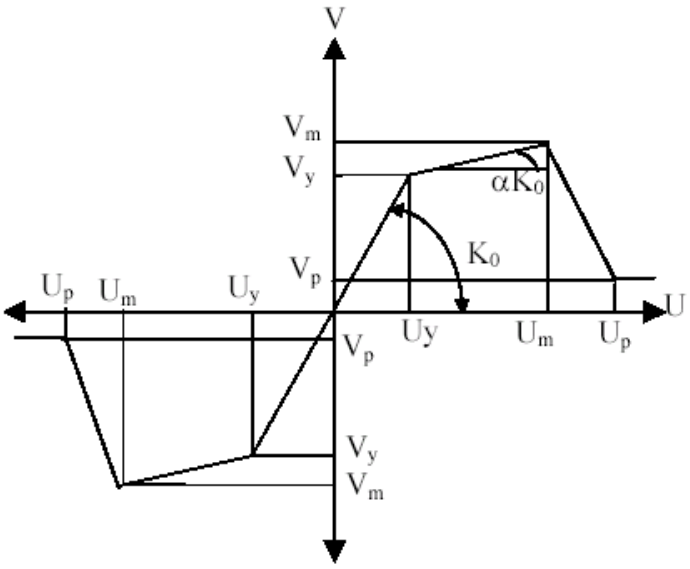

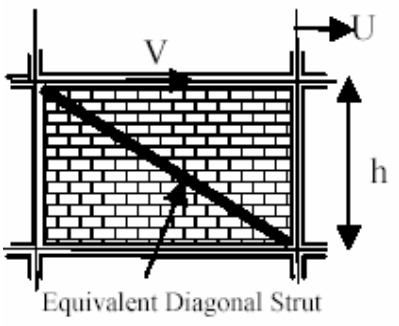

(Mostafaei et al, 2003)

Fig. 4.2.4.5 Strength Envelope for Masonry Infill Panel.

Where: V_m, U_m - Maximum shear force and corresponding displacement respectively.

V_y, U_y - Shear force at yielding and corresponding displacement respectively.

V_p, U_p - Post-peak residual shear force and corresponding displacement respectively.

K_0 - Initial Stiffness of the infill panel.

α - The ratio of the post-yield stiffness to the pre-yield stiffness.

Maximum lateral strength, V_m , should be estimated considering the two critical failure modes, sliding shear and compression failures. The maximum displacement at the maximum lateral force is:

$$U_m = \frac{\varepsilon_m^{'} d_m}{\cos\theta} \quad ; \quad \varepsilon_m^{'} = \frac{f_m^{'}/\cos\theta}{E_m}$$

Where: U_m - Maximum displacement at the maximum lateral force.

$\varepsilon_m^{'}$ - Masonry compression strain at the maximum compression stress.

Hence the initial stiffness of the infill panel is given by:

$$K_0 = 2\left(\frac{V_m}{U_m}\right)$$ (Madan et al, 1997)

Where: K_0 - Initial stiffness of the masonry infill panel.

From the geometry of figure 4.2.4.5, $V_y = \frac{V_m - U_m \alpha K_0}{1-\alpha}$ *and* $U_y = \frac{V_y}{K_0}$

4.2.5 Energy Dissipation Model for Hysteretic Damping

In addition to the viscoelastic behavior of materials, their hysteretic behavior is also a factor that leads to damping. It is most significant, especially, for high values of deformation such as those resulting from earthquake.

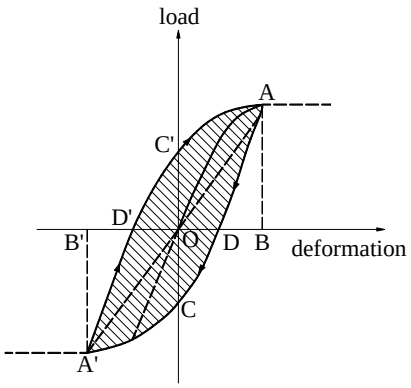

Fig. 4.2.5.1 Typical Hysteretic Loop.

The area of the shaded loop represents the energy that is dissipated in every loading cycle in the form of heat, due to the plastic behavior of the material (Penelis and Kappos, 1997).

Modified Bouc-Wen model (Bouc, 1967 ; Wen, 1981) for hysteretic behavior has been adopted. The modification includes stiffness degradation, strength deterioration, and pinching. A smooth hysteretic force displacement relationship between force ***V*** and displacement ***u*** is furnished by the model. The program **ASSDMI** attached in appendix A has been developed based on modified Bouc-Wen model.

$$V_i = V_y\left[\alpha\mu_i + (1-\alpha)Z_i\right] \quad ; \quad \mu_i = \frac{u_i}{u_y} \qquad \text{---------- (4.2.5.1)}$$

Where: *i* and *y* are instantaneous and yield values respectively.

μ_i - ductility.

u_i - instantaneous inter-story drift.

u_y - inter-story drift at yielding.

α - the ratio of the post-yield stiffness to the pre-yield stiffness.

Z_i - hysteretic component determined from the differential equation.

$$dZ_i = \left\{A - |Z_i|^n \left[\beta \,\mathrm{sgn}(d\mu_i Z_i) + \gamma\right]\right\} d\mu_i \qquad \text{---------- (4.2.5.2)}$$

Where: A, β, and γ are constants that control the shape of the generated hysteretic loops.

The parameter η_i is directly incorporated for the hysteretic parameter Z in order to control the *stiffness decay* in the model.

$$dZ_i = \left\{A - |Z_i|^n \left[\beta \,\mathrm{sgn}(d\mu_i Z_i) + \gamma\right]\right\} (d\mu_i / \eta_i) \qquad \text{---------- (4.2.5.3)}$$

$$\eta_i = \left[s_k + \alpha(\mu_i - 1) + 1\right] / \left[s_k + \mu_i\right] \quad for\ \mu_i > 1.0 \qquad \text{---------- (4.2.5.4)}$$

Where: η_i - Parameter controlling the stiffness decay.

s_k - V_y multiplier to define the pivot for stiffness deterioration branches.

The *strength deterioration* is modeled by reducing the yield force V_y from the original value V_y^0 at each step k as follows,

$$V_y^k = V_y^0 (1 - DI) \qquad \text{---------- (4.2.5.5)}$$

where DI is the cumulative damage parameter given as,

$$DI = \frac{\mu_{\max} - 1}{\mu_c - 1}\left[1 - 0.25 s_{p1} \int \left(\frac{V}{V_y}\right) \frac{d\mu}{(\mu_c - 1)}\right]^{-s_{p2}} \qquad \text{---------- (4.2.5.6)}$$

In which, μ_{max} - maximum attained ductility.

μ_c - monotonic ductility capacity.

s_{p1} and s_{p2} - parameters controlling the rate of deterioration.

The concept of slip-lock element (Baber and Noori, 1984) is incorporated in series in order to account for *pinching* of hysteresis loops due to opening and closing of masonry cracks. Therefore, the following equation is a modification of displacement ductility capacity.

$$\mu = \mu_1 + \mu_2 \qquad \text{---------- (4.2.5.7)}$$

in which μ_1 is for the smooth degrading element previously given and μ_2 is for the slip-lock element given by:

$$d\mu_2 = a f(Z_i) dZ \qquad \text{---------- (4.2.5.8)}$$

Where: $a = A_s(\mu_r - 1)$ - constant defined as the slip length.

$$f(Z_i) = \exp\left(-\frac{\left\{Z_i - \bar{Z}\right\}^2}{Z_s^2}\right); \quad -1 \le Z_i,\ \bar{Z} \le 1 \qquad \text{---------- (4.2.5.9)}$$

A_s - control parameter to vary the slip length

μ_r - ductility attained at the load reversal.

$\bar{Z}$ - value of Z_i at which $f(Z_i)$ reaches its maximum.

Z_s - range of Z_i, about $Z_i = \bar{Z}$, in which the slip occurs.

Finally combining equations 4.2.5.3, 4.2.5.7, 4.2.5.8, and 4.2.5.9, Z_i will satisfy the following differential equation (Madan et al, 1997).

$$\frac{dZ_i}{d\mu} = \frac{\left[A - |Z_i|^n \{\beta \operatorname{sgn}(d\mu_i Z_i) + \gamma\}\right]}{\eta_i \left[1 + a \exp\left(-\frac{\{Z - \bar{Z}\}^2}{Z_s^2}\right)\left(A - |Z_i|^n \{\beta \operatorname{sgn}(d\mu_i Z_i) + \gamma\}\right)\right]} \quad \text{---------- (4.2.5.10)}$$

The following sketches indicate the qualitative variation, for a wall subjected to cyclic loading, beginning from the nil effect up to the combined effect of degradations.

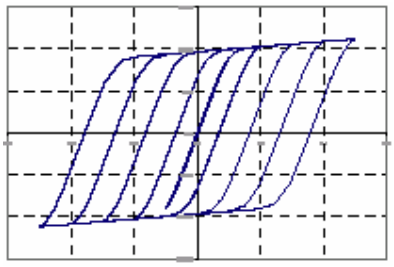

Nonlinear unloading – no degradations

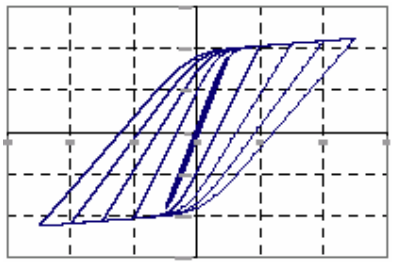

Stiffness degradation

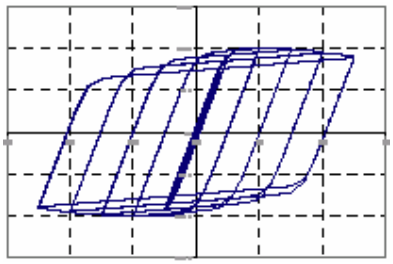

Strength degradation

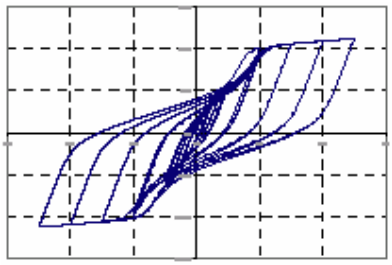

Slip (Pinching)

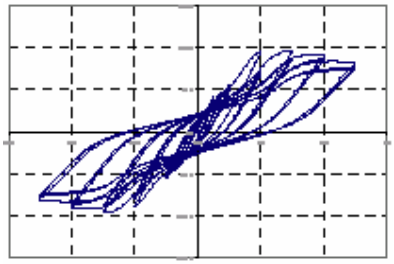

Combined degradations

(Manual of IDARC-2D 6.0, 2004)

Fig. 4.2.5.2 Qualitative view of effects of degradations on hysteretic Behavior (smooth model)

4.2.6 Assessment of Nonlinear Response of Masonry Infill Panel in MDOF System

The dynamic inelastic time-history analysis involves stepwise solution in the time domain of the multi-degree-of freedom equations of motion representing a multistory building response. It requires one or more design accelerograms representing the design earthquakes. These are normally generated as artificial earthquakes analytically or by "massaging" recorded accelerograms to provide the requisite elastic spectral response. For this particular research the software SYNTH was used in order to generate artificial earthquake record from the elastic design spectrum curve of EBCS-8.

The time-stepping method based on interpolation of excitation has been used. Direct step-by-step integration for small successive time steps is performed for the dynamic analysis of MDOF inelastic systems (Chopra, 1995). The end conditions of one step are initial conditions for the next step. The method considers the response of the inelastic system within every integration interval as linear. The slope of the local tangent to the load deflection curve is equal to the value of the stiffness during the iteration interval. While yielding occurs in some members and the stiffness of the structure changes, the response of the nonlinear system is considered to be the response of successive linear systems, with different stiffnesses.

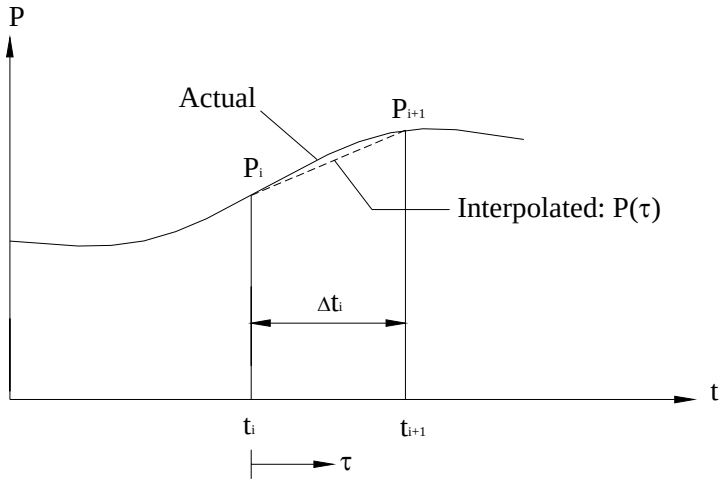

Fig. 4.2.6.1 Notation for linearly interpolated excitation.

The response $U(\tau)$ over the time interval $0 \le \tau \le \Delta t_i$ is the sum of the three parts: (1) free vibration due to initial displacement U_i and velocity $\dot{U}_i$ at $\tau = 0$, (2) response to step force

P_i with zero initial conditions, and (3) response to ramp force $(\Delta P_i/\Delta t_i)\tau$ with zero initial conditions. Combining the solution for these three cases at each successive time interval, $\tau = \Delta t_i$, gives the recurrence formula for displacement U_{i+1} at time i+1.

For MDOF system the modal coordinate q is used in the recurrence formula and U is obtained as the sum of the contributions of the various modes.

MDOF: $$q_{i+1} = Aq_i + B\dot{q}_i + CP_i + DP_{i+1} \quad \text{---------- (4.2.6.1a)}$$

$$\dot{q}_{i+1} = A'q_i + B'\dot{q}_i + C'P_i + D'P_{i+1} \quad \text{---------- (4.2.6.1b)}$$

$$U_i(t) = \sum_{j=1}^{n} \phi_{ji} q_{ji}(t) \quad \text{---------- (4.2.6.2)}$$

Where: j – counts the number of modes involved.

i – an index to count the time steps in the history of loading

For the modes normalized with respect to mass.

$$K_n = \phi_n^T [k] \phi_n = \omega_n^2 M_n = \omega_n^2 \quad \text{---------- (4.2.6.3)}$$

Throughout the analysis viscous damping, $\xi = 5\%$.

$$\omega_D = \omega_n \sqrt{1-\xi^2} \quad \text{---------- (4.2.6.4)}$$

Where: ω_n - The natural circular frequency of a system.

ω_D - The natural circular frequency of a damped vibration of a system.

Coefficients in the recurrence formulas of MDOF.

$$A = e^{-\xi \varpi_n \Delta t}\left(\frac{\xi}{\sqrt{1-\xi^2}}\sin\omega_D\Delta t + \cos\omega_D\Delta t\right)$$

$$B = e^{-\xi \varpi_n \Delta t}\left(\frac{1}{\omega_D}\sin\omega_D\Delta t\right)$$

$$C = \frac{1}{\omega_n^2}\left\{\frac{2\xi}{\omega_n\Delta t} + e^{-\xi\omega_n\Delta t}\left[\left(\frac{1-2\xi^2}{\omega_D\Delta t} - \frac{\xi}{\sqrt{1-\xi^2}}\right)\sin\omega_D\Delta t - \left(1+\frac{2\xi}{\omega_n\Delta t}\right)\cos\omega_D\Delta t\right]\right\}$$

$$D = \frac{1}{\omega_n^2}\left[1 - \frac{2\xi}{\omega_n\Delta t} + e^{-\xi\omega_n\Delta t}\left(\frac{1-2\xi^2}{\omega_D\Delta t}\sin\omega_D\Delta t + \frac{2\xi}{\omega_n\Delta t}\cos\omega_D\Delta t\right)\right]$$

$$A' = -e^{-\xi \varpi_n \Delta t}\left(\frac{\omega_n}{\sqrt{1-\xi^2}}\sin\omega_D\Delta t\right)$$

$$B' = e^{-\xi\varpi_n\Delta t}\left(\cos\omega_D\Delta t - \frac{\xi}{\sqrt{1-\xi^2}}\sin\omega_D\Delta t\right)$$

$$C' = \frac{1}{\omega_n^2}\left\{-\frac{1}{\Delta t} + e^{-\xi\omega_n\Delta t}\left[\left(\frac{\omega_n}{\sqrt{1-\xi^2}} + \frac{\xi}{\Delta t\sqrt{1-\xi^2}}\right)\sin\omega_D\Delta t + \frac{1}{\Delta t}\cos\omega_D\Delta t\right]\right\}$$

$$D' = \frac{1}{\omega_n^2\Delta t}\left[1 - e^{-\xi\omega_n\Delta t}\left(\frac{\xi}{\sqrt{1-\xi^2}}\sin\omega_D\Delta t + \cos\omega_D\Delta t\right)\right]$$

The constant time step, Δt = 0.01sec and therefore the above coefficients will vary with the variation of ω_n because of the nonlinearity of stiffness in the masonry panel.

5 ANALYSIS FOR THE EVALUATION OF INTERACTION BETWEEN MASONRY INFILLS AND FRAMES

5.1 The Synthetic Record of Earthquake as an Exciting Acceleration

For the *non-linear dynamic procedure* the response calculations are carried out using *time history analysis*. Hence the design displacements are not established using a target displacement, but instead are determined directly through dynamic analysis using ground motion time histories. Earthquake shaking shall be characterized by discretized records or synthetic earthquake records as base motion.

For the particular use in this research the synthetic earth quake time history has been generated from the elastic design spectrum curve for soil class A of EBCS-8 using the software SYNTH. The generated synthetic record is obtained as the sum of sine waves with random phase angles (uniformly distributed between zero and 2π) and iteratively adjusted to fit the target spectrum (Meskouris, K., 2000). It has been scaled down by 0.3g in order to meet the requirement of moderate seismic force that may occur in our country.

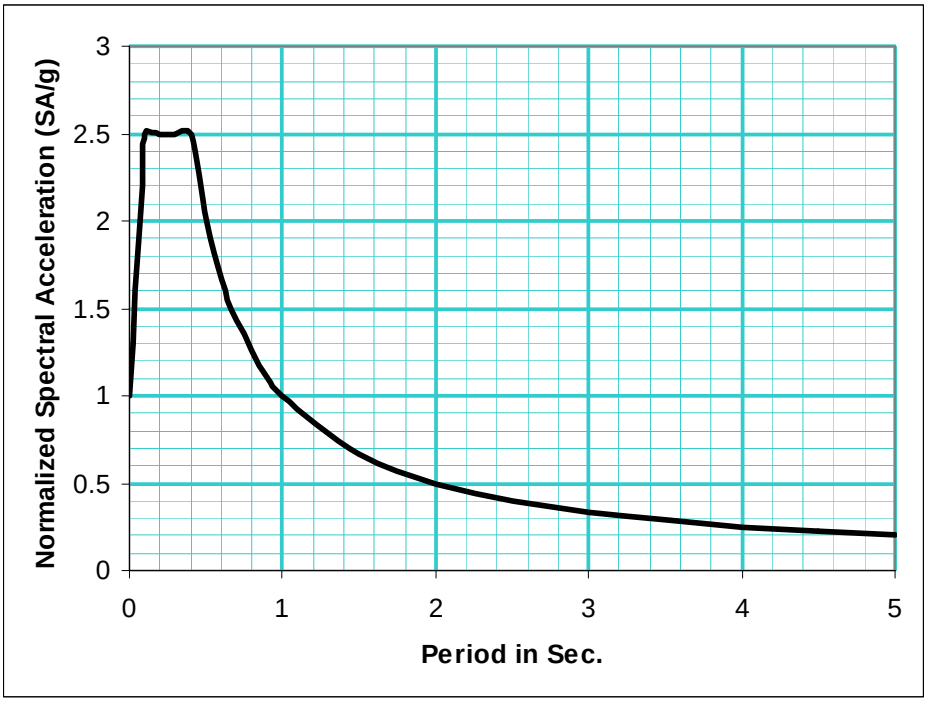

Fig. 5.1.1 Normalized elastic design spectrum of EBCS-8

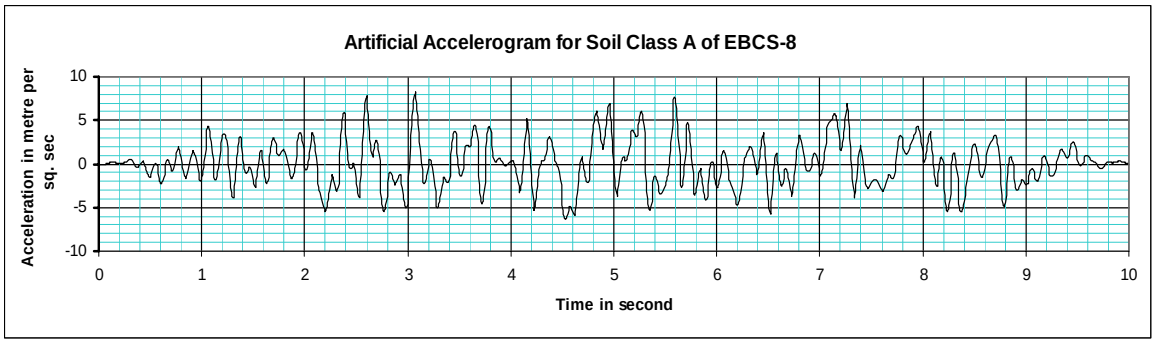

Fig. 5.1.2 Synthetic record of earthquake derived from elastic design spectrum curve of EBCS-8.

The above synthetic record has been verified by carrying out time history analysis using SAP2000 (Fig. 5.1.3) so as to get back the design spectrum curve of EBCS-8 (Fig. 5.1.1).

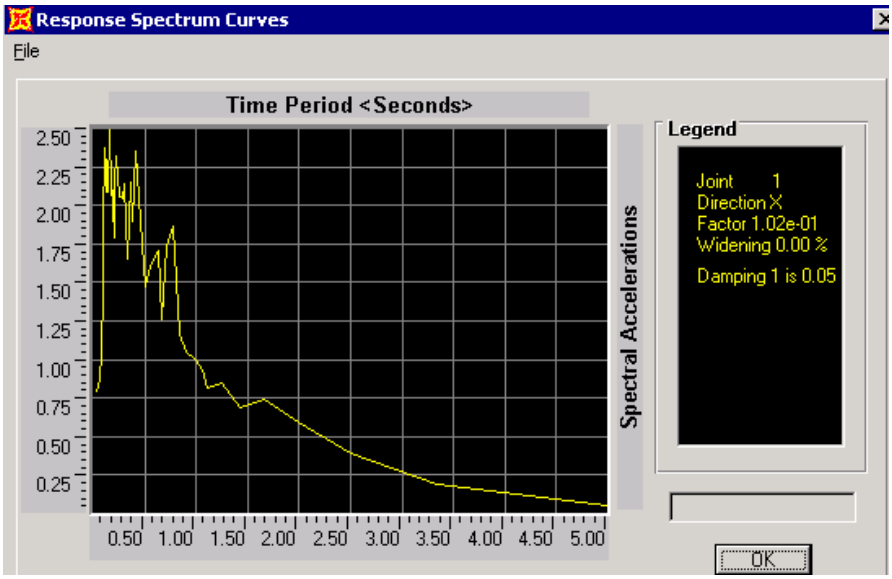

Fig. 5.1.3 Elastic design spectrum curve of EBCS-8 - verified using SAP2000

5.2 Determination of Masses at the Story Levels

Since the masses are lumped at the floor level all the vertical elements, the columns and walls, at each story level will have half of their heights tributary to their respective floors. Similarly, the horizontal elements, out-of-plane beams and diaphragms, contribution to the mass will be half of their length in the lateral direction of both sides together with the additional entire length of the in-plane beam. The example that follows clearly shows the determination of lumped mass at a floor level for FRAME-3 (ref. section 5.3)

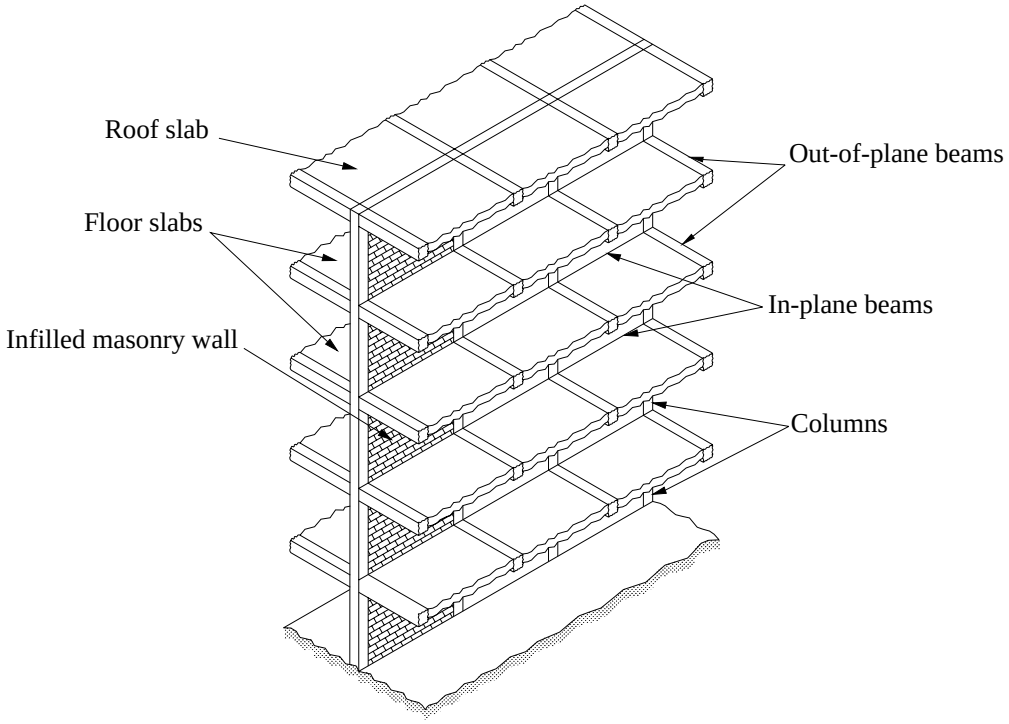

Fig. E5.2.1 3-D view of FRAME-3 with elements tributary to a floor mass

Example 3.7.1 The mass lumped at the floor level of FRAME-3 is determined from different components in the following manner, aspect ration for the infilled bay is 2.0:

Columns tributary to a floor (Fig. E5.2.2):

Tributary length = 3m,

Cross section = 40 X 40 cm

Number of columns = 4

Unit wt. of concrete = 25 KN/m^3

Mass = 4 * 0.4 * 0.4 * 3.0 * 25/9.81 = 4.89 ton

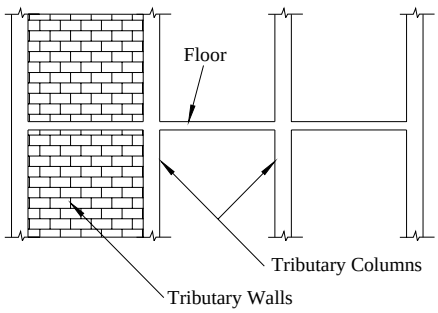

Fig. E5.2.2 Tributary columns and walls

Wall tributary to the floor (Fig. E5.2.2):

Aspect ratio = 2.0, Hence length = 2.0 * 3.0 = 6.0

Tributary height = 3m,

Thickness = 12 cm

Number of walls = 1

Unit wt. of brick masonry = 22 KN/m^3

Mass = 1 * 0.12 * 22 * (3.0 – 0.4) * (6.0 – 0.4)/9.81 = 3.92 ton

Beams and floors tributary to the floor (Fig. E5.2.3)

Out-of-plane length of beam = 5.0m

In-plane length of beam = 6.0m

No. of out-of-plane beams = 4

No. of in-plane beams = 3

Beam cross section = 30 X 40 cm

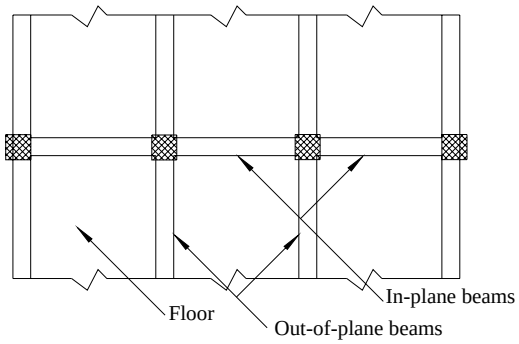

Fig. E5.2.3 Tributary beams and floors.

Slab thickness = 18 cm

Beam mass = 25*0.3*0.4*((5.0–0.4)*4 + 1*(6.0 – 0.4) + (4 – (1+1))*(6–0.4))/9.81=10.76 ton

Floor mass = 25*0.18*(5-0.3)*(1*(6-0.3) + (6-0.3)*(4-(1+1)))/9.81 = 36.87 ton

The above calculation is in harmony with the shaded result of Table C-1 in Appendix C.

5.3 Determination of Stiffnesses

Since basically the frame is assumed to be shear frame with the horizontal rigid element (slab + beam) only the vertical elements (columns) are emphasized. Rigidity of beams makes it easy to calculate the stiffness of the story as direct sum of the stiffnesses of the columns.

Unless the span of adjacent beams is very different, the earthquake-induced axial forces will normally affect only the outer columns in a frame. Moreover the frame elements are assumed to respond elastically throughout the time history of the earthquake. Hence the following average moments of inertia are adopted for the exterior and interior columns (Table 4.1.1).

$$I_{ex} = 0.6I_g \quad \text{and} \quad I_{in} = 0.8I_g \quad \text{(Paulay and Priestley, 1992)}$$

Stiffness contribution of columns at a story level,

$$K_f = \frac{12E_f \sum I_{col}}{h^3}$$

and the initial stiffness , K_0, of the masonry infill is:

$$K_0 = 2\left(\frac{V_m}{U_m}\right)$$

Hence the total stiffness, K, at the floor level,

$$K = K_f + K_0$$

Where: K_f - The sum of the stiffness of columns in a story.

$\sum I_{col}$ - The sum of moments of inertia of exterior and interior columns at a story.

V_m - Maximum shear force.

U_m - Maximum displacement.

Throughout the analysis in this work cross sectional area and height of the columns are 40 X 40 cm and 300 cm respectively.

***Example 5.3.1*:** Determination of equivalent strut width and shear forces at sliding shear and compression failures for the panel aspect ratio (L/H) of 2.0.

E_f = 24000 MPa ; E_m = 3300 MPa ; $f_m^{'} = 4.37\,MPa$ (Paulay and Priestlley, 1992)

Column size = 40 X 40 cm.
Beam size = 30 X 40 cm
h = 300cm
} → constants adopted throughout the analysis

Panel size = 600 X 300 cm.

With reference to fig. 4.2.1.1:

h_m = 300 – 40 = 260 cm

l_m = 600 – 40 = 560 cm

t_m = 12 cm

Equivalent strut width:

$$I_{col} = I_g = \frac{40^4}{12} = 213333.33\,cm^4$$

$$d_m = \sqrt{h_m^2 + l_m^2} = 621.69\,cm$$

$$\theta = \arctan\left(h_m / l_m\right) = 24.90^0$$

$$\lambda_I = \left[\frac{E_m t_m \sin 2\theta}{4E_f I_{col} h_m}\right]^{\frac{1}{4}} = 0.00868\,cm^{-1}$$

$$Z = 0.175\left(\lambda_I h\right)^{-0.4} d_m = 74.19\,cm$$

Shear force at sliding shear failure:

$$\tau_0 = 0.04 f_m^{'} = 0.175$$

$$\therefore \; V_f = \frac{\tau_0 t_m l_m}{1-\mu \tan\theta} = \frac{0.175*120*5600}{1-0.5*\tan\left(24.90^0\right)}*10^{-3} = 153.14\,KN$$

Shear force at compression failure:

$$V_c = Z t_m f_m^{'} \cos\theta = 741.9*120*4.37*\cos\left(24.9^0\right)*10^{-3} = 352.89\,KN$$

Example 5.3.2: Determination of initial shear force and displacement at yielding.

From the previous example,

$f_m^{'} = 4.37\,MPa$; $E_m = 3300\,MPa$; $\theta = 24.90^0$; $d_m = 621.69\,cm$

V_m is the minimum of V_f and V_c, $V_m = 153.14\,KN$.

$\alpha = 0.01$ - Default value

$$\varepsilon_m^{'} = \frac{f_m^{'}/\cos\theta}{E_m} = 0.00146 \;\Rightarrow\; U_m = \frac{\varepsilon_m^{'} d_m}{\cos\theta} = 1.00\,cm = 10\,mm$$

$$K_0 = 2\left(\frac{V_m}{U_m}\right) = 30628\,KN/m$$

$$V_y = \frac{V_m - U_m \alpha K_0}{1-\alpha} = 151.59\,KN \;\Rightarrow\; U_y = \frac{V_y}{K_0} = 4.95\,mm$$

The above examples indicate the procedure used to determine the stiffness parameters. It has been summarized in an excel sheet for various bay widths in Table C-2 of Appendix C.

5.3 Degradation Behavior of Masonry Infill Panel

Four types of frames were involved in the analysis. The basic difference between the frames arises from the number of bare bays incorporated in addition to the infilled bay. Always the infilled bay is located at the left end of the frame and additional bare bays will have a constant width of 6m for each. FRAME-1 is a single bay infilled frame and FRAME-2, FRAME-3, FRAME-4 are identified by the one additional more bare bay they have incorporated successively (Fig. 5.3.1 – Fig. 5.3.4). Three important variables deserving attention are the story level, aspect ratio (length/height) and number of bays in the frame.

$$Aspect\ ratio = \frac{L}{H}$$

Where: H – height of a story and a constant height, H = 3.0m is adopted throughout the

analysis.

L – Length of the infilled bay.

L varies from 3.0m to 9.0m but for the sake of showing the charts only L = 4.5m, L = 6.0m and L = 7.5m are included – APPENDIX B.

The figures (Fig. 5.3.5 – Fig. 5.3.6) are clear indications of the stiffness deterioration and strength degradation of the masonry infill wall.

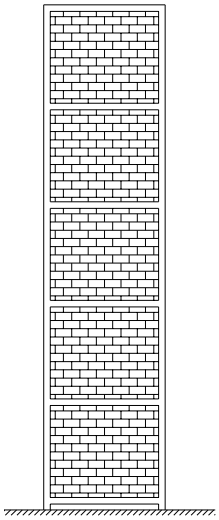

Fig. 5.3.1 FRAME-1 Single bay frame.

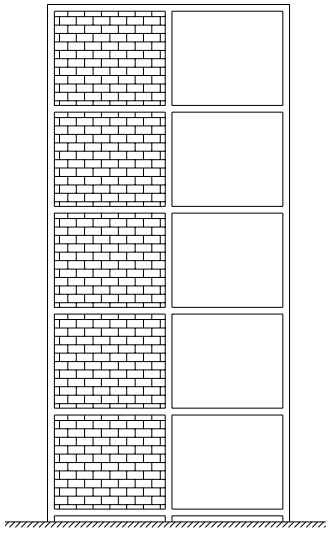

Fig. 5.3.2 FRAME-2 Double bay frame.

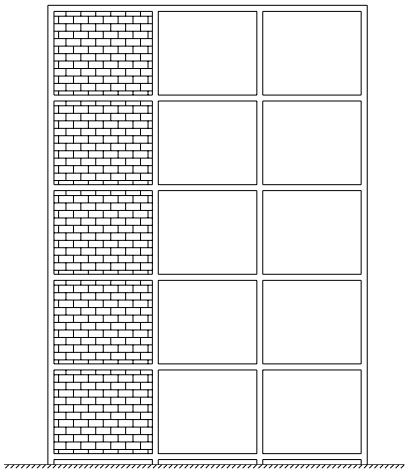

Fig. 5.3.3 FRAME-3 Triple bay frame.

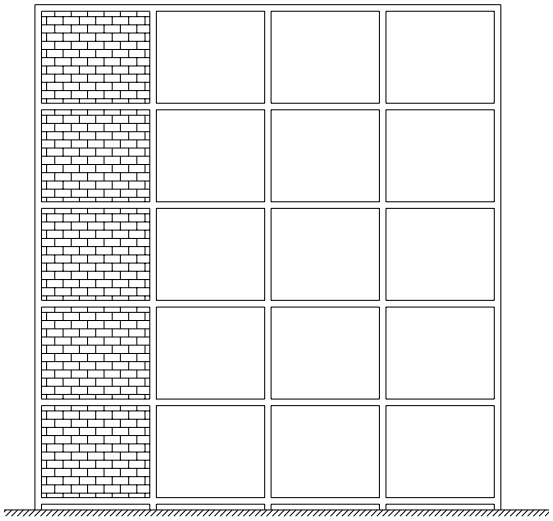

Fig. 5.3.4 FRAME-4 Quadruple bay frame.

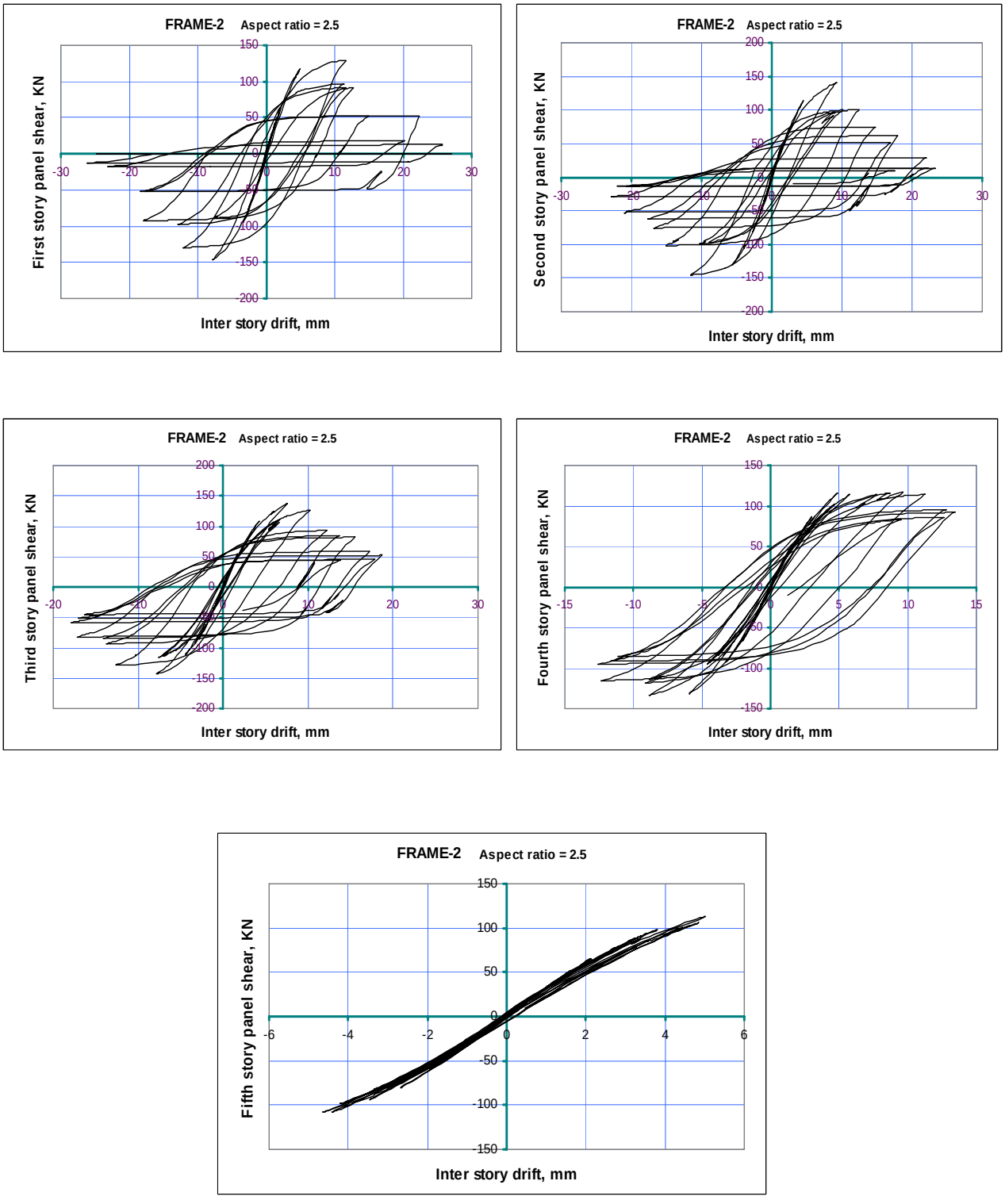

Fig. 5.3.5 Infill shear vs. inter-story drift at different story levels – FRAME-2 with aspect ratio = 2.5

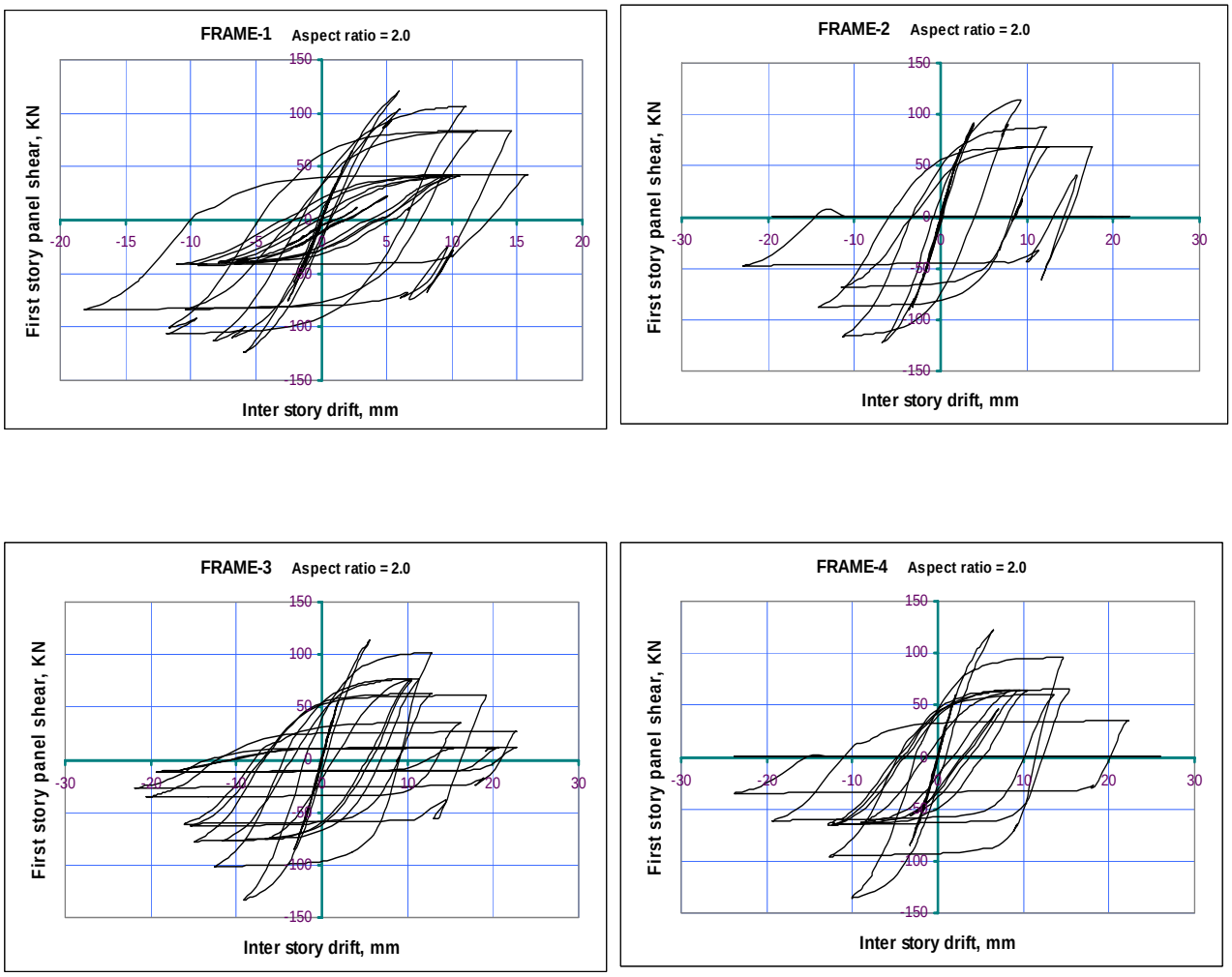

Fig. 5.3.6 Infill shear vs. inter-story drift of different frames at the first story level – Aspect ratio = 2.0

Discussion

The above figures typically represent the force deformation relationship. FRAME-2 with aspect ratio of 2.5 (Fig. 5.3.5) has been included in order to show the nature of stiffness decay and strength degradation at different story levels. Moreover, figure 5.3.6 shows variations in force deformation relationships for the first story of the different frame types. Sets of figures for more information in relation to various aspect ratios in different frames are depicted in appendix B. As it can be seen from the successive decrease in stiffness and strength at each

cycle of load-deformation history, the program has successfully executed the degradations of stiffness and strength. Moreover, the graphs clearly indicate the nonlinearity of force-deformation relationship at the lower stories gradually giving a way to linearity at the upper stories as anticipated. Generally, the higher the aspect ratio the more heavily the masonry infill is degraded, even sometimes followed by the complete loss of stiffness. Similarly, the higher frames received higher degradations because of the increased inertia force imparted to the infilled frame.

The peak value of a hysteretic loop (maximum shear in a loop) will gradually increase from cycle to cycle till the infill panel confronts strength degradation due to large displacement, after which peak values decline. Sometimes infill panels at lower story levels may begin degrading at earlier time history of the load as a consequence of which they can lose strength before attaining the expected peak shear. That is why panels in the upper story levels can have peak shear values higher than those in the lower story levels depending on the nature of degradations. It is also qualitatively observed in the figures that the energy dissipated increases from cycle to cycle of hysteresis unless degradation is so high that it will be minimized towards the collapse of the panel.

5.4 Comparison of Columns Shear in Bare Frame and Infilled Frame

In addition to the frames already used in section 5.3 corresponding bare frames are included in the analysis. Corresponding bare frame meant frames without any infill at all but with the same dimensions of the beams and columns as that of the infilled frame. In the commonly used design practice (bare frame assumption), though the stiffness of infill is not considered the inertia contributed by the infill is incorporated in design. Hence the bare frame analysis has taken into account the mass contribution of the infill wall.

Shear calculation was carried out for the column at left extreme end in all the frame types at each story level. Shear for bare frame column, infilled frame column shear and infilled frame column plus panel shear are all plotted against height of the frame in a single chart for the comparison purpose in the next pages. Aspect ratios (L/H) accounted in each type of frame are 1.0, 1.5, 2.0, 2.5, 3.0 selected based on the conventionally recommended ratio in the range of 1.0 – 3.0 (section 2.3).

Figures 5.4.1 – 5.4.4 show the time history response of the first story column shears of the bare frame, infilled frame and infilled frame plus infill. In bare frame the inertia of the infilled panel is included while its stiffness is omitted in the analysis. The infilled frame column shear accounts the stiffness contribution of the infill panel but doesn't incorporate the interaction of the infill and frame. The infilled frame plus infill column shear accounts the inertia and stiffness contribution of the infill and also the interactions of infill and frame.

The maximum shear of such time history analysis is calculated for each story with different aspect ratios and plotted in figures 5.4.5 – 5.4.9. The summary of the variation of column shear for the first story of the different aspect ratios is presented in figure 5.4.10.

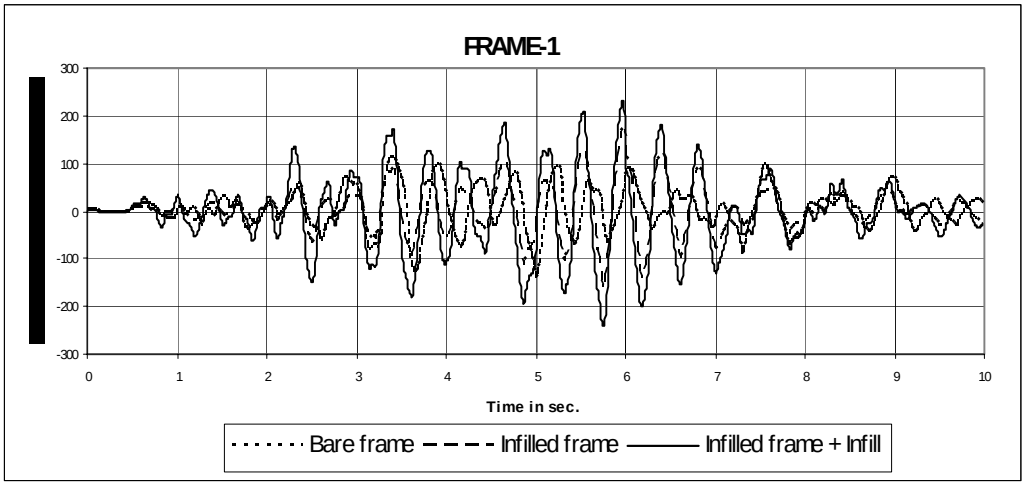

Fig. 5.4.1 Time history of column shears at the left end of FRAME-1 – aspect ratio = 1.0

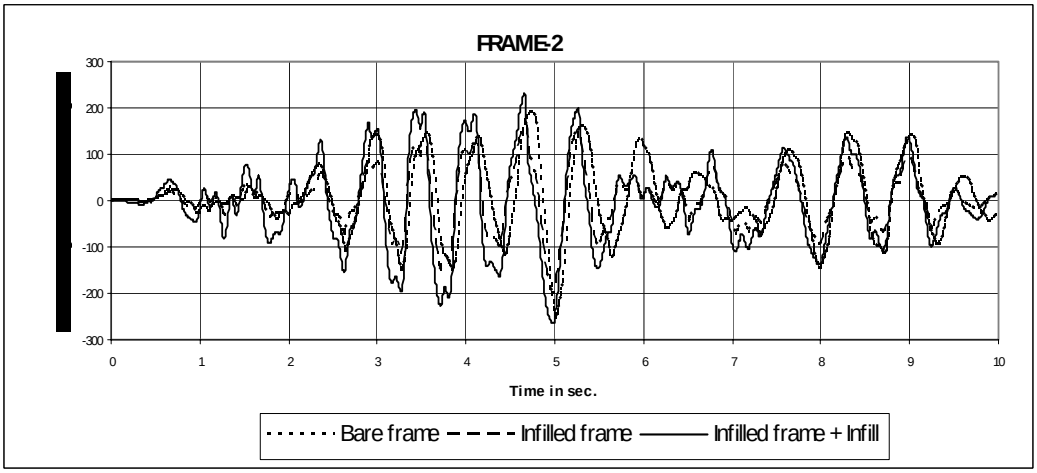

Fig. 5.4.2 Time history of column shears at the left end of FRAME-2 – aspect ratio = 1.0

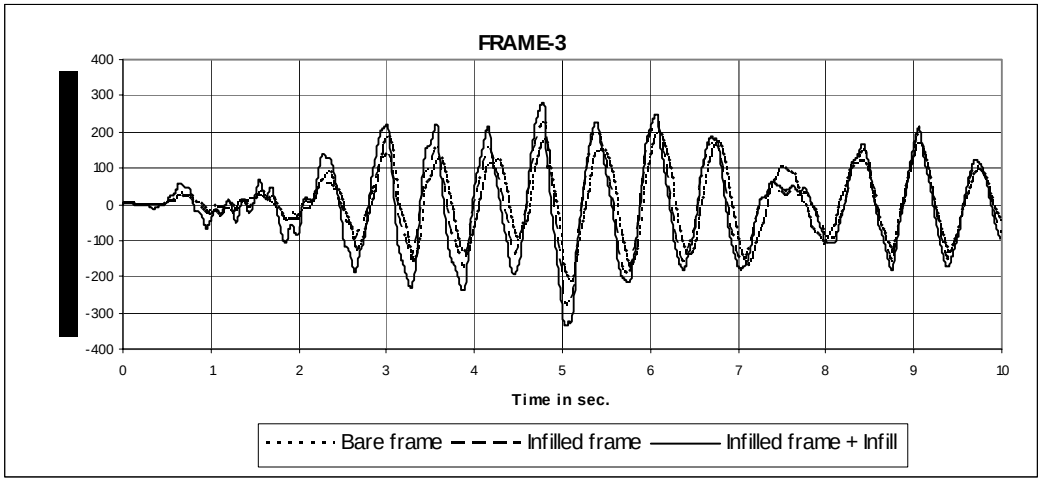

Fig. 5.4.3 Time history of column shears at the left end of FRAME-3 – aspect ratio = 1.0

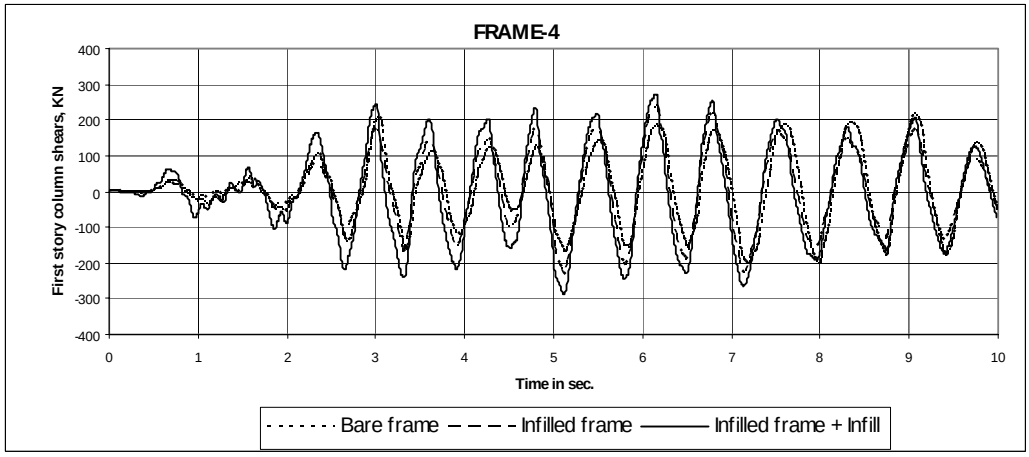

Fig. 5.4.4 Time history of column shears at the left end of FRAME-4 – aspect ratio = 1.0

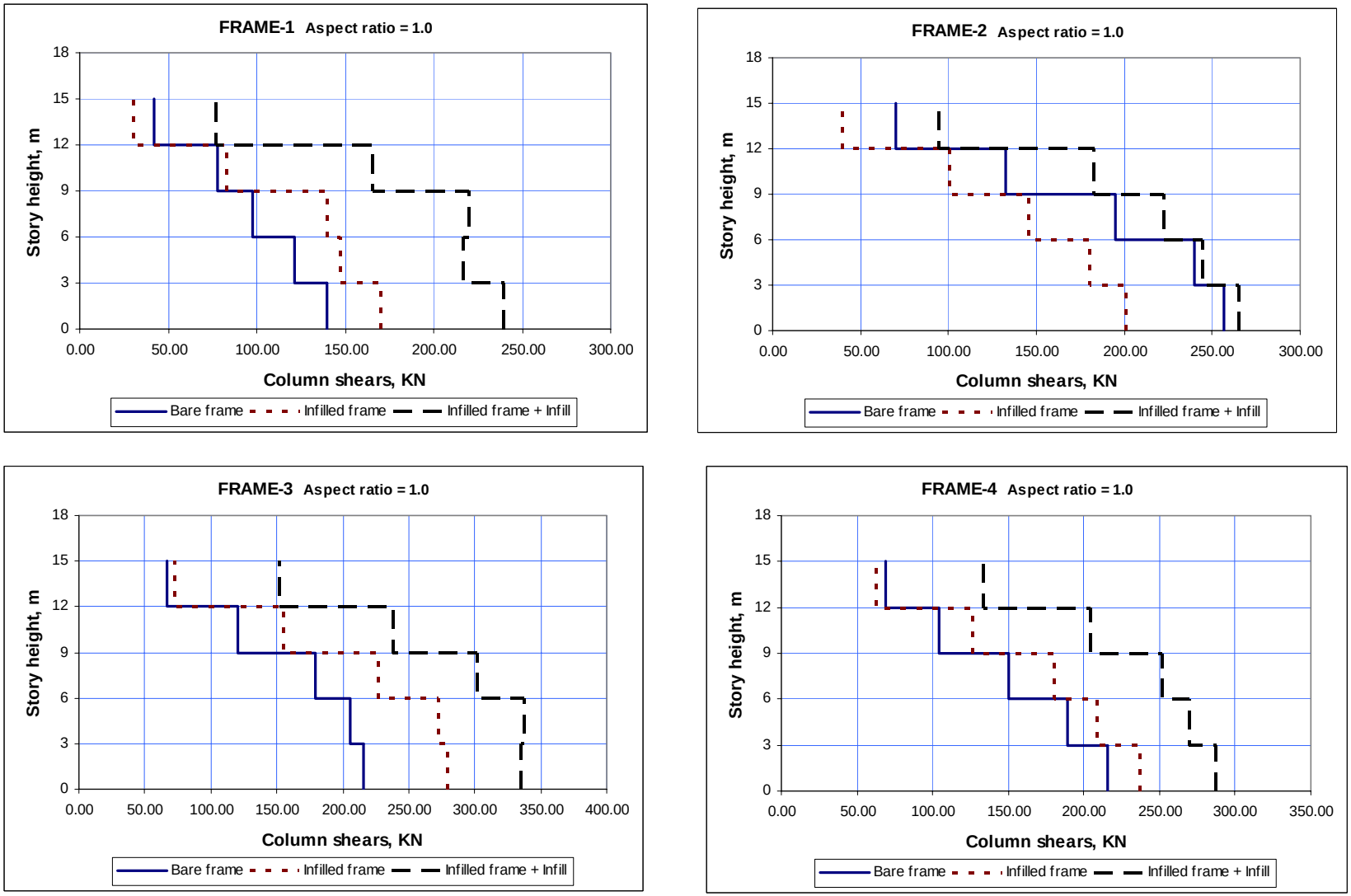

Fig. 5.4.5 Column shears at the left end of frames – aspect ratio = 1.0

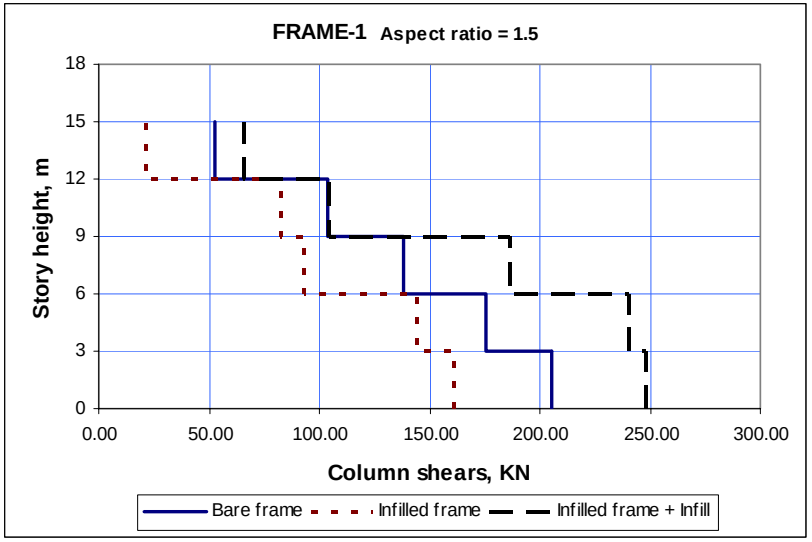

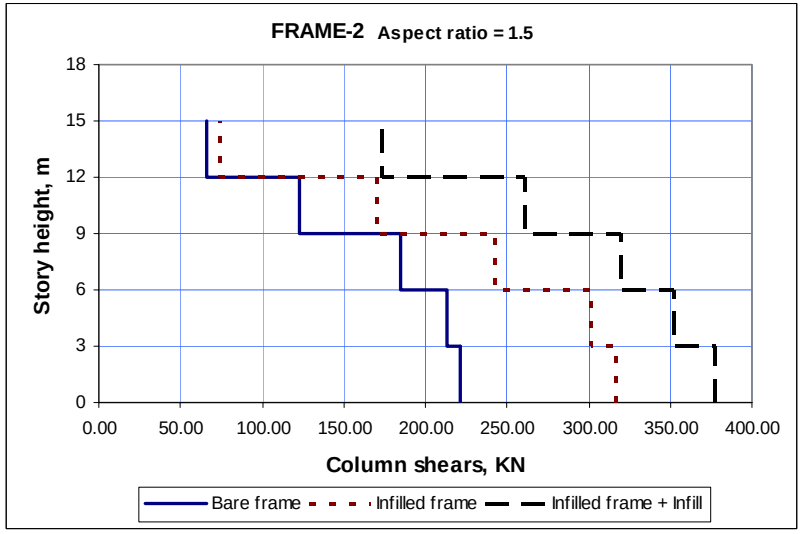

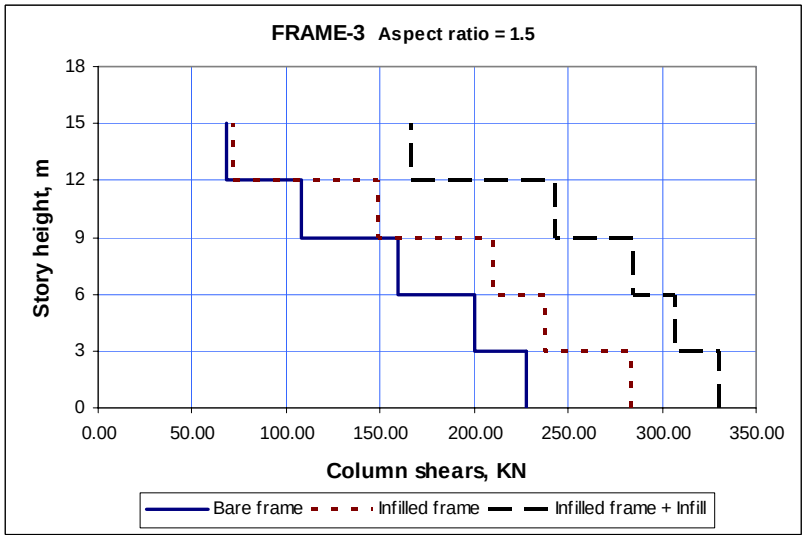

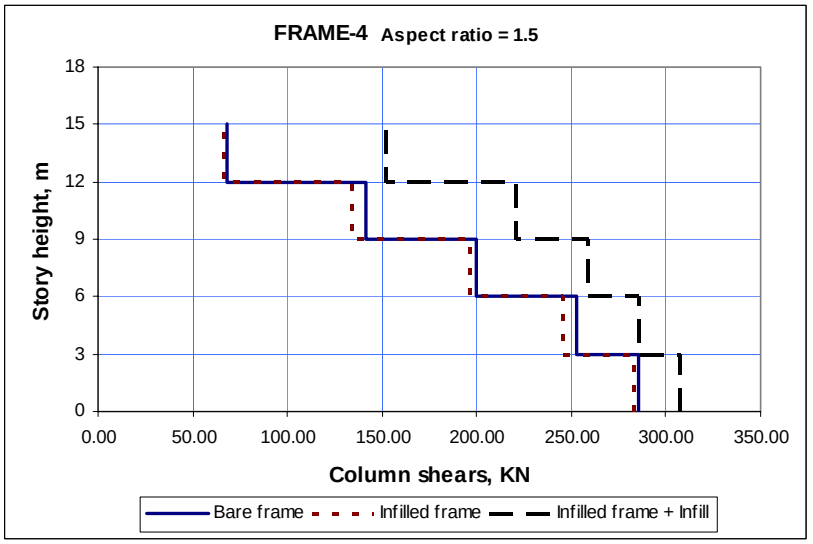

Fig. 5.4.6 Column shears at the left end of frames – aspect ratio = 1.5

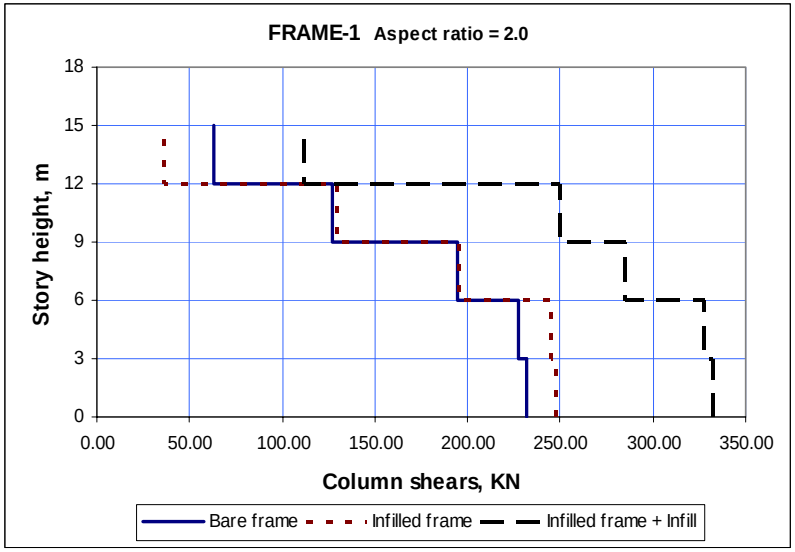

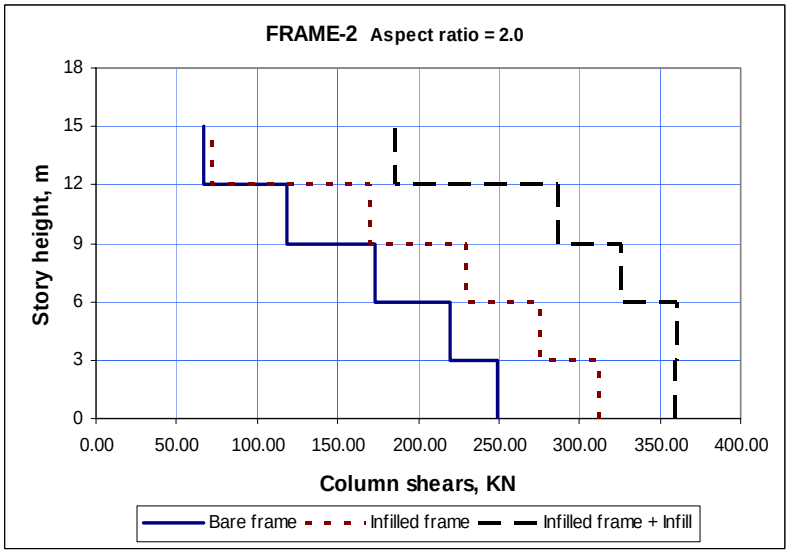

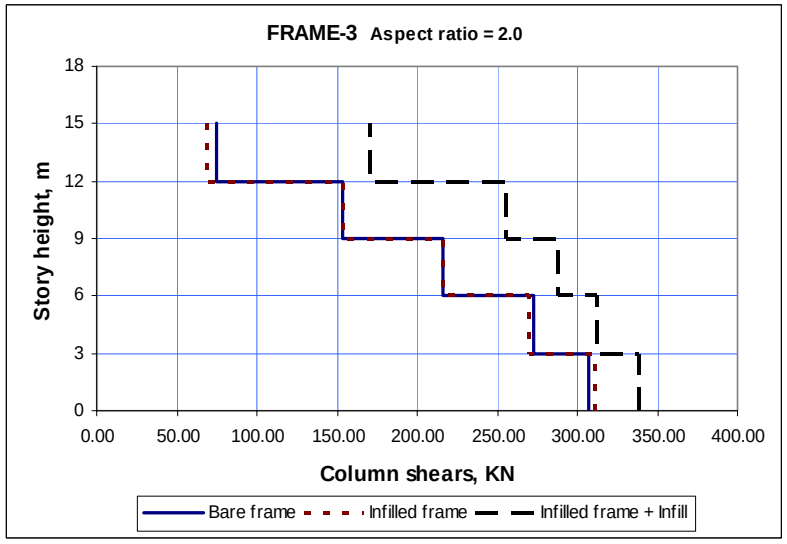

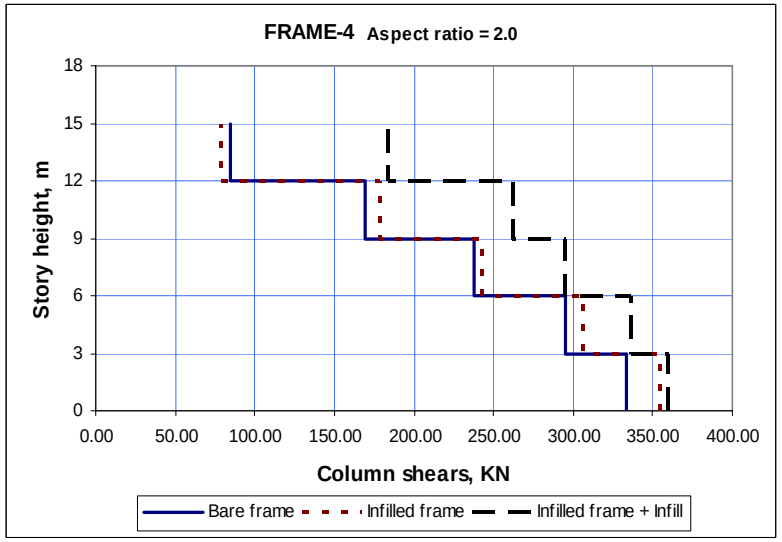

Fig. 5.4.7 Column shears at the left end of frames – aspect ratio = 2.0

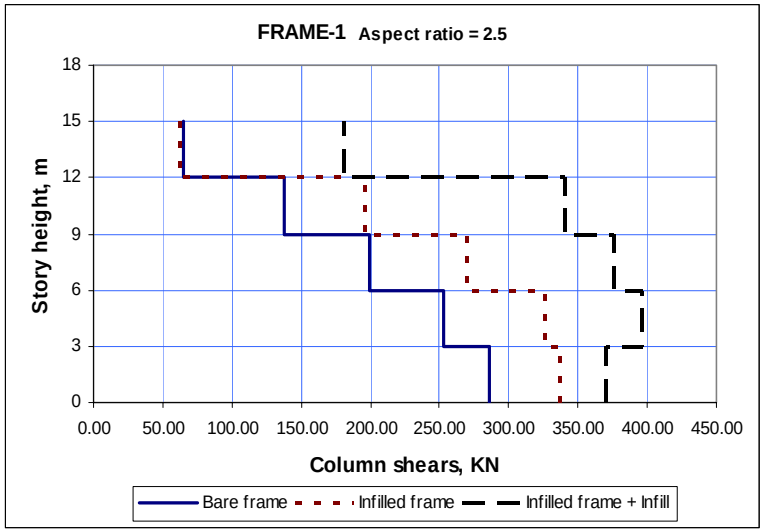

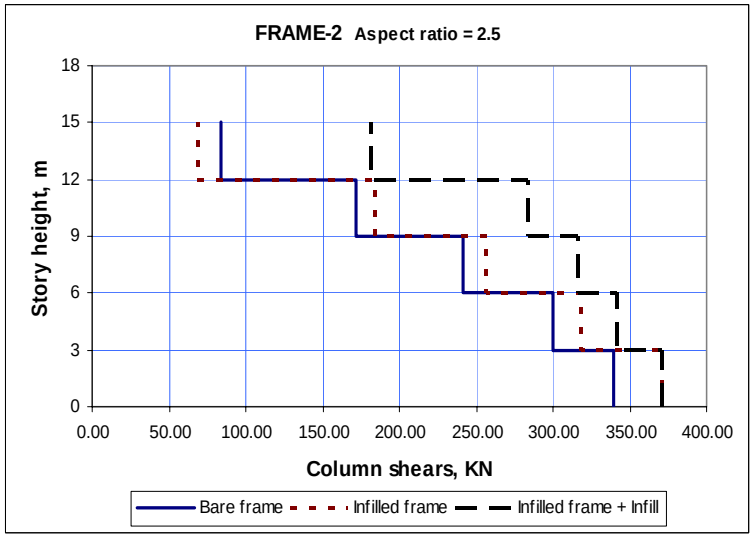

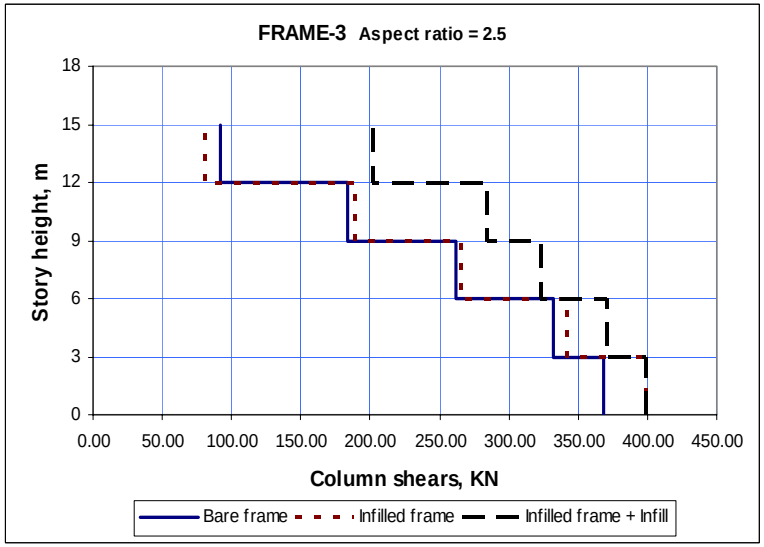

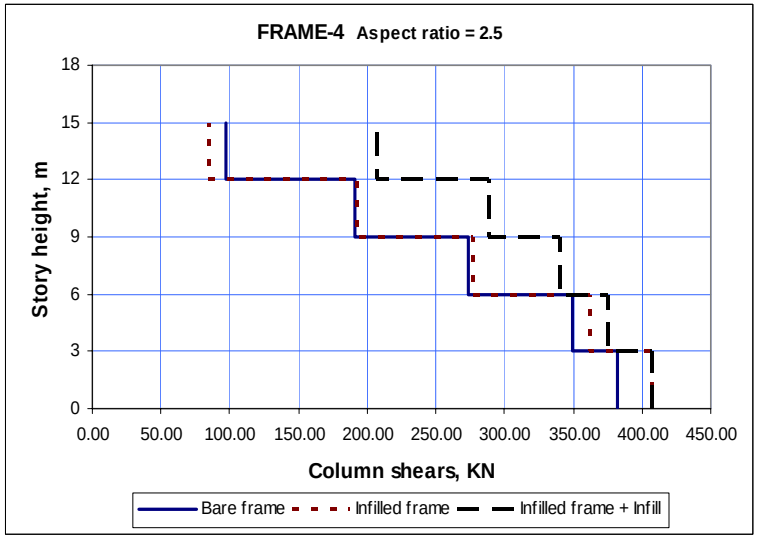

Fig. 5.4.8 Column shears at the left end of frames – aspect ratio = 2.5

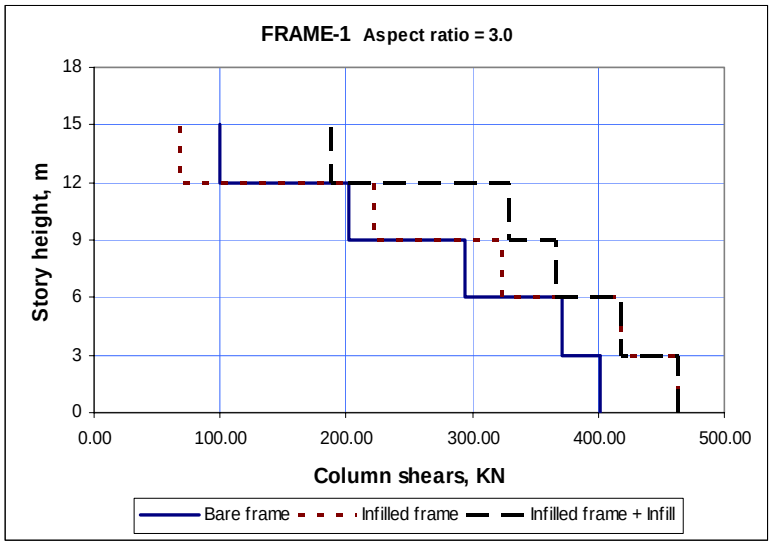

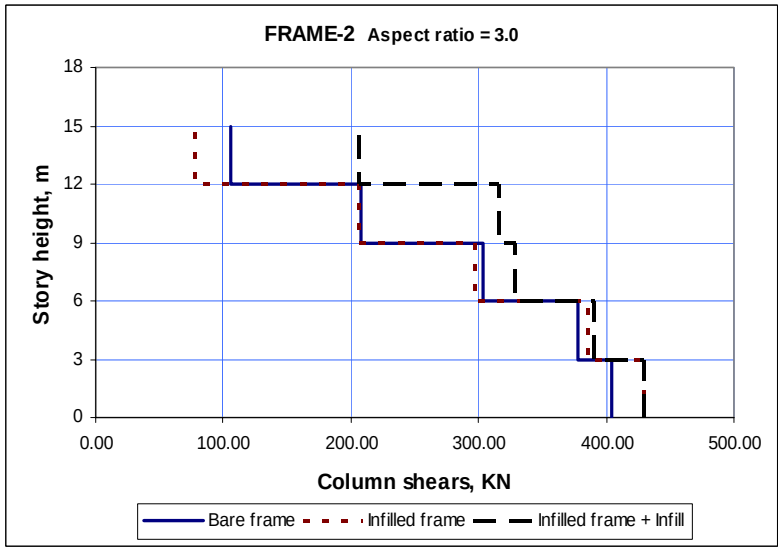

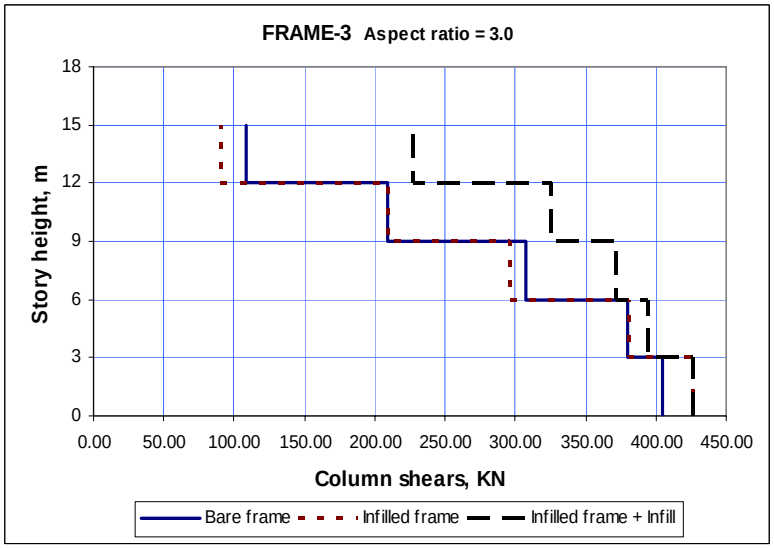

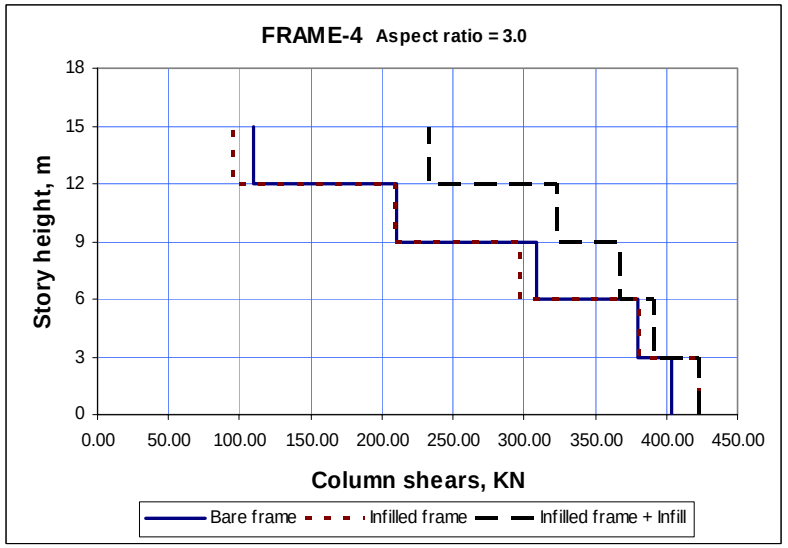

Fig. 5.4.9 Column shears at the left end of frames – aspect ratio = 3.0

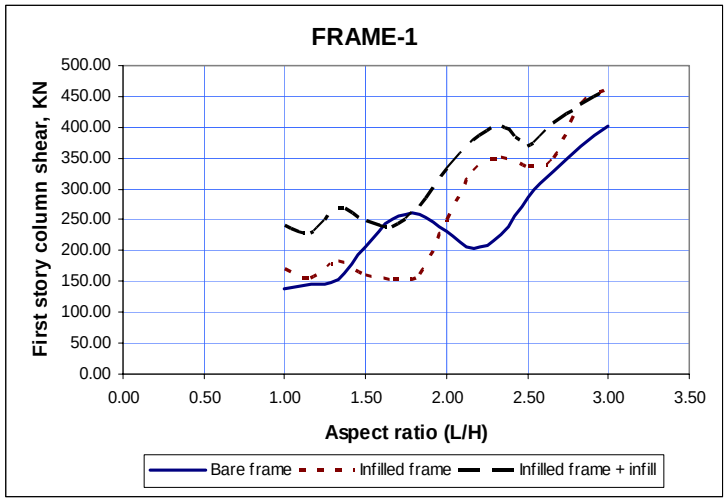

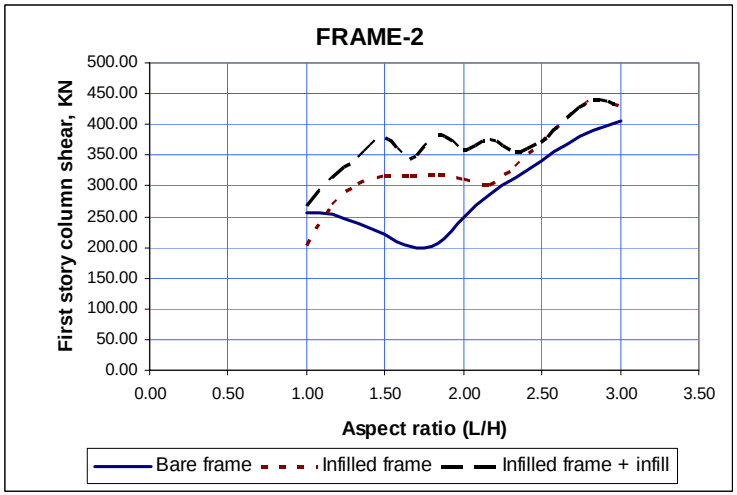

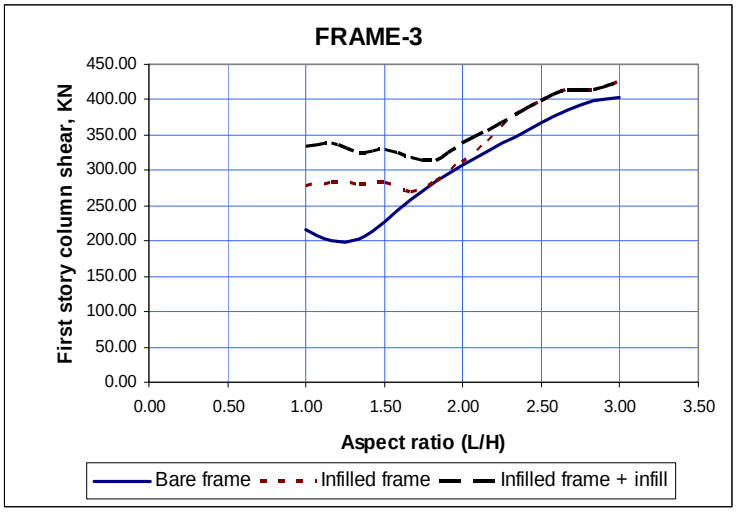

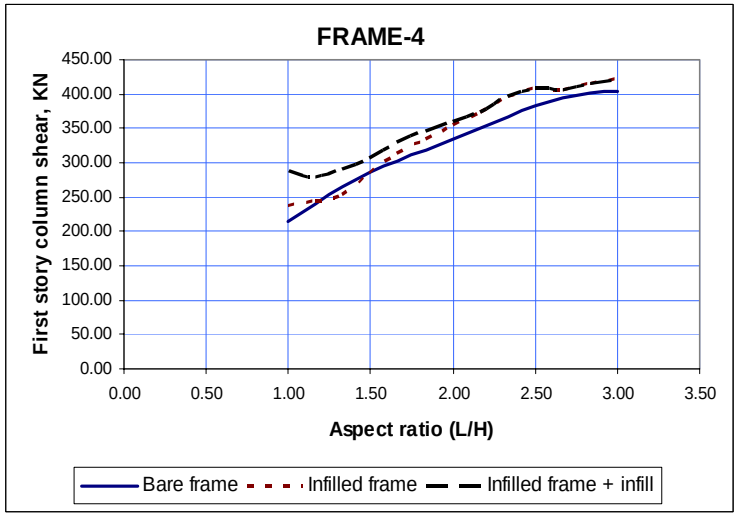

Fig. 5.4.10 First story column shears at the left end of frames vs aspect ratio

Discussion

Highly accurate prediction of the behavior of the infill-frame interaction is beyond the scope of this research work. Simply the time histories of shears in the frame and infill were added with the assumption that equivalent strut is eccentrically placed on the columns (Fig. 4.2.4.1). In each graph peak values of column shear obtained from time history analysis were plotted versus aspect ratio. In the majority of the cases column shear in the bare frame was exceeded by column shear in the infilled frame without the additional shear for the interaction in the panel. A gradual shift of significant difference (25 – 35%) between the shears was observed from higher aspect ratio for FRAME-1 to the lowest aspect ratio for FRAME-4. The observation of such significance shear difference with the bare frame exceeded by the infill frame lie in the following ranges of aspect ratio for the different frames : 2.0 – 2.5 for FRAME-1, 1.5 – 2.0 for FRAME-2, 1.0 – 1.5 for FRAME-3 and less than 1.0 for FRAME-4 (Fig. 5.4.10).

5.5 EBCS-8 and Column Shear

5.5.1 Infilled Frames

Clause 3.9.4 of EBCS-8 provides a guide for the modification of design seismic action effects of bare frame, except the displacements, in account of the frame infill. Due to the reduced natural period caused by the addition of infills, the design seismic action effects shall be modified with regard to the response of the bare structure as follows:

(a) The ordinate S_d of the design spectrum is calculated using an average value T_1' of the first mode period of the structure, which is determined as follows:

$$T_1' = \frac{(T_{1b} + T_{1i})}{2}$$

Where: T_{1b} – first mode period of the bare structure without taking into account any stiffness of the infills.

T_{1i} – first mode period of the structure taking into account the infills as structural elements

(b) Except for the calculation of displacements, all seismic action effects, determined with the model of the bare structure, are multiplied by the ratio of $S_d(T_1')/S_d(T_{1b})$

The first mode period may be estimated by the following simplified expressions.

$$T_{1i} = \min \begin{cases} 0.065n \\ 0.080\left(\frac{H}{\sqrt{B}}\right)\left(\frac{H}{H+B}\right) \\ 0.075H^{3/4} \end{cases}$$

Where: n – number of stories.

H – height of the building in m.

B – width of the building in m in the direction considered.

Example 5.5.1.1. FRAME-1 with aspect ratio of 2.5 is considered for the determination of a factor used to modify the bare frame in account of the infill effect.

n = 5 H = 15m B = 7.5m

T_{1b} = 0.689sec - from the program ASSDMI.

$$T_{1i} = \min \begin{cases} 0.065*5 = 0.325 \\ 0.080\left(\frac{15}{\sqrt{7.5}}\right)\left(\frac{15}{15+7.5}\right) = 0.292 \\ 0.075*15^{3/4} = 0.572 \end{cases}$$

$\therefore$ *Use* $T_{1i} = 0.292$

$$T_1^{'} = \frac{(0.292+0.689)}{2} = 0.4905$$

The ratio of the spectral acceleration to ground acceleration, β_o, for $T_1^{'}$ *and* T_{1b} is given by:

$\beta_{01}^{'} = (1/0.4905) = 2.0387 \leq 2.5$

$\beta_{01b} = (1/0.689) = 1.4514 \leq 2.5$

Therefore, the modifying factor ,M_f, becomes,

$$M_f = \frac{2.0387}{1.4514} = 1.4046$$

Table 5.5.1.1 shows the modifying factors prepared in an excel sheet for some of the aspect ratios used in the analyses.

Table 5.5.1.1 Determination of modification factor for bare frame in account of infill

				Simplified formulea for periods in sec.						
Aspect ratio (L/H)	Number of stories, n, in m	Height of Frame, H, in m	Width of bay, B, in m	$T_1 = 0.065n$	$T_2 = 0.080\left(\frac{H}{\sqrt{B}}\right)\left(\frac{H}{H+B}\right)$	$T_3 = 0.075H^{3/4}$	T_{1i} = Min of T_1, T_2 and T_3	T_{1b} from ASSDMI	$T_1^{`} = \frac{(T_{1b}+T_{1i})}{2}$	Modification factor, M_f
1.0	5	15	3.0	0.325	0.577	0.572	0.325	0.48	0.403	1.193
1.5	5	15	4.5	0.325	0.435	0.572	0.325	0.559	0.442	1.265
2.0	5	15	6.0	0.325	0.350	0.572	0.325	0.627	0.476	1.317
2.5	5	15	7.5	0.325	0.292	0.572	0.292	0.689	0.491	1.405
3.0	5	15	9.0	0.325	0.250	0.572	0.250	0.745	0.498	1.497

In figure 5.5.1.1 plots of column shear versus story height are shown for FRAME-1 under different conditions. The aspect ratio varies from 1.0 to 3.0 and the comparison is among infilled frame column, infilled frame column plus infill, bare frame column and bare frame column subject to modification of EBCS-8.

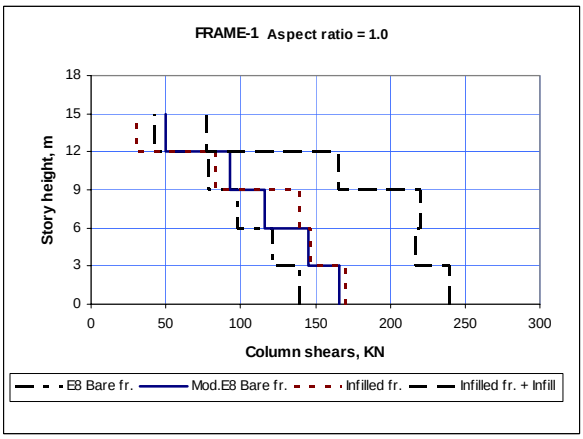

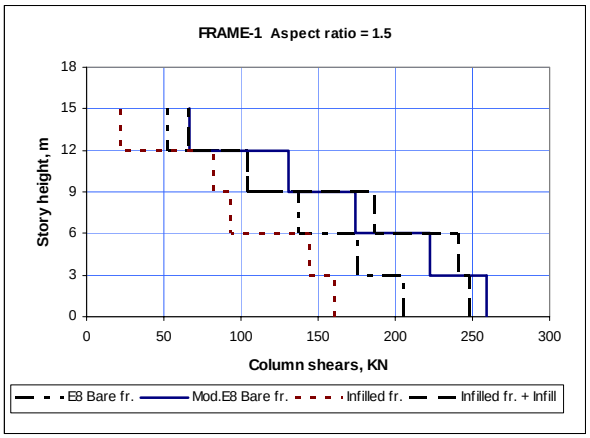

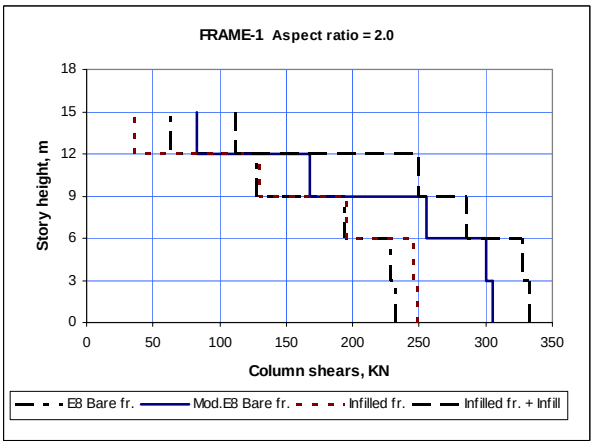

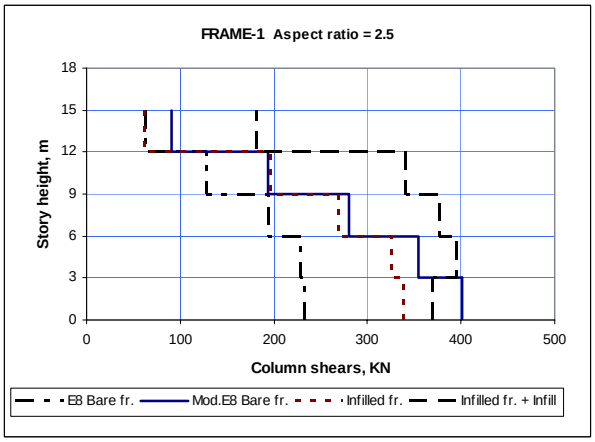

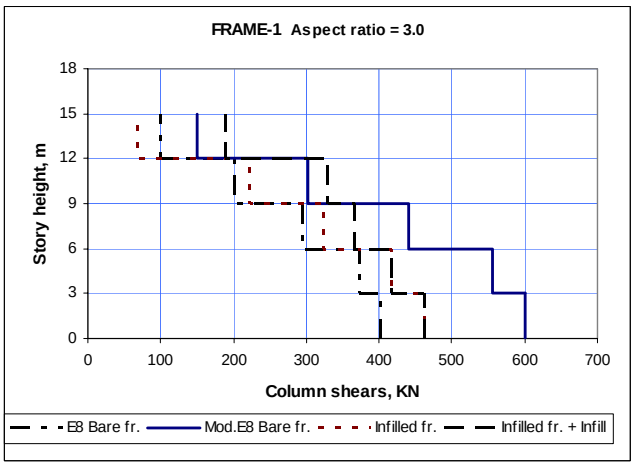

Fig. 5.5.1.1 Modification of column shears based on EBCS-8 for FRAME-1

Discussion

The provision by EBCS-8 to account for the effect of infill does not clearly specify the distribution of the infill in a frame. In reality all or parts of bays in a frame might be infilled. Anyhow the procedure in EBCS-8 has been applied for FRAME-1. It is more confusing to apply for the other frames which are characterized by infill bay and bare bay irregularity. The code provides a modification factor so as to amplify the shear obtained in bare frames. The modification factor improves the shear in the bare frame (Fig. 5.5.1.1). However, there are significant differences with the analysis results of infilled frame plus infill for the first and the last aspect ratios. For the aspect ratio of 3.0 modification of shear using EBCS-8 gives conservative results for most of the stories whereas for the lower aspect ratios shears using EBCS-8 are less than the infilled frame plus infill shears.

5.5.2 Bare Frames

The analysis has been compared using approximate static procedure provided in EBCS-8.

The seismic base shear force ,F_b, is given by,

$$F_b = S_d(T_1)W$$

Where: $S_d(T_1)$ – ordinate of the normalized elastic response spectra at period T_1.

T_1 – fundamental period of vibration of the structure.

W – seismic dead load.

Since the building height is less than 80m the value of T_1 may be approximated from the following formula:

$$T_1 = C_1 H^{3/4}$$

Where: T_1 – fundamental period of building, in seconds.

H – height of the building above the base in meters.

C_1 = 0.075 for reinforced concrete moment-resisting frames.

The base shear shall be distributed over the height of the structure in conformance with the equation given below.

$$F_b = F_t + \sum_{i=1}^{n} F_i$$

$$F_t = 0.07 T_1 F_b$$

Where: F_t – The concentrated force at the top

The base shear shall be distributed over the height of the structure , including level n in accordance to the following formula:

$$F_i = \frac{(F_b - F_t)W_i h_i}{\sum_{i=1}^{n} W_i h_i}$$

Where: F_i – lateral force at a story level i.

W_i – Seismic dead load at the story level i.

h_i – height of a story level above the base.

The charts included in figures 5.5.2.1 – 5.5.2.2 show the comparison of shears in the column at extreme left end of the different frame types. The randomly selected aspect ratios of the infilled bay are 2.0 and 3.0.

Example 5.5.2.1 Shear determination of the left end column in FRAME-1 with aspect ratio of 2.0 using static analysis procedure of EBCS-8. The mass at each floor level is 23.18 Kg whereas at the roof level it is 20 Kg (Table C-1).

Seismic dead load, W = (4*23.18 + 20) * 9.81 = 1105.78 KN

Fundamental period, $T_1 = 0.075 * (15)^{3/4} = 0.572 \text{ sec.}$

Ground exciting acceleration = 0.3g

Spectral acceleration/ Ground acceleration, $\beta_0 = 1/0.572 = .75$

Ordinate of ERSC, $S_d(T_1) = 0.3*1.75 = 0.525$

∴ $F_b = 0.525*1105.78 = 580.54$ KN $\qquad F_t = 0.07*0.572*580.54 = 23.24$ KN

$F_b - F_t = 557.30$ KN

$$\sum_{i=1}^{5} W_i h_i = 3 * 23.18 * (1+2+3+4) + 15 * 20 = 995.40 \, KN$$

Lateral forces at the story levels:

$$F_1 = 557.30 * 23.18 * 3 / 995.40 = 38.93 \, KN$$

$F_2 = F_1*2 = 77.86$ KN $\qquad F_4 = F_1*4 = 155.72$ KN

$F_3 = F_1*3 = 116.76$ KN $\qquad F_5 = 557.30*20*15/995.4 = 168.00$ KN

Shear forces at the story levels:

$V_1 = 38.93 + 77.86 + 116.76 + 155.72 + 168.00 = 557.27$ KN

$V_2 = 77.86 + 116.76 + 155.72 + 168.00 = 518.34$ KN

$V_3 = 116.76 + 155.72 + 168.00 = 440.48$ KN

$V_4 = 155.72 + 168.00 = 323.72$ KN

$V_5 = 168.00$ KN

Shear forces at the left end columns at each story level:

$V_{c1} = V_1/2 = 278.64$ KN

$V_{c2} = V_2/2 = 259.17$ KN

$V_{c3} = V_3/2 = 220.24$ KN

$V_{c4} = V_4/2 = 161.86$ KN

$V_{c5} = V_5/2 = 84$ KN

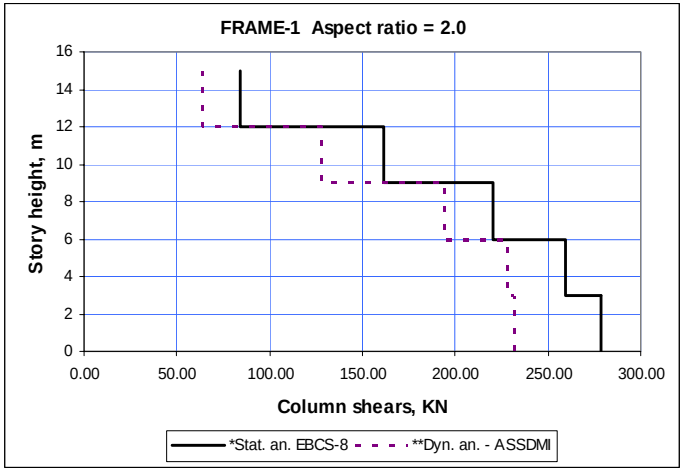

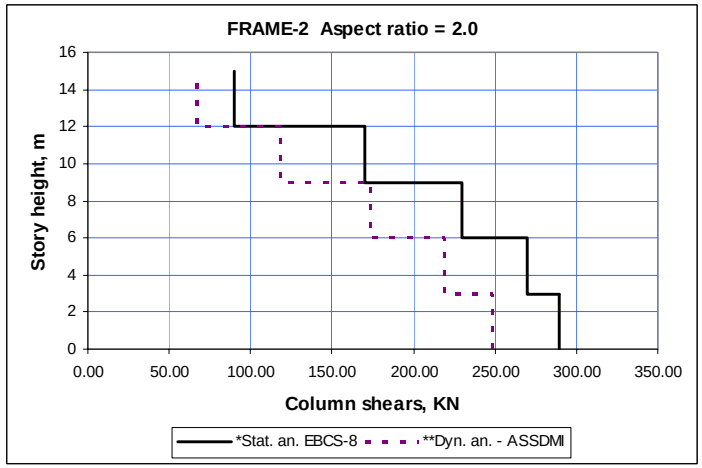

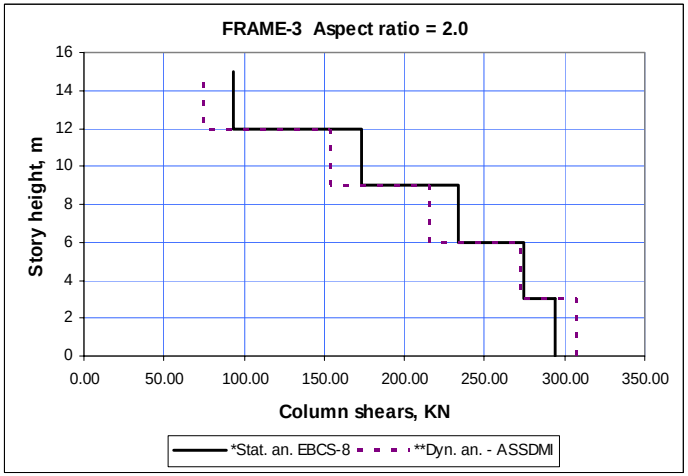

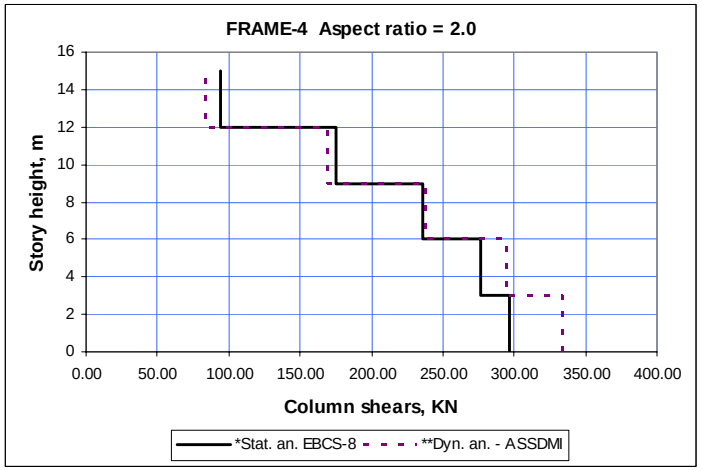

Fig. 5.5.2.1Comparison of static and dynamic analyses for the frames with aspect ratio = 2.0

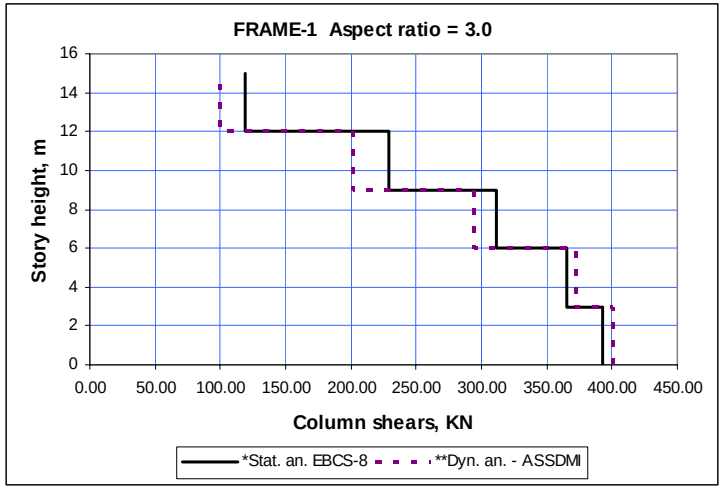

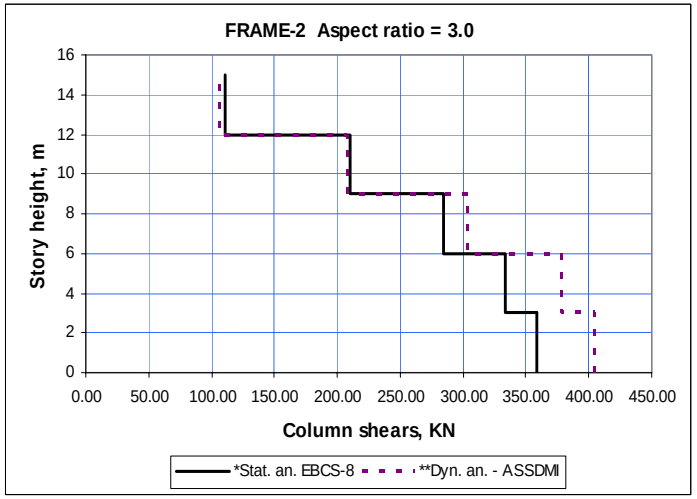

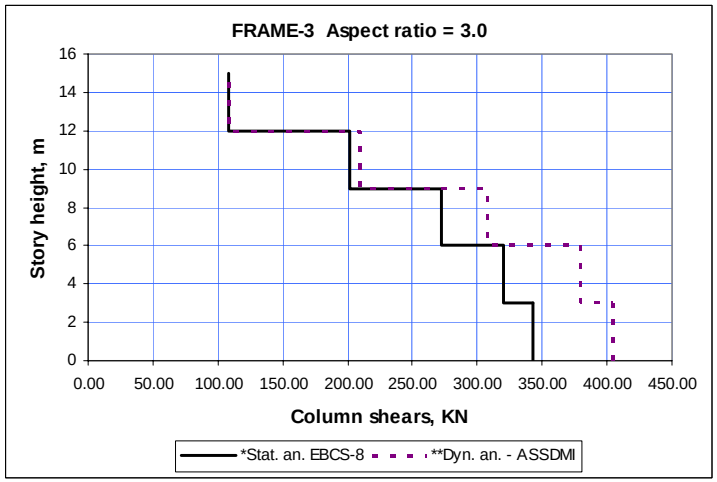

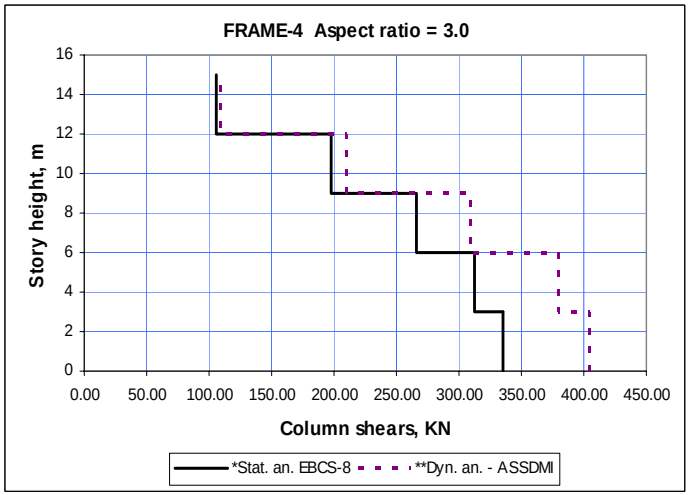

Fig. 5.5.2.2 Comparison of static and dynamic analyses for the frames with aspect ratio = 3.0

* Static analysis using EBCS-8
** Dynamic analysis using ASSDMI

Discussion

The analysis result using ASSDMI for bare frame is more or less in harmony with the equivalent static analysis of EBCS-8 since the frames don't exhibit serious irregularity. FRAME-1 and FRAME-2 with aspect ratio of 2.0 show relatively higher differences of shears obtained by EBCS-8 and ASSDMI whereas lower differences are observed for FRAME-3 and FRAME-4 (Fig. 5.5.2.1). The reverse is true for the frames with aspect ratio 3.0 (Fig. 5.5.2.2). There is a tendency of decrease in shear of the equivalent static analysis with the increase in the number of bays. The difference is magnified at the lower stories where higher in-plane shear is registered.

6 CONCLUSIONS AND RECOMMENDATIONS

6.1 Conclusions

The analysis was carried out for shear forces of a column at different situations. The first condition assumes that the infill has inertia force contribution but no stiffness contribution (bare frame). The second state considers the mass and stiffness contributions but no interaction between infill and frame (infilled frame). The third condition accounts the mass and stiffness contributions plus the infill-frame interaction (infilled frame plus infill).

The following are some of conclusions that can be deduced from the analysis.

1. The increase in the aspect ratio (L/H) heavily degrades the masonry infill. At higher aspect ratios such as 2.5 or 3.0 complete loss of stiffness of infill panel was recorded. Such big changes in stiffness during the cyclic loading in earthquake are causes for the attraction of larger shear forces towards columns neighborhood of the infill panels.

2. As the bare frame analysis yielded less shear force for most aspect ratios, the common design practice assumption of neglecting stiffness of the infill is unsafe.

3. The mystery of actual interaction between infill and frame is yet complex. The consideration of infill-frame interaction, with the simple addition of infill shear and frame shear, gives the overestimation of shear force and remains safe value for conservative design.

4. A close scrutiny to EBCS-8 provides a factor, based on the fundamental period, to amplify the bare frame shear to account the effect of the infill. When applied to FRAME-1 the improved shear for most of the aspect ratios lies in between the infilled frame column shear and infilled frame column plus infill shear. Hence, the clue in EBCS-8 provision is in harmony with ASSDMI analysis.

5. The program used for the analysis proved to be more flexible and can be applied for various irregular 2D-frames. Hence the limitations imposed in the EBCS-8 can easily be overcome.

6.2 Future Recommendations

This thesis work is an inch towards the complex phenomena of the interaction of masonry infills and frames. Especially micro-level investigations are beyond the scope of this study. The rational advice is to get acquainted with the variables involved so as to pick out certain related variables while keeping the others constant. Bit by bit one may arrive at an integrated and harmonious result otherwise dawdling away ones time in the meanders may lead to drowning in the sea of variables. Among the possibilities for future study, the following are the main ones that deserve attention.

1. Modifying the program (ASSDMI) developed in the thesis can broaden the scope so as to encompass other irregularities in the infilled frame.

2. In this study the columns deformation is assumed to be linearly elastic. The inelastic deformation has been left for future investigation.

3. Because of the 2-D analyses, the frames were subjected only to the in-plane action of seismic forces. The out-of-plane action and its interaction with the in-plane action is a subject for further study in 3-D analysis.

4. Due to the limitation of the experimental data the material of infill was unreinforced brick. It can be replaced by other materials such as reinforced brick, hollow concrete block (HCB) and stone masonry in order to reveal the influence in the variation of materials. The thickness of the brick infill was a single wythe. Future study can accommodate a double wythe, enabling the incorporation of thick external walls.

5. Solid masonry infills at alternate bays can easily be extended from this thesis work. Moreover, partial masonry infills at story levels and perforations due to doors and windows provision in walls are inevitably common practices. Since they are the major causes for the behavioral changes under seismicity, they deserve attention in the future study.

REFERENCES

1. Ali, S., 1987. *Concentrated Loads on solid masonry*, diss. 1143, University of Newcastle, *passim.*
2. Andreaus, U., Jan.1996. *"Failure Criteria for Masonry Panels under In-Plane Loading"*. Journal of Structural Engineering, PP 37 – 46.
3. Asteris, P.G. and Tzamtzis, A.D. ,2003. *"On the Use of a Regular Yield Surface for the Analysis of Unreinforced Masonry Walls"*. Electronic Journal of Structural Engineering 3.
4. ATC-40, 1996, *Seismic Evaluation and Retrofit of Concrete Building*s, prepared by the Applied Technology Council (Report No. ATC-40), Redwood City, California for the California Seismic Safety Commission (Report No. SSC 96-01). http://www.atcouncil.org/atc40.shtml
5. Baber, T. T., and Wen, Y. K., 1981. *"Random vibration of hysteretic degrading systems."* Journal of Engineering Mechanics, ASCE, 107(6), 1069 – 1087.
6. Benjamin, J.R., and Williams, H.A., 1958, *"The behavior of one-story shear walls," Proc. ASCE,* ST. 4, Paper 1723: 30.
7. Blondet, M., Torrealva D. and García, G. V. , 2002. *"Adobe in Peru: Tradition, Research and Future."*
8. Bouc, R., 1967. *"Forced vibration of mechanical systems with hysteresis."* Proceedings, 4th Conference on Non-linear Oscillation.
9. Chopra, A. K. ,1995. *Dynamics of Structures – Theory and Applications to Earthquake Engineering.* Prentice Hall of India.
10. Chrysostomou, C.Z., Gergely, P, and Abel, J.F., 1988, *Preliminary Studies of the Effect of Degrading Infill Walls on the Nonlinear Seismic Response of Steel Frame*s, National Center for Earthquake Engineer-ing Research, Technical Report NCEER-88-0046.
11. Dhanasekar, M., (1985), *The performance of brick masonry subjected to in-plane loading,* diss. 990**,** University of Newcastl**e,** *passi*m.
12. EBCS-8, 1995 , *Design of Structures for Earthquake Resistance*. Ethiopian Building Code Standard prepared by Ministry of Works and Urban Development. Addis Ababa, Ethiopia.
13. Ellul, F. and D'Ayala, D., July 2003. *"Field Report on the Bingol, Turkey Earthquake of the 1st of May 2003"*. University of BATH - Architecture & Civil Engineering Department.
14. FEMA 306, 1998, *Evaluation of Earthquake-Damaged Concrete and Masonry Wall Buildings— Basic Procedures Manua*l, prepared by the Applied Technology Council

(ATC-43 Project), for the Federal Emergency Management Agency, Washington, D.C. (FEMA Publication No. 306).
http://www.conservationtech.com/FEMA-publications/FEMA-306-8.htm

15. FEMA 307, 1998, *Evaluation of Earthquake-Damaged Concrete and Masonry Wall Buildings—Technical Resource*s, prepared by the Applied Technology Council (ATC-43 Project), for the Federal Emergency Management Agency, Washington, D.C. (FEMA Publication No. 307).
http://www.conservationtech.com/FEMA-publications/FEMA-306-8.htm
16. FEMA 356, 2000, *Prestandard and Commentary for the Seismic Rehabilitation of Buildings.* Prepared by the American Society of Civil Engineers, for Federal Emergency Management Agency, Washington, D.C.
http://www.degenkolb.com/0_0_Misc/0_1_FEMADocuments/fema356/ps-fema356.html
17. Gergely, P., White, R. N., and Mosalam, K.M., 1994, *"Evaluation and Modeling of Infilled Frames,"* Pro-ceedings of the NCEER Workshop on Seismic Response of Masonry Infills, D.P. Abrams editor, National Center for Earthquake Engineering Research, Technical Report NCEER-94-0004, pp.1-51 to 1-56.
18. Hilsdorf, H. K., May 1969, *"An Investigation into the Failure Mechanism of Brick Masonry Under Axial Compression in Designing," in Engineering and Constructing with Masonry Products,* F. B. Johnson, Ed., Gulf Publishing, Houston, pp. 34 – 41.
19. Idarc 2D version 6.0, 2004. *Users Manual*. University at Buffalo, Department of Civil, Structural and Environmental Engineering
http://civil.eng.buffalo.edu/idarc2d50/
20. Kusunoki, K., Apr. 2002, *"Report on the Damage Investigation of the 2001 Atico Earthquake in Peru"*. Building Research Institute of Japan.
21. Madan, A., Reinhorn, A.M., Mander, J.B. and Valles, R.E., 1997. *"Modeling of Masonry Infill Panels for Structural Analysis"*. Journal of Structural Engineering, October, PP 1295 - 1302.
22. Maghaddam, H.A. and Dowling, P.J., 1987, *The State of the Art in Infilled Frame*s, Civil Engineering Department, Imperial College, ESEE Research Report No. 87-2, London.
23. Mander, J. B., Aycardi, L.E., and Kim, D-K, 1994, *"Physical and Analytical Modeling of Brick Infilled Steel Frames,"* Proceedings of the NCEER Work-shop on Seismic Response of Masonry Infills, D.P. Abrams editor, National Center for Earthquake Engineering Research, Technical Report NCEER-94-0004.
24. Meskouris, K., 2000, *Structural Dynamic – Models, Methods, Examples*. CD-ROM

inclusive. Structural Engineering Practice. Ernst & Sohn – A Wiley Company

25. Mosalam, K.M., Gergely, P., and White, R., 1994 *"Per-formance and Analysis of Frames with "URM" Infills,"* Proceedings of the Eleventh Conference (formerly Electronic Computation Conference) held in conjunction with ASCE Structures Congress 94 and International Symposium '94, Atlanta, Georgia, pp. 57-66.
26. Mostafaei, H. and Kabeyasawa, T.. *"3-D Nonlinear Response Simulations of Bam Telephon Center RC Building to the 2003 Bam Earthquake Considering the Effect of Masonry Infill Walls"*. Earthquake Research Institute, The University of Tokyo.
27. Nichols, J. ,2000. *"A Study of the Progressive Degradation of Masonry Shear Walls Subjected to Harmonic Loading"*. A Thesis submitted to the University of Newcastle in partial fulfilment of the requirements for the degree of Doctor of Philosophy.
28. Paulay, T. and Priestley, M.J.N., 1992, *Seismic Design of Reinforced Concrete and Masonry Building*s, John Wiley & Sons, New York.
29. Penelis, G. G. and Kappos, A. J. ,1997. *Earthquake Resistant Concrete Structures.* St. Edmundsbury Press Limited, Bury St. Edmunds, Suffolk.
30. Polyakov, S.V., 1956, *Masonry in framed building*s, pub. by Gosudarstvennoe Izdatelstvo po Stroitel-stvu I Arkhitekture (Translation into English by G.L.Cairns).
31. Saneinejad, A. and Hobbs, B., 1995. *"Inelastic design of infilled frames." J. Struct. Engrg*., ASCE, 121(4), 634-650.
32. Shing, P.B., Mehrabi, A.B., Schuller, M., and Noland, J.D., 1994, *"Experimental evaluation and finite ele-ment analysis of masonry-infilled R/C frames,"* Proc. of the Eleventh Conference (formerly Electronic Computation Conference) held in conjunction with ASCE Structures Congress '94 and International Symposium '94, Atlanta, Georgia., pp. 84-93.
33. Smith, B. S. and Coull, A. ,1991. *Tall Building Structures – Analysis and Design.*
34. Stafford-Smith, B.S., 1966, *"Behavior of square infilled frames,"* ASCE (92)1: 381-403.
35. Thiruvengadam, V., 1985, *"On the natural frequencies of infilled frames,"* Earthquake Engineering and Structural Dynamics, 13: 401-419.

APPENDIX-A The Program ASSDMI

ASSDMI – Analyses for Stiffness and Strength Degradation of Masonry Infill.

Definition of Variables Used in the Program.

AA - One dimensional array for Slip length in pinching of hysteresis loops. It is **a** in modified Bouc-Wens model.

Acc – One dimensional array for synthetic accelerogram record.

Alf - Post-yield to pre-yield stiffness ratio. It is α in Bouc-Wen model.

As - Constant that controls the shape of the generated hysteretic loops ; As = A, in Bouc-Wen model; Default value, As = 1, based on IDARC-2D manual.

Ax - Slip-lock parameters; Ax = As in modified Bouc-wen model; Default values, Ax = 0.5.

Bt - Constant that controls the shape of the generated hysteretic loops ; Bt = β, in Bouc-Wen model; Default value, Bt = 0.1, based on IDARC-2D manual.

Dp - Viscous damping ; Dp = 0.05 has been used.

Dr - Two dimensional array for the time history of inter story drifts.

FL - Flag used to differentiate the absence or presence of infill wall; For presence of infill FL= 1 , for the absence FL=0.

FR - One dimensional array for frequency of free vibration of the system.

FRd - One dimensional array for frequency of damped vibration of the system.

Gr - Factor used to multiply the *Time History Record.* Gr = 0.4 (400 so as to convert displacement in m to mm) used in the program

Gm - Constant that controls the shape of the generated hysteretic loops ; Gm = γ in Bouc-Wen model; Default value, Gm = 0.9 – based on IDARC-2D manual.

ID - Subdivision of the inter-story drift in a time step, used for high accuracy *Runge-Kutta* integration (Subroutine *STIFDEG, RUNGEKUTTA*)

ITN – Iteration number in the power series method used in for determination of *Frequency* and *Mode Shapes* (Subroutine *EIGVAL*)

M - Story number used for the convenience in the subroutines *ORTHOG, MULTIPL* and *MULTIPL1*

Mas - One dimensional array for mass(in Ton) of a bldg assumed to be lumped at the floor level.

Masa - Two dimensional diagonal mass matrix.

Mc - Monotonic ductility capacity ; Mc = μ_c in Bouc-Wen model; Default value Mc = 25

Mode - One dimensional array for the mode shape.

Modn - One dimensional array for the normalized mode shape.

Mx - One dimensional array for the maximum displacement in the time history.

NC - One dimensional array for number of columns at each story.

NN - Parameter controlling the rate of transition from the elastic to yielded state ; NN = n in Bouc-Wen model ; Default value NN = 2.

Ns - Story number

Nt - Number of time steps used for ***THA*** ; Nt = 1000 for the synthetic record used in the program.

P - Two dimensional matrix for *Seismic Inertia Force* for each incremental of time step and at

each story level.

Sk - Multiplier for Vy to define the pivot for deterioration branches. Defaul value Sk = 0.1.

Sp1, Sp2 - Parameters controlling the rate of deterioration ; Default values Sp1 = 0.8, Sp2 = 1.0.

Stc - One dimensional array for stiffness of columns.

Stin - One dimensional array for initial stiffness (in KN/m) of the masonry panel before stiffness degradation.

Stm - One dimensional array for stiffness (in KN/m) of the masonry panel, varying with degradation.

T - One dimensional array for time in seconds increasing with time stepping of 0.01sec.

Ts - Time step ; Ts = 0.01sec for the synthetic record.

U - Two dimensional array for the time history of displacement at the floor levels of the system.

Uy - Inter-story drift of panel at yielding.

VC - Two dimensional array for the time history of shear force of column at the story levels.

VI - Two dimensional array for the time history of shear force of panel at the story levels.

Vy - Shear at yielding of the panel.

Vyk - One dimensional array for yielding of panel at each story level, varying with strength degradation.

VV - One dimensional array for the cumulative energy dissipated. It is the sum of the areas under the hysteretic loop.

Zb - Slip-lock parameter; Zb = $\bar{Z}$, in modified Bouc-wen model; Default value Zb = 0.0.

Zi - Two dimensional array for the time history of hysteretic component determined from the differential equation in modified Bouc-Wen model.

Zs - Slip-lock parameter; Zs = Zs, in modified Bouc-wen model; Default value Zs = 0.1.

Brief Description of Subroutines.

1. **STIFFDIST** – Used to distribute the one dimensional stiffness of stories based on shear building requirement.
2. **MATINV** – Inverts the matrix obtained in 1.
3. **MULTIPL** – Multipies the inverted matrix in 2 with mass matrix **Masa**.
4. **EIGVAL** – Carries out the eigen value and eigen vector determination by iterative procedure of power method. The eigen value is the frequency and the eigen vector is the mode shape(later on a normalized one).
5. **ORTHOG -** Uses the advantage of orthogonality of eigen vectors for the determination of consecutive frequencies and mode shapes.
6. **MULTIPL1** – Facilitates *orthogonality transformation.*
7. **TIMESTEP** – Time stepping method, as described in Anil K. Chopra(Chapter 5 modified MDFS), for the determination of the response of structure.
8. **STIFDEG** – Accounts the stiffness and strength deterioration also including pinching.
9. **RUNGEKUTTA2 -**Fourth order Runge-Kutta for the determination the *hysteretic component* Zi.

```
PROGRAM ASSDMI
IMPLICIT NONE
INTEGER::M,Ns,I,J,ITN,MON(50),Nt,NC(20)
INTEGER,PARAMETER::KK=25
REAL,DIMENSION(20,20)::Stifa,Masa,C,Mode,Modn
REAL,DIMENSION(0:1700,0:20)::Dr,VI,VC,VS
REAL,DIMENSION(100)::FR,FRd
REAL,DIMENSION(1700)::T,Acc
REAL,DIMENSION(20)::Mas,VV,Stif,Stin,Stc,Stm,AA,Vyk,Mx
REAL,DIMENSION(1700,20)::P
REAL::Ts,Dp,Kon,My,Gr,Vy,Alf,U(-1:3000,0:20),As,Bt,Gm,NN,Uy,ID,Sk,Mc,Sp1,Sp2,Zb,Zs,Ax,FL

CHARACTER*50 INPUT,OUTPUT1,OUTPUT2,OUTPUT3
!-------------------------------------------------------------------------------------------------------!
PRINT*,'ENTER THE NAME OF THE INPUT FILE'
 READ(*,*) INPUT
PRINT*,'ENTER THE NAME OF THE OUTPUT FILE 1'
 READ(*,*)  OUTPUT1
PRINT*,'ENTER THE NAME OF THE OUTPUT FILE 2'
 READ(*,*)  OUTPUT2
PRINT*,'ENTER THE NAME OF THE OUTPUT FILE 3'
 READ(*,*)  OUTPUT3

 OPEN(UNIT=KK, FILE=INPUT, STATUS = "OLD")
 OPEN(UNIT=35, FILE=OUTPUT1, STATUS = "UNKNOWN")
 OPEN(UNIT=45, FILE=OUTPUT2, STATUS = "UNKNOWN")
 OPEN(UNIT=55, FILE=OUTPUT3, STATUS = "UNKNOWN")

!READING THE DIMENSION OF THE MASS MATRIX AND THE STIFFNESS MATRIX
 READ(KK,*) M,Ns,ITN,Nt,Ts !M AND Ns - STORY No..; ITN - ITERATION No.; Nt - No. OF TIME
STEPS; Tst - TIME STEP
 READ(KK,*) Dp,Gr,Vy,Alf,ID  !,Kon,My  !Dp - DAMPING. NON-LINEAR STIFF COEFF..GRAVI.ACC..
MOMENT AT YIELD
 READ(KK,*) As,Bt,Gm,NN,Uy,Sk
 READ(KK,*) Mc,Sp1,Sp2,Zb,Zs,Ax,FL

!READING THE STIFFNESS MATRIX
 READ(KK,*) (Stm(J),J=1,Ns) !INITIAL STIFFNESS OF MASONRY
 READ(KK,*) (Stc(J),J=1,Ns) !STIFFNESS OF COLUMNS
 READ(KK,*) (NC(J),J=1,Ns)  !NUMBER OF COLUMNS AT EACH STORY

!READING THE MASS MATRIX
 READ(KK,*) (Mas(I),I=1,Ns)
          DO I=1,Ns
           DO J=1,Ns
            IF(I/=J)THEN
```

```
     Masa(I,J) = 0.0
    ELSE
     Masa(I,J) = Mas(I)
    END IF
   END DO
  END DO

  DO I=1,Nt
   T(I) = (I-1)*Ts
  END DO

!READING THE ACCELEROGRAM
  READ(KK,*)  (Acc(I),I=1,Nt)
   DO I=1,Nt
    DO J=1,Ns
     P(I,J) = -Gr*Acc(I)*Mas(J)
    END DO
   END DO

IF(FL==0)THEN
 DO J=1,Ns
  Stm(J) = 0
 END DO
ENDIF

  DO I=1,Ns
   Stin(I) = Stm(I)
   Vyk(I) = Vy
   VV(I) = 0.0
   Mx(I) = 0.0
   AA(I) = 0.0
  END DO

 DO I=1,Nt-1

  DO J = 1,Ns
   Stif(J) = Stm(J) + (2 + (NC(J)-2)*(4/3))*Stc(J)
  END DO

   CALL STIFFDIST(Ns,Stif,Stifa)

   CALL MATINV(Ns,Stifa)

   CALL MULTIPL(M,Ns,Stifa,Masa,C)

   CALL EIGVAL(Ns,ITN,Mas,Masa,C,Mode,Modn,FR)
```

```
          DO J=1,Ns
            FRd(J) = FR(J)*SQRT(1-Dp**2)
          END DO

         CALL RECCONS(I,Ns,Dp,Ts,P,FR,FRd,Modn,U,Dr,VC,Stc,NC,FL)

  CALL
STIFDEG(Ns,I,Alf,U,As,Bt,Gm,NN,Uy,Vy,Vyk,VI,Stm,Stin,ID,Sk,Mc,Sp1,Sp2,VV,Mx,Zb,Zs,Ax,AA, FL)

         DO J=1,Ns
           VS(I,J) = VI(I,J) + VC(I,J)
         END DO

         END DO

 IF(FL==1)THEN
  WRITE(35,"(/'RESPONSES AT THE FLOOR LEVELS'/)")
   WRITE(35,"(/'TIME',10X,5('DRIFT.',8X,'SHEAR',10X)/)")
  WRITE(45,"(/'RESPONSES AT THE FLOOR LEVELS'/)")
   WRITE(45,"(/'TIME',10X,5('DISPL.',8X,'SHEAR',10X)/)")
  WRITE(55,"(/'RESPONSES AT THE FLOOR LEVELS'/)")
   WRITE(55,"(/'TIME',10X,5('SHEAR',10X)/)")
              DO I=1,Nt-1
               WRITE(35,"(F5.2,4X,10(F10.3,5X))") T(I),(Dr(I,J),VI(I,J),J=1,Ns)
               WRITE(45,"(F5.2,4X,10(F10.3,5X))") T(I),(U(I,J),VC(I,J),J=1,Ns)
               WRITE(55,"(F5.2,4X,5(F10.3,5X))") T(I),(VS(I,J),J=1,Ns)
              END DO
            ELSE
             WRITE(35,"(/'DISPLACEMENTS OF FLOORS'/)")
             WRITE(35,"(/'TIME',10X,5('DISPL.',8X,'SHEAR',10X)/)")
              DO I=1,Nt-1
               WRITE(35,"(F5.2,4X,10(F10.3,5X))") T(I),(U(I,J),VS(I,J),J=1,Ns)
              END DO
            ENDIF

             REWIND KK
             CLOSE (KK)
             CLOSE (35)
             CLOSE (45)
             CLOSE (55)
 END PROGRAM ASSDMI

!-----------------------------------------------------------------------------------------------!

 SUBROUTINE MATINV(N,A)
```

```
IMPLICIT NONE
INTEGER::N,I,J,K
REAL::FA1,FA2
REAL,DIMENSION(20,20)::A

            DO I=1,N
            DO J=N+1,2*N
             A(I,J) = 0.0
            END DO
            A(I,I+N) = 1.0
           END DO

           DO I=1,N
            FA1 = A(I,I)
            DO J=1,2*N
             A(I,J) = A(I,J)/FA1
            END DO
            DO K=1,N
             IF(K/=I)THEN
              FA2 = A(K,I)
             DO J=1,2*N
              A(K,J) = A(K,J) - FA2*A(I,J)
             END DO
             END IF
            END DO
           END DO

           DO I=1,N
            DO J=1,N
             A(I,J) = A(I,J+N)
            END DO
           END DO

END SUBROUTINE MATINV

!-----------------------------------------------------------------------------------------------!

 SUBROUTINE EIGVAL(N,ITN,Mas,B,C,EVE,EVE3,W)
 IMPLICIT NONE
 REAL, DIMENSION(20,20)::B,C,EVE,D,E,F,G,RES,EVE1,EVE3
 REAL, DIMENSION(100)::W,SUM1
 REAL::SUM2,Mas(20)
 INTEGER I,J,K,L,N,ITN,P

 !RESERVING THE ARRAY C
         DO I=1,N
```

```
DO J=1,N
 RES(I,J) = C(I,J)
END DO
END DO

DO K=1,N   !BEGINNING OF K
 !INITIALIZING THE EIGEN VECTOR
 DO I=1,N
  EVE(I,K) = 1.0
 END DO
!ITERATION FOR THE MODE SHAPE
 DO I=1,ITN
   DO J = 1,N
    SUM1(J) = 0.0
   DO L=1,N
    SUM1(J) = SUM1(J) + C(J,L)*EVE(L,K)
   END DO !END OF L
  END DO  !END OF J

   SUM2 = 0.0
  DO J=1,N
   EVE(J,K) = SUM1(J)
   SUM2 = SUM2 + (EVE(J,K)**2)*MAS(J)
  END DO !END OF J

  DO J=1,N
   EVE3(J,K) = EVE(J,K)/SQRT(SUM2)
  END DO

   W(K) = ABS(EVE(1,K))
  DO J=1,N
   EVE(J,K) = EVE(J,K)/W(K)
  END DO !END OF J

 END DO  !END OF I

  W(K) = SQRT(1/W(K))

  DO I=1,N
   EVE1(K,I) = EVE(I,K)
  END DO !END OF I

  IF(K<N.AND.N>1)THEN  !BEGINNING OF IF STATEMENT

  CALL ORTHOG(K,N,B,EVE1,D,E)
  CALL MATINV(K,D)
```

```
            P = N-K
           CALL MULTIPL1(K,P,D,E,F)

           DO I=1,K
            DO J=1,N
             G(J,I) = 0.0
            END DO !END OF J
             DO J=K+1,N
              G(I,J) = F(I,J)
             END DO !END OF J
           END DO !END OF I

           DO I=K+1,N
           DO J=K+1,N
             IF(I==J)THEN
              G(I,J) = 1.0
             ELSE
              G(I,J) = 0.0
             END IF
           END DO
           END DO

          CALL MULTIPL(N,N,RES,G,C)
          END IF  !END OF IF STATEMENT

          END DO  !END OF K
END SUBROUTINE EIGVAL

!-------------------------------------------------------------------------------------------!

!SBROUTINE FOR ORTHOGONALITY TRANSFORMATION
SUBROUTINE ORTHOG(M,N,B,EVE1,D,E)
IMPLICIT NONE
INTEGER::M,N,I,J
REAL,DIMENSION(20,20)::B,EVE1,D,E,ORT,ORT1

           CALL MULTIPL(M,N,EVE1,B,ORT)

           DO I=1,M
             DO J=1,M
              D(I,J) = ORT(I,J)
             END DO !END OF J
             DO J=M+1,N
              E(I,J-M) = -ORT(I,J)
             END DO !END OF J
           END DO !END OF I
```

```
 END SUBROUTINE ORTHOG

!-----------------------------------------------------------------------------------------!

 SUBROUTINE MULTIPL(M,N,A,B,C)
 IMPLICIT NONE
 INTEGER::M,N,I,J,K
 REAL, DIMENSION(20,20)::A,B,C
 REAL::SUM1

            DO I=1,M
            DO J=1,N
             SUM1 = 0.0
             DO K=1,N
              SUM1 = SUM1 + A(I,K)*B(K,J)
             END DO
              C(I,J) = SUM1
            END DO
            END DO
           END SUBROUTINE MULTIPL

!-----------------------------------------------------------------------------------------!

 SUBROUTINE MULTIPL1(M,N,A,B,C)
 IMPLICIT NONE
 INTEGER::M,N,I,J,K
 REAL, DIMENSION(20,20)::A,B,C
 REAL::SUM1

             DO I=1,M
             DO J=1,N
              SUM1 = 0.0
              DO K=1,M
               SUM1 = SUM1 + A(I,K)*B(K,J)
              END DO
               C(I,J+M) = SUM1
             END DO
             END DO
 END SUBROUTINE MULTIPL1

!-----------------------------------------------------------------------------------------!

SUBROUTINE STIFFDIST(N,ST,A)
IMPLICIT NONE
REAL,DIMENSION(20,20)::A
```

```
REAL,DIMENSION(20)::ST
INTEGER::I,J,N,Lc(20)

            DO I=1,N
             IF(I/=N)THEN
              DO J=I,I+1
               A(I,J) = -ST(I+1)
               A(J,I) = A(I,J)
               A(I,I) = ST(I)+ST(I+1)
              END DO
             END IF
              DO J = I+2,N
               A(I,J) = 0.0
               A(J,I) = A(I,J)
              END DO
             END DO
             A(N,N) = ST(N)

END SUBROUTINE STIFFDIST

!-----------------------------------------------------------------------------------------------!

 SUBROUTINE RECCONS(I,Ns,Dp,Ts,P,FR,FRd,Modn,U,Dr,VC,Stc,NC,FL)
 IMPLICIT NONE
 INTEGER::I,Ns,J1,J2,L,NC(20)
 REAL,DIMENSION(20)::FR,FRd,Stc
 REAL,DIMENSION(1700,20)::Qd,Qv,P,V,PP
 REAL,DIMENSION(0:1700,0:20)::Dr,VC
 REAL::S,C,E,D,W,Y,Z,X,AC,BC,CC,DC,AD,BD,CD,DD,Sd,Sv,Modn(20,20),Ts,Dp,SUM1,U(-1:3000,
       0:20), FL

          DO J1=1,Ns !COUNT OF STORIES
           Qd(1,J1) = 0.0
           Qv(1,J1) = 0.0
          END DO
           U(I,0) = 0.0

           DO J1=1,Ns  !COUNT OF FREQUENCIES
            DO L=I,I+1
              SUM1 = 0.0
             DO J2=1,Ns  !COUNT OF STORIES
              SUM1 = SUM1 + Modn(J2,J1)*P(L,J2)
             END DO
              PP(L,J1) = SUM1
            END DO
           END DO
```

```
  DO J1=1,Ns  !COUNT OF FREQUENCIES
   S = SIN(FRd(J1)*Ts) ; C = COS(FRd(J1)*Ts) ; E = EXP(-Dp*FR(J1)*Ts) ; D = Dp/SQRT(1-Dp**2)
   W = (1-2*(Dp**2))/(FRd(J1)*Ts) ; Y = (2*Dp)/(FR(J1)*Ts) ; Z = FR(J1)/SQRT(1-Dp**2) ; X =
Dp/(Ts*SQRT(1-Dp**2))

              AC = E*(D*S+C)
              BC = E*S/FRd(J1)
              CC = (Y + E*((W-D)*S - (1+Y)*C))/(FR(J1)**2)
              DC = (1 - Y + E*(-W*S + Y*C))/(FR(J1)**2)
              AD = -E*Z*S
              BD = E*(C - D*S)
              CD = (-(1/Ts) + E*((Z+X)*S + C/Ts))/(FR(J1)**2)
              DD = (1 - E*(D*S + C))/((FR(J1)**2)*Ts)

              Qd(I+1,J1) = AC*Qd(I,J1) + BC*Qv(I,J1) + CC*PP(I,J1) + DC*PP(I+1,J1)
              Qv(I+1,J1) = AD*Qd(I,J1) + BD*Qv(I,J1) + CD*PP(I,J1) + DD*PP(I+1,J1)
            END DO

            DO J2=1,Ns  !COUNT OF STORIES
             Sd = 0.0
             Sv = 0.0
             DO J1=1,Ns  ! COUNT OF FREQUENCIES
              Sd = Sd + Modn(J2,J1)*Qd(I,J1)
              Sv = Sv + Modn(J2,J1)*Qv(I,J1)
             END DO
             U(I,J2) = Sd
             V(I,J2) = Sv
             Dr(I,J2) = U(I,J2) - U(I,J2-1)
             VC(I,J2) = Stc(J2)*Dr(I,J2)/1000
            END DO

 END SUBROUTINE RECCONS
!-----------------------------------------------------------------------!

 SUBROUTINE
STIFDEG(Ns,I,Alf,U,As,Bt,Gm,NN,Uy,Vy,Vyk,VI,Stm,Stin,ID,Sk,Mc,Sp1,Sp2,VV,Mx,Zb,Zs,Ax,AA,FL)
 IMPLICIT NONE
 INTEGER::I,J2,Ns,LL,J3,J,Nv(20)
 REAL,DIMENSION(0:1700,0:20)::VI
 REAL,DIMENSION(-1:3000,0:20)::U
 REAL::As,Alf,Bt,Gm,NN,Uy,Vy,ID,Sk,H,H1,H2,Mc,Sp1,Sp2,DI,UU,DV,Zb,Zs,Ax,Zi(-1:10000,0:20)
       ,FL,CT(1000,20)
 REAL,DIMENSION(20)::AA,Stm,Stin,M1,M2,Vyk,VV,Mx

            DO J2=1,Ns
```

```
 VI(0,J2) = 0.0
 U(0,J2) = 0.0
 U(-1,J2) = 0.0
END DO
 U(-1,0) = 0.0
 U(0,0) = 0.0
 U(I,0) = 0.0
 DO J2=1,Ns      !COUNTING THE STORY BEGINS HERE
  IF(FL==0)THEN
   VI(I,J2) = 0.0
  ELSE

   UU = (U(I,J2)-U(I,J2-1))/Uy
   H2 = ((U(I,J2)-U(I,J2-1)) - (U(I-1,J2)-U(I-1,J2-1)))
  IF(UU<=1.0) THEN
   IF(ABS(H2)>ID)THEN
     LL = ABS(H2/ID)
     H = H2/LL
    DO J3=1,LL
      J = I+J3-2
     CALL RUNGEKUTTA2(I,Ns,J,J2,Alf,Bt,Gm,As,NN,U,H,Sk,Zi,UU,Uy,AA,Zb,Zs)
    END DO
      Zi(I,J2) = Zi(I+LL-1,J2)
   ELSE
     H = H2
     J = I-1
    CALL RUNGEKUTTA2(I,Ns,J,J2,Alf,Bt,Gm,As,NN,U,H,Sk,Zi,UU,Uy,AA,Zb,Zs)
   ENDIF
     VI(I,J2) = Vyk(J2)*(Alf*UU + (1-Alf)*Zi(I,J2))
  ENDIF

 IF(UU>1.0)THEN
  IF(ABS(H2)>ID)THEN
   LL = ABS(H2/ID)
   H = H2/LL
   DO J3=1,LL
     J = I+J3-2
     CALL RUNGEKUTTA2(I,Ns,J,J2,Alf,Bt,Gm,As,NN,U,H,Sk,Zi,UU,Uy,AA,Zb,Zs)
   END DO
      Zi(I,J2) = Zi(I+LL-1,J2)
  ELSE
    H = H2
    J = I-1
   CALL RUNGEKUTTA2(I,Ns,J,J2,Alf,Bt,Gm,As,NN,U,H,Sk,Zi,UU,Uy,AA,Zb,Zs)
  ENDIF
     VI(I,J2) = Vyk(J2)*(Alf*UU + (1-Alf)*Zi(I,J2))
```

```
            ENDIF

             VV(J2) = VV(J2) + (VI(I,J2)+VI(I-1,J2))*H/(2*Uy)
             H1 = ((U(I-1,J2)-U(I-1,J2-1)) - (U(I-2,J2)-U(I-2,J2-1)))

             IF((H2<=0.0).AND.(H1>=0.0))THEN
              M1(J2) = ABS(U(I-1,J2)-U(I-1,J2-1))
              M2(J2) = 0.0
             ELSEIF((H2>=0.0).AND.(H1<=0.0))THEN
              M2(J2) = ABS(U(I-1,J2)-U(I-1,J2-1))
              M1(J2) = 0.0
             ELSE
              M1(J2) = 0.0 ; M2(J2) = 0.0
             ENDIF
               Mx(J2) = MAX(M1(J2),M2(J2),Mx(J2))

            IF((VI(I-1,J2)<0.0).AND.(VI(I,J2)>0.0).AND.Mx(J2)>1.0)THEN
             DI = ((Mx(J2)-1)/(Mc-1))*(1 - 0.25*Sp1*(VV(J2))/(Vy*(Mc-1)))**(-Sp2)
             Vyk(J2) = Vy*(1-DI)
             AA(J2) = Ax*((Mx(J2)/Uy) - 1)
            ENDIF

             DV = VI(I,J2) - VI(I-1,J2)
             IF(H2/=0)THEN
              Stm(J2) = (DV/H2)*1000
              CT(I,J2) = Stm(J2)
              IF(Stm(J2)>=Stin(J2))THEN
                Stm(J2) = Stin(J2)
              ELSEIF((I>=10).AND.((CT(I-2,J2)<=0.OR.CT(I-1,J2)<=0).OR.(CT(I,J2)<=0)))THEN
                Stm(J2) = 0.0
                VI(I,J2) = 0.0
              ENDIF
             ENDIF
             IF((I>=5).AND.(VI(I-1,J2)==0.0))THEN
                Stm(J2) = 0.0
                VI(I,J2) = 0.0
             ENDIF
            ENDIF
           END DO  !END OF STORY COUNTING

  END SUBROUTINE STIFDEG
!---------------------------------------------------------------------------!

  SUBROUTINE RUNGEKUTTA2(I,Ns,J,J2,Alf,Bt,Gm,As,NN,U,H,Sk,Zi,UU,Uy,AA,Zb,Zs)
  IMPLICIT NONE
  INTEGER::I,J,J2,Ns,K
```

```
REAL,DIMENSION(-1:3000,0:20)::U
REAL::H,Sk,Alf,Bt,Gm,As,NN,Mi,Y,Y1,X,X1,K1,K2,K3,K4,UU,Uy,Mu,AA(20),Zb,Zs,CC,C1,Zi(-1:10000,
      0:20)

        DO K=1,Ns
         Zi(0,K) = 0.0
        END DO

        IF(UU<=1.0) THEN
          Mu = H/Uy
          Y = Zi(J,J2)
          CC = As - ((ABS(Y))**NN)*(Bt*SIGN(1,Mu*Y) + Gm)
          K1 = CC/(1+AA(J2)*(EXP(-((Y-Zb)/Zs)**2))*CC)
          Y1 = Y + K1*Mu/2
          C1 = As - ((ABS(Y1))**NN)*(Bt*SIGN(1,Mu*Y1) + Gm)
          K2 = C1/(1+AA(J2)*(EXP(-((Y1-Zb)/Zs)**2))*C1)
          Y1 = Y + K2*Mu/2
          C1 = As - ((ABS(Y1))**NN)*(Bt*SIGN(1,Mu*Y1) + Gm)
          K3 = C1/(1+AA(J2)*(EXP(-((Y1-Zb)/Zs)**2))*C1)
          Y1 = Y + K3*Mu
          C1 = As - ((ABS(Y1))**NN)*(Bt*SIGN(1,Mu*Y1) + Gm)
          K4 = C1/(1+AA(J2)*(EXP(-((Y1-Zb)/Zs)**2))*C1)
          Zi(J+1,J2) = Y + (K1+2*(K2+K3)+K4)*Mu/6
        ELSEIF(UU>1.0)THEN
          Mu = H/Uy
          Mi = (U(I-1,J2)-U(I-1,J2-1))/Uy + (J-I+1)*Mu
          X = (Sk+Alf*(Mi-1)+1)/(Sk+Mi)
          Y = Zi(J,J2)
          CC = As - ((ABS(Y))**NN)*(Bt*SIGN(1,Mu*Y) + Gm)
          K1 = (CC/(1+AA(J2)*(EXP(-((Y-Zb)/Zs)**2))*CC))/X
          X1 = X+Mu/2
          Y1 = Y + K1*Mu/2
          C1 = As - ((ABS(Y1))**NN)*(Bt*SIGN(1,Mu*Y1) + Gm)
          K2 = (C1/(1+AA(J2)*(EXP(-((Y1-Zb)/Zs)**2))*C1))/X1
          Y1 = Y + K2*Mu/2
          C1 = As - ((ABS(Y1))**NN)*(Bt*SIGN(1,Mu*Y1) + Gm)
          K3 = (C1/(1+AA(J2)*(EXP(-((Y1-Zb)/Zs)**2))*C1))/X1
          X1 = X+Mu
          Y1 = Y + K3*Mu
          C1 = As - ((ABS(Y1))**NN)*(Bt*SIGN(1,Mu*Y1) + Gm)
          K4 = (C1/(1+AA(J2)*(EXP(-((Y1-Zb)/Zs)**2))*C1))/X1
          Zi(J+1,J2) = Zi(J,J2) + (K1+2*(K2+K3)+K4)*Mu/6
        ENDIF

END SUBROUTINE RUNGEKUTTA2
```

APPENDIX-B Degradation of Infill Panel

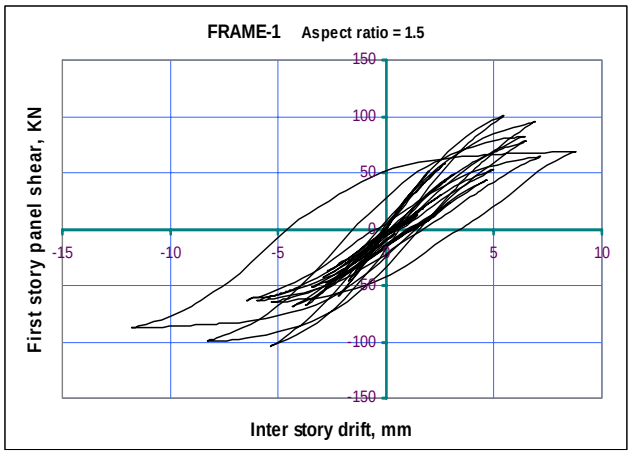

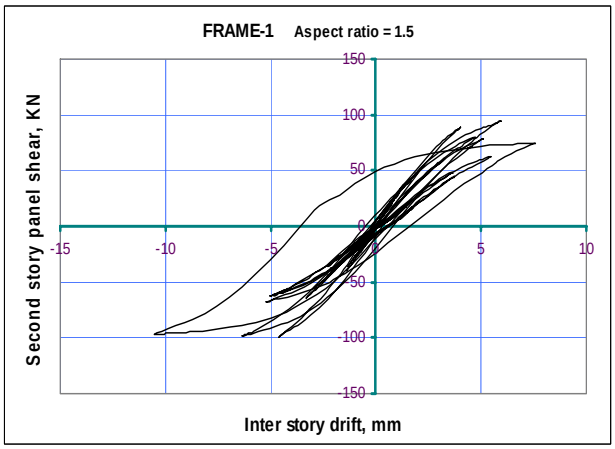

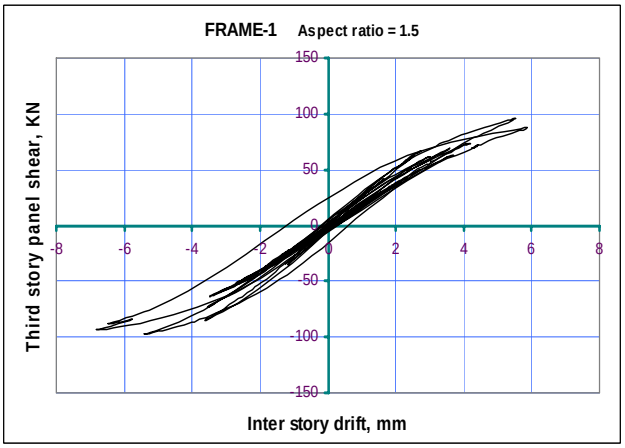

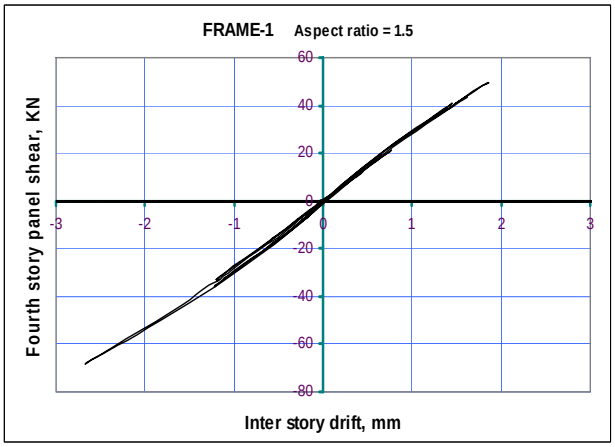

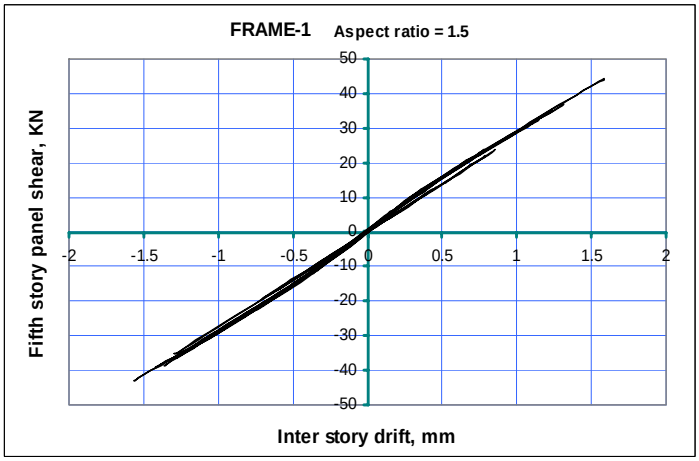

Fig. B.1 Infill shear vs. inter-story drift at different story levels – FRAME-1 with aspect ratio = 1.5.

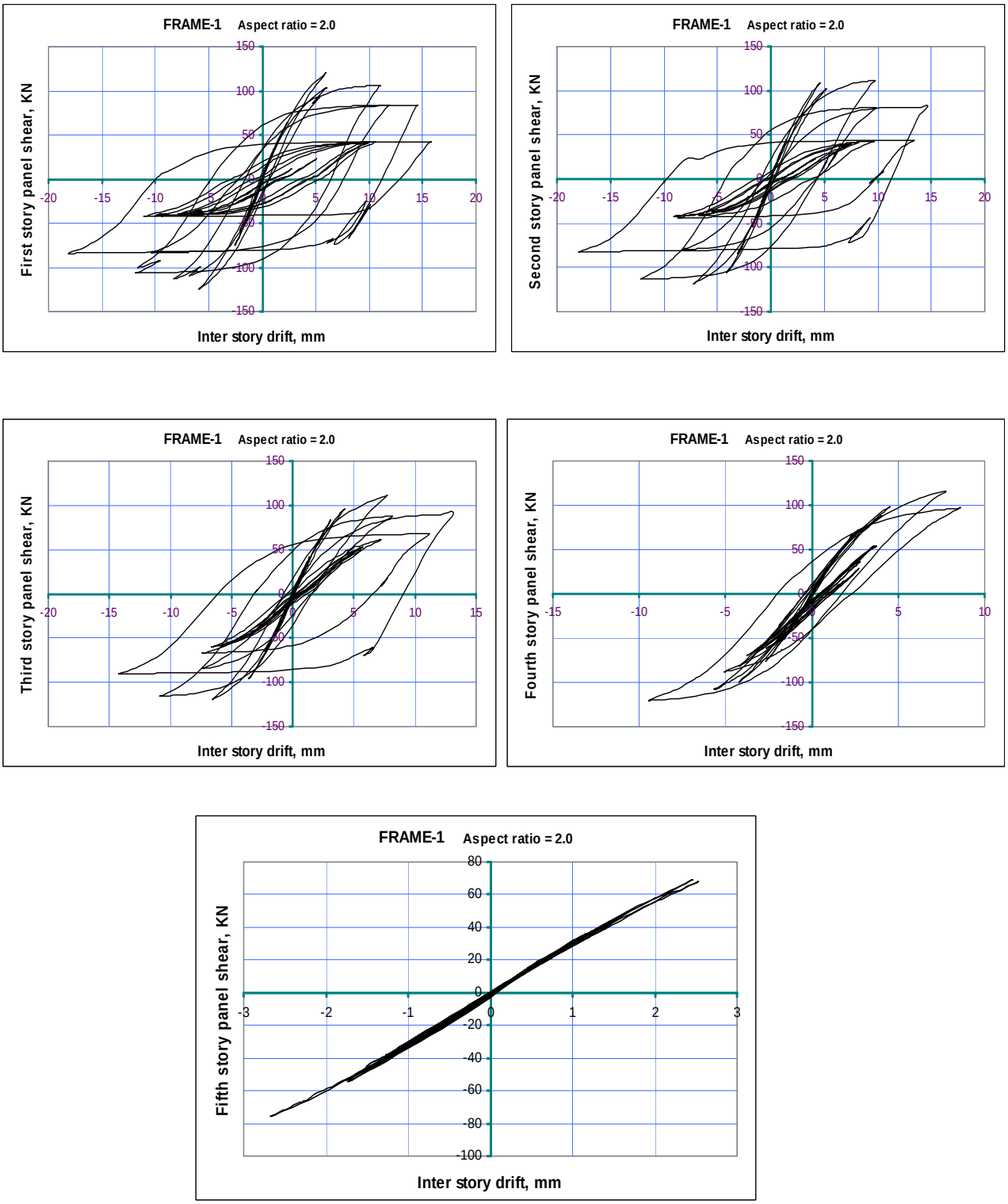

Fig. B.2 Infill shear vs. inter-story drift at different story levels – FRAME-1 with aspect ratio = 2.0

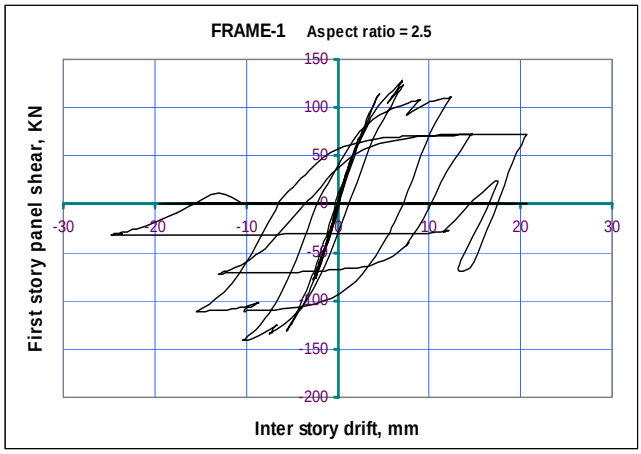

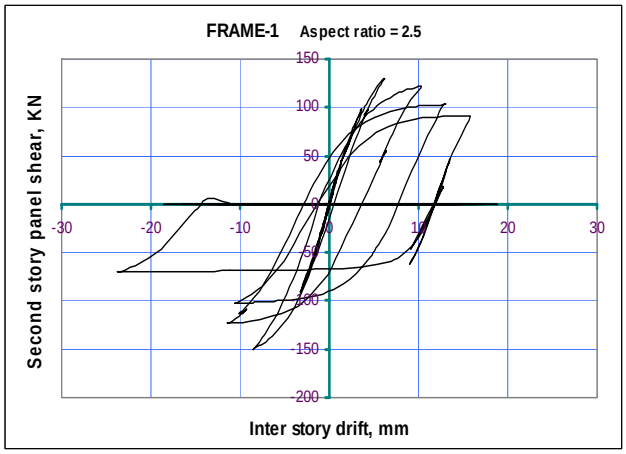

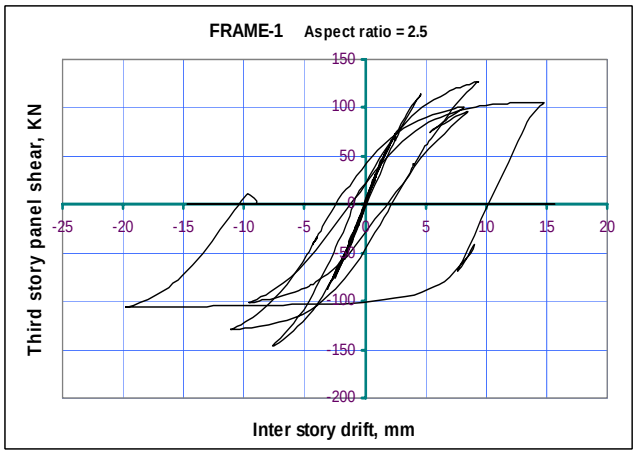

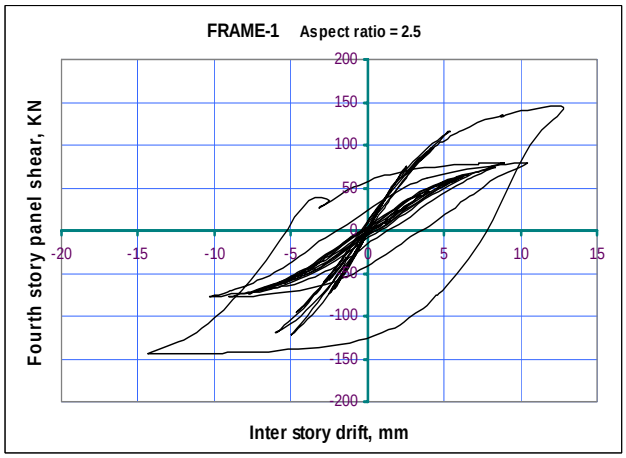

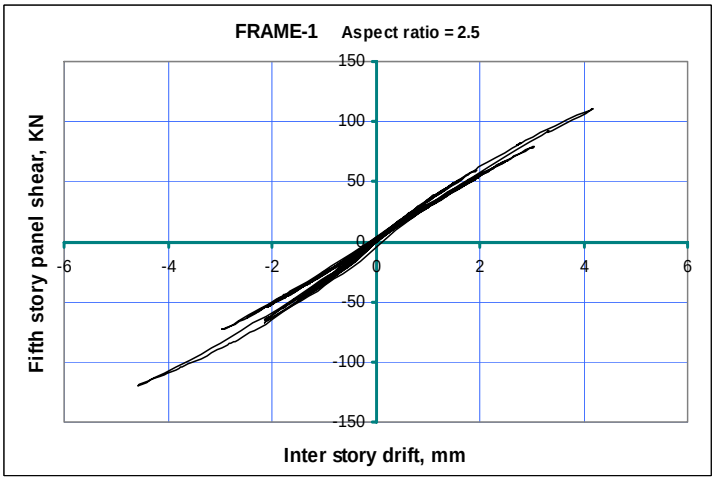

Fig. B.3 Infill shear vs. inter-story drift at different story levels – FRAME-1 with aspect ratio = 2.5

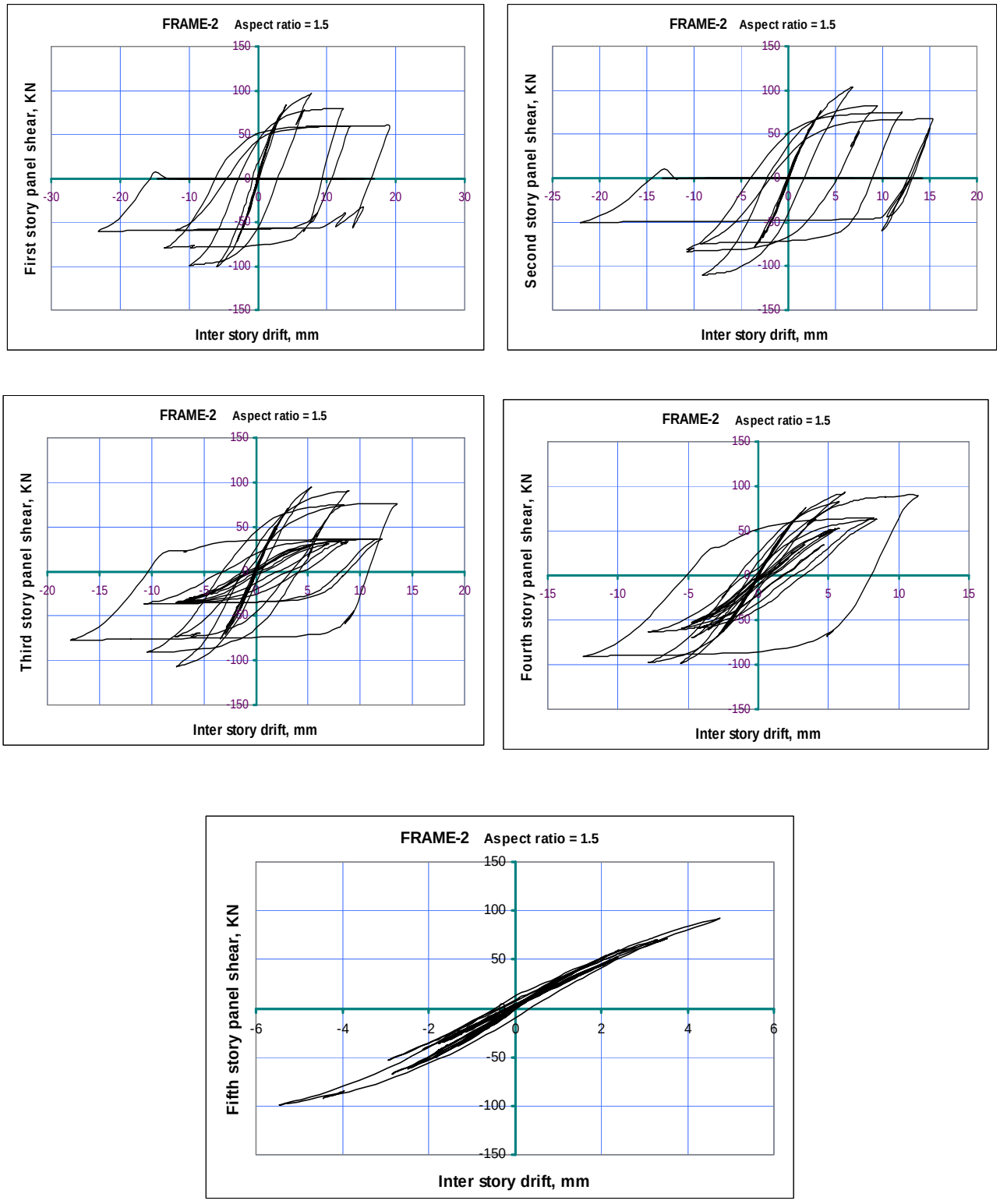

Fig. B.4 Infill shear vs. inter-story drift at different story levels – FRAME-2 with aspect ratio = 1.5

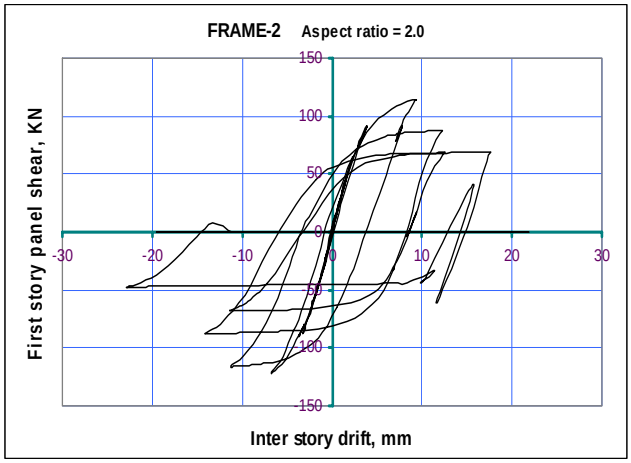

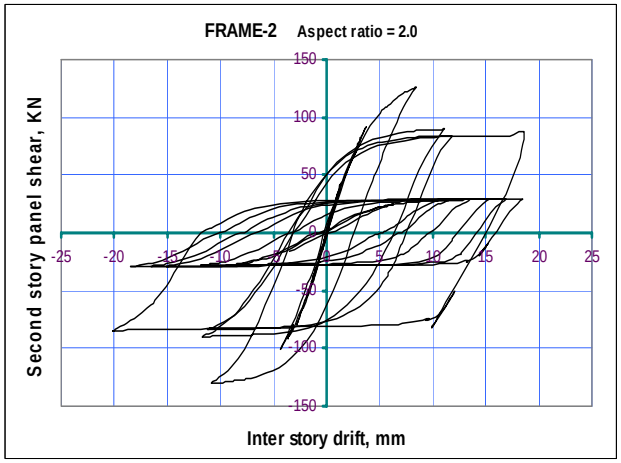

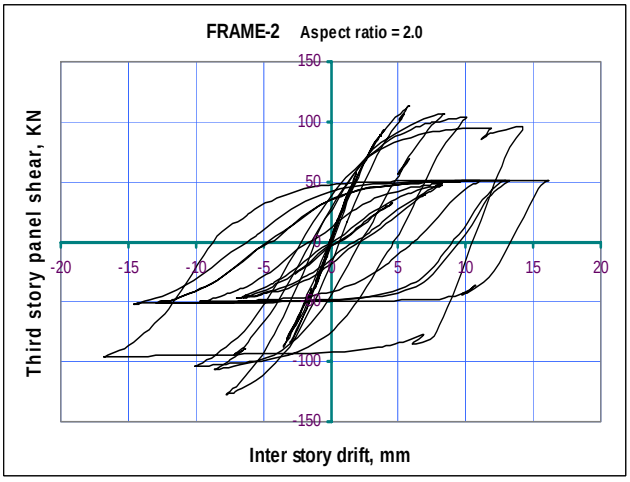

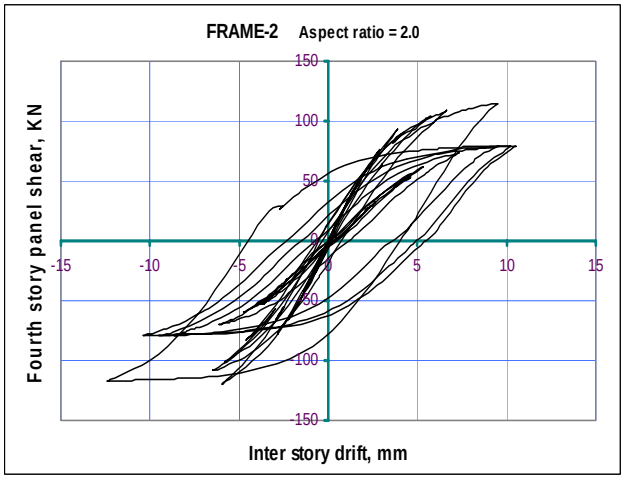

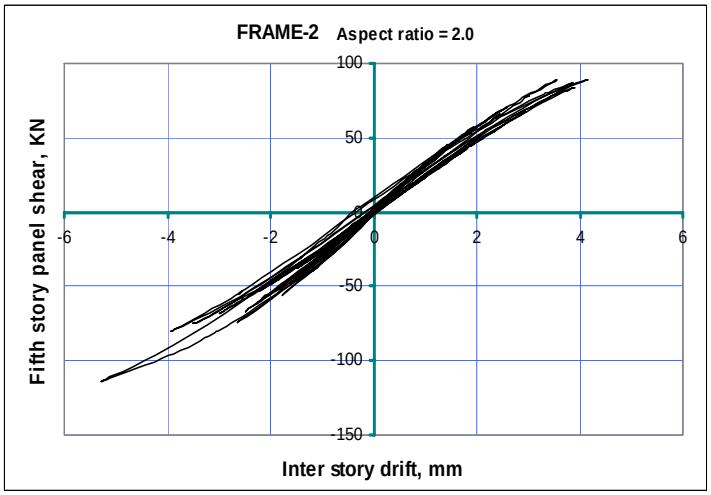

Fig. B.5 Infill shear vs. inter-story drift at different story levels – FRAME-2 with aspect ratio = 2.0

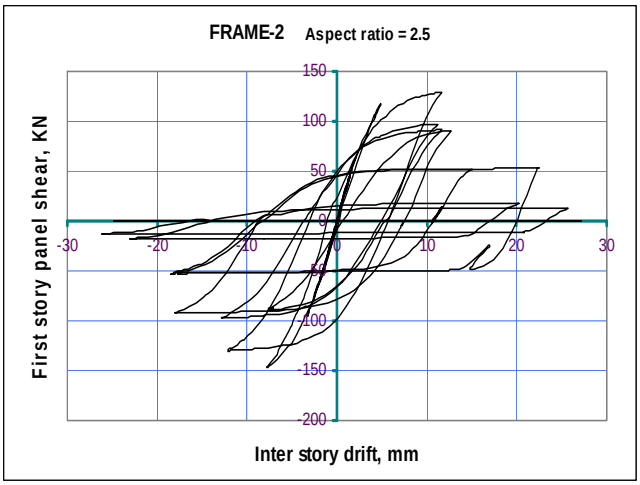

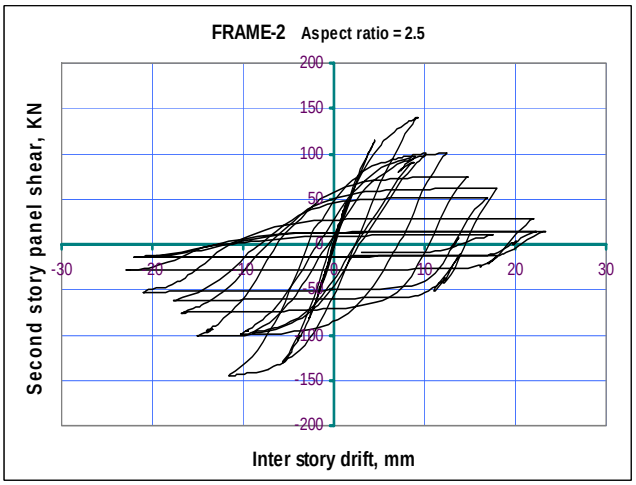

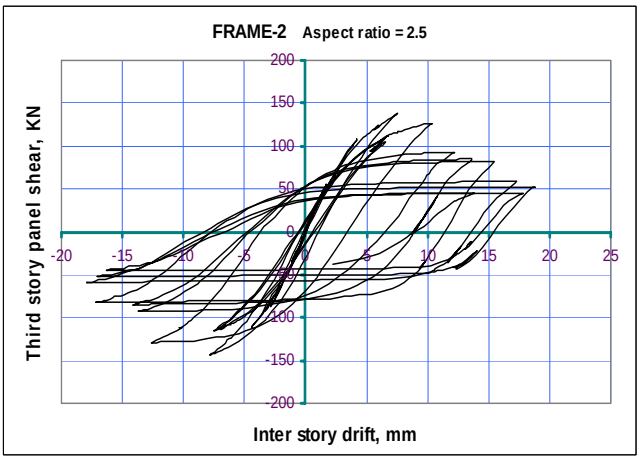

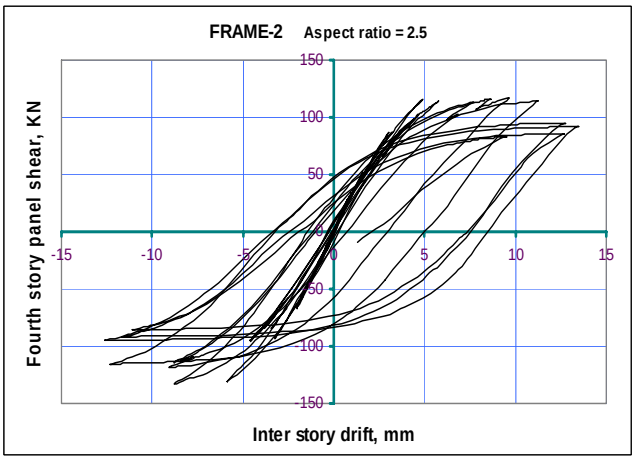

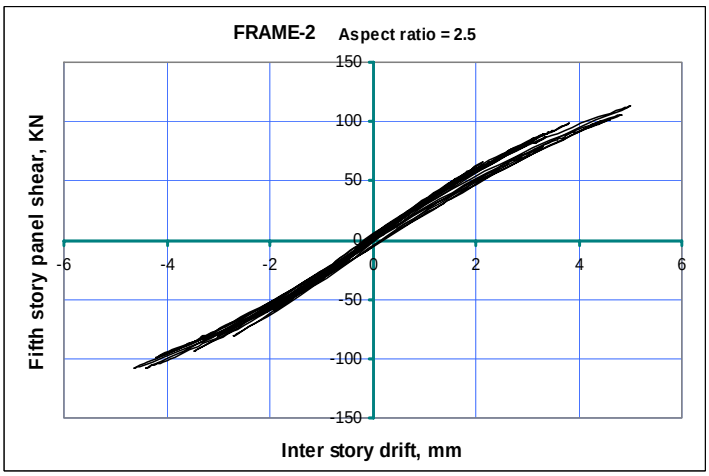

Fig. B.6 Infill shear vs. inter-story drift at different story levels – FRAME-2 with aspect ratio = 2.5

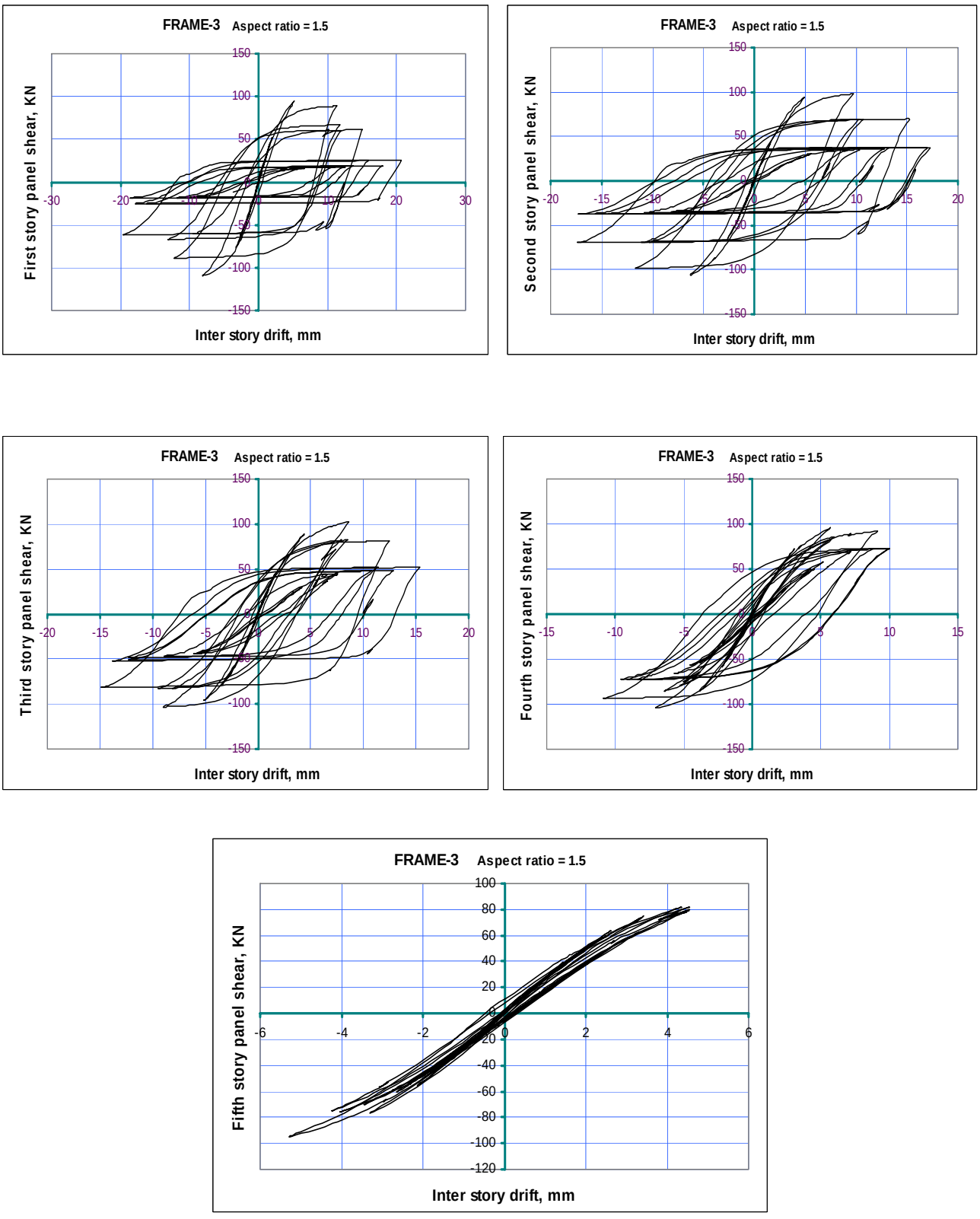

Fig. B.7 Infill shear vs. inter-story drift at different story levels – FRAME-3 with aspect ratio = 1.5

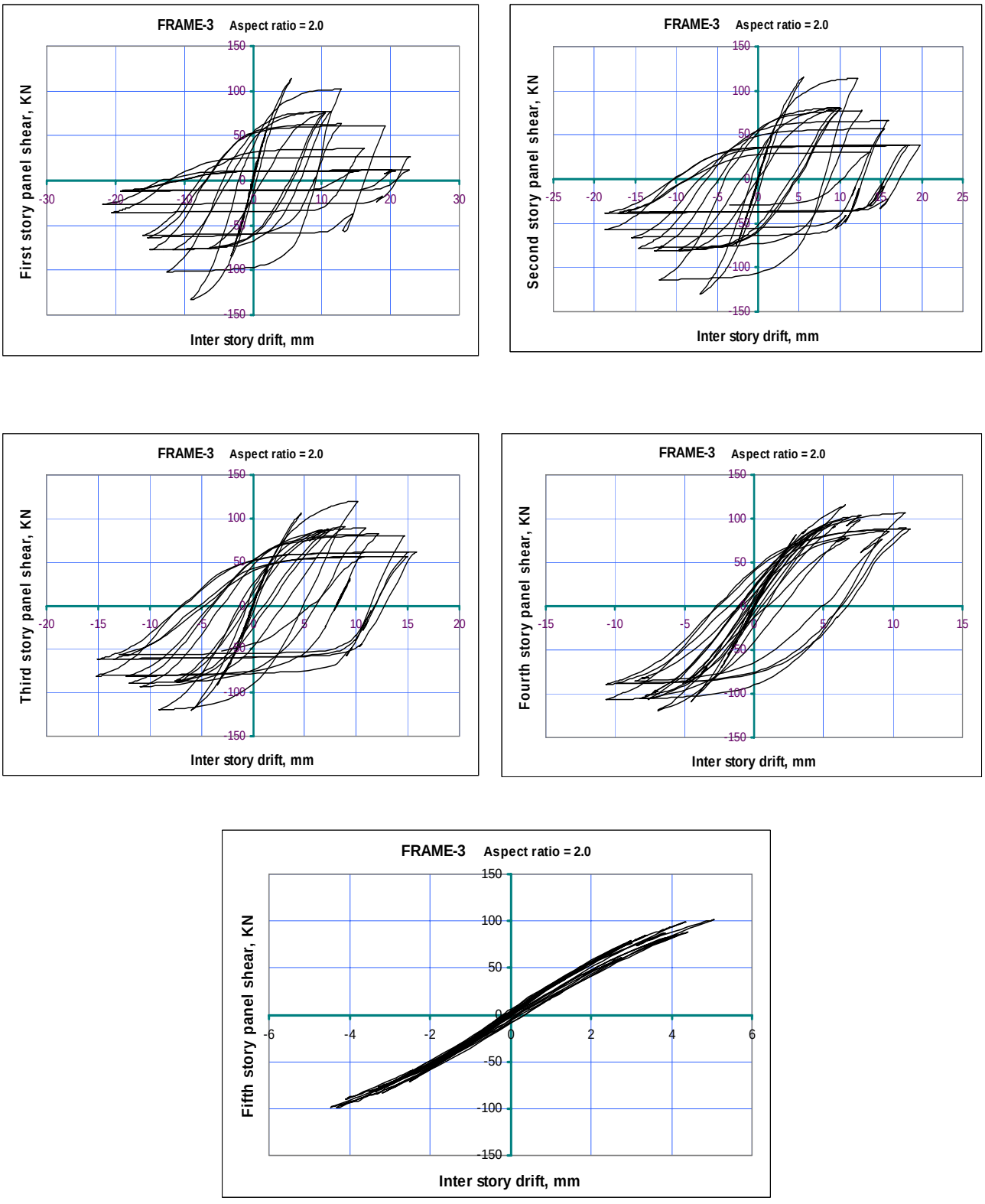

Fig. B.8 Infill shear vs. inter-story drift at different story levels – FRAME-3 with aspect ratio = 2.0

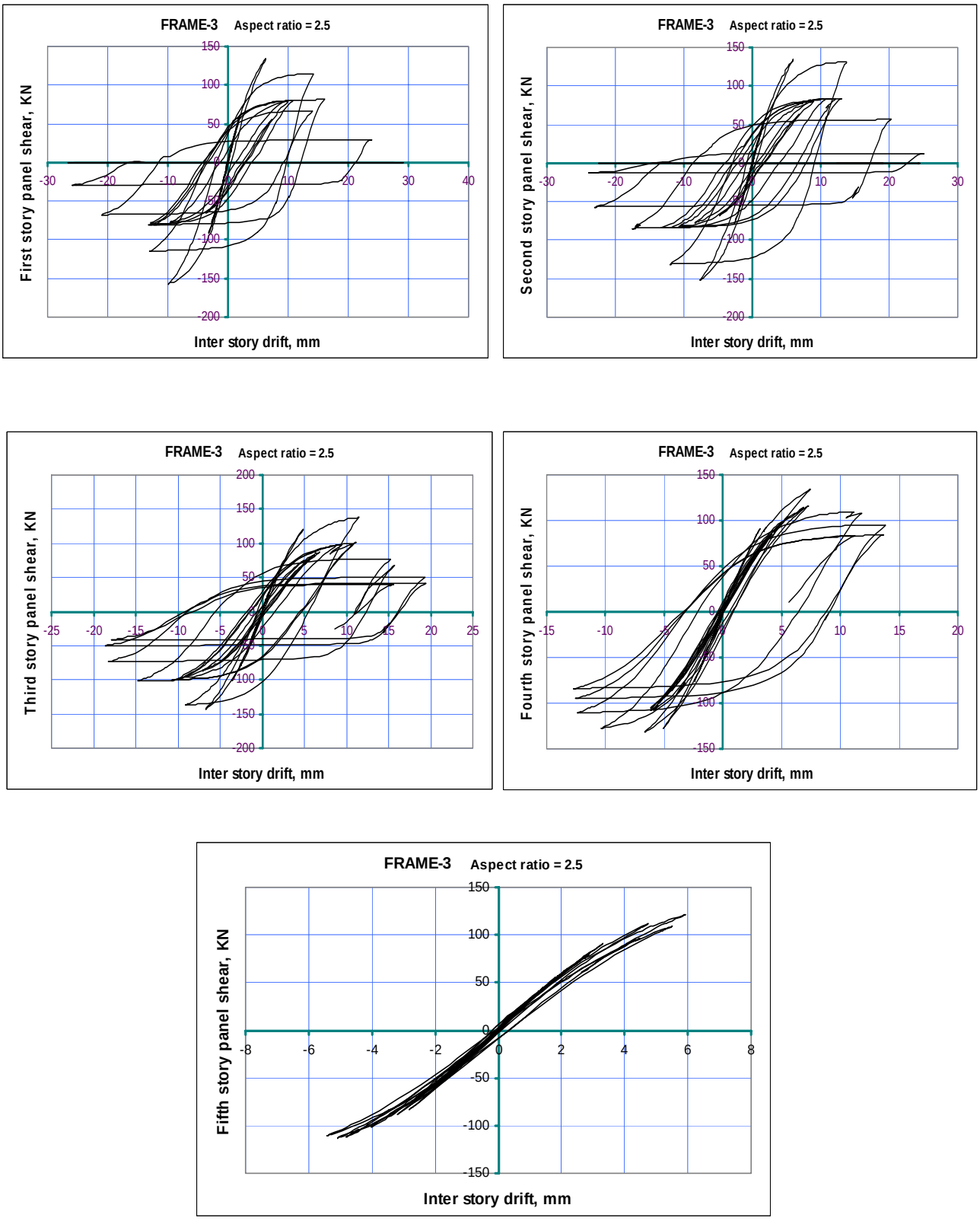

Fig. B.9 Infill shear vs. inter-story drift at different story levels – FRAME-3 with aspect ratio = 2.5

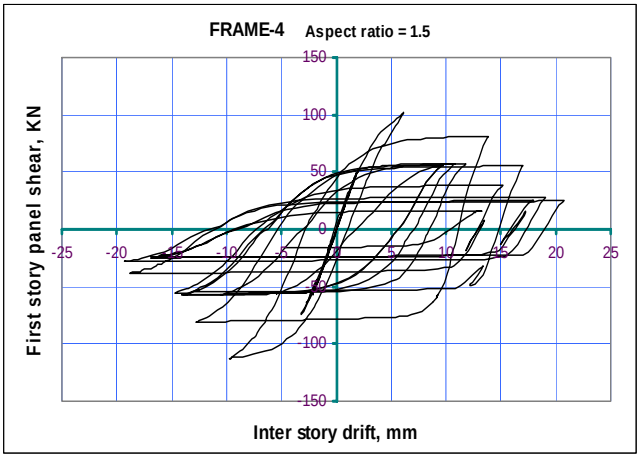

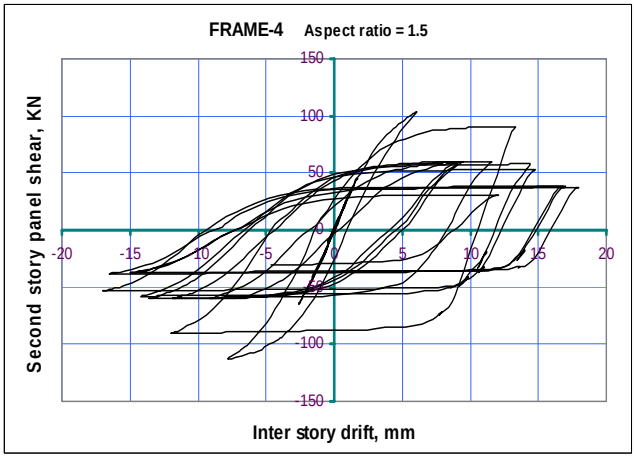

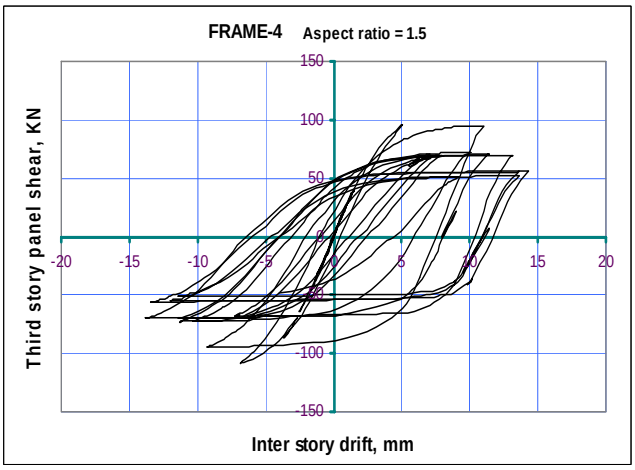

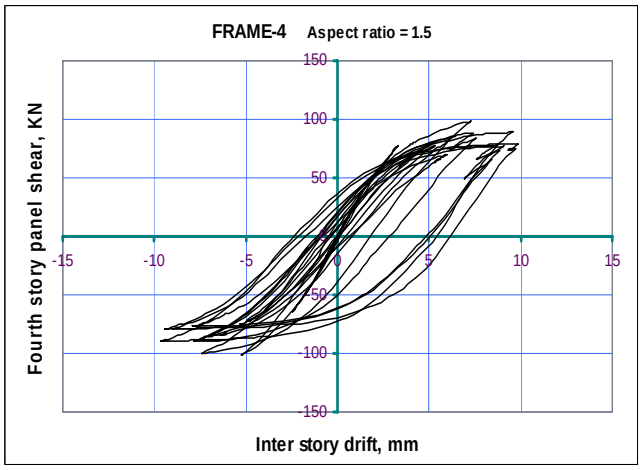

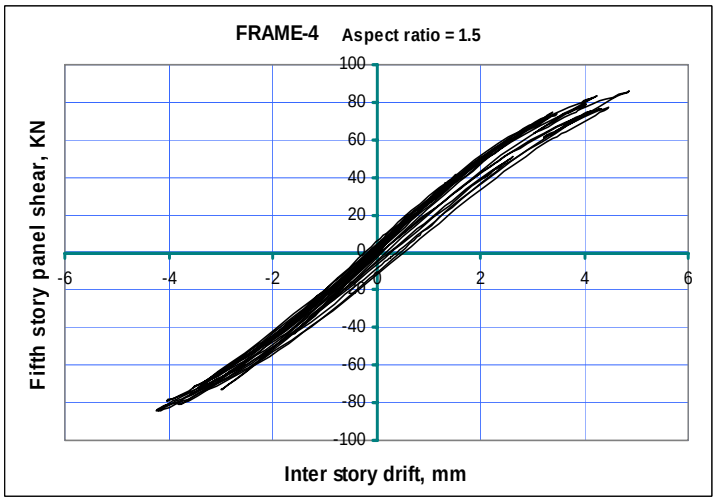

Fig. B.10 Infill shear vs. inter-story drift at different story levels – FRAME-4 with aspect ratio = 1.5

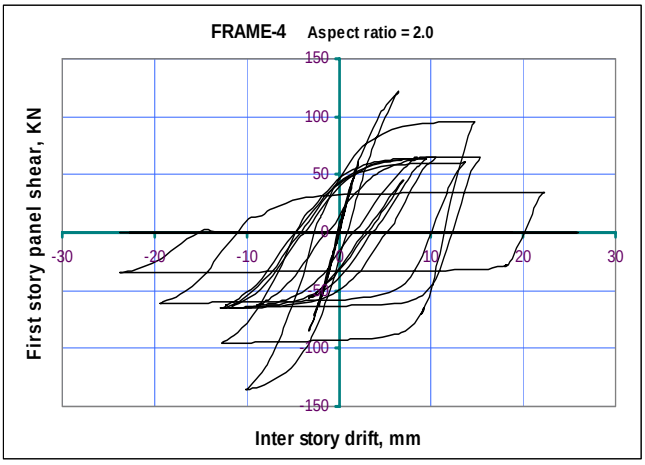

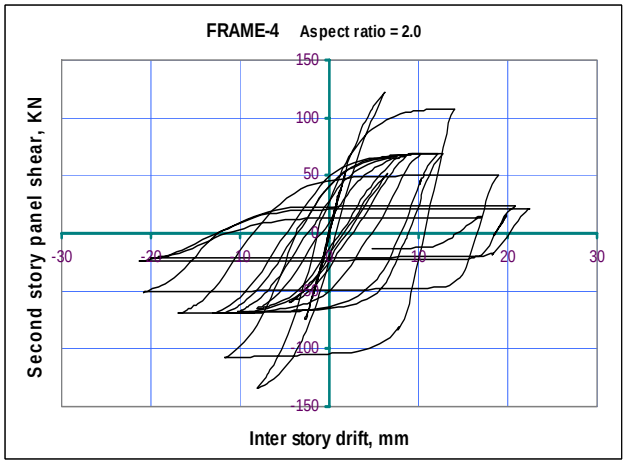

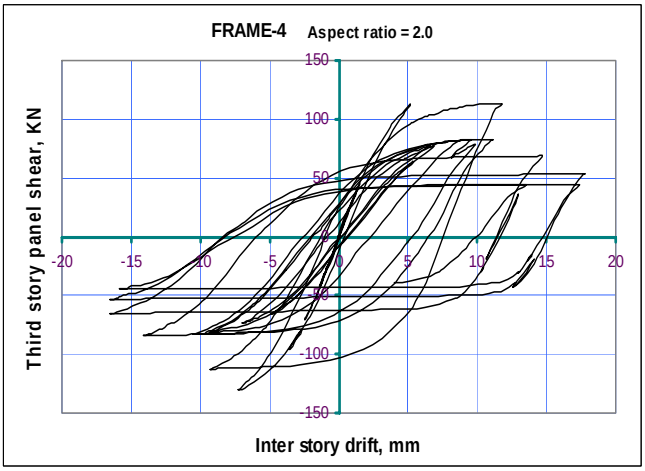

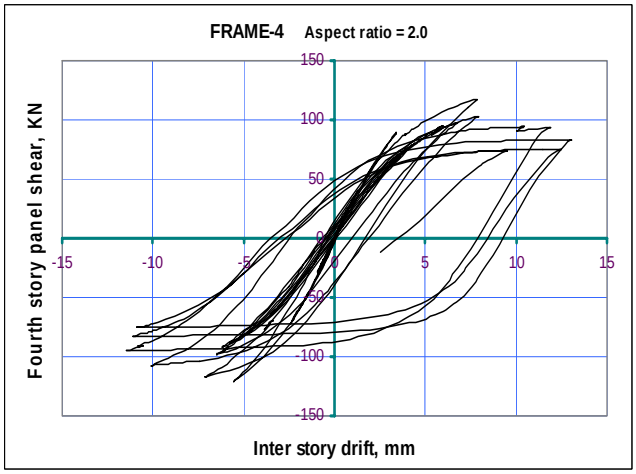

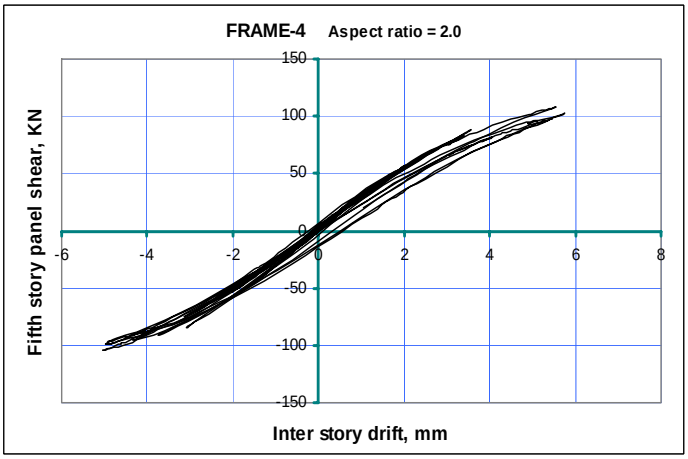

Fig. B.11 Infill shear vs. inter-story drift at different story levels – FRAME-4 with aspect ratio = 2.0

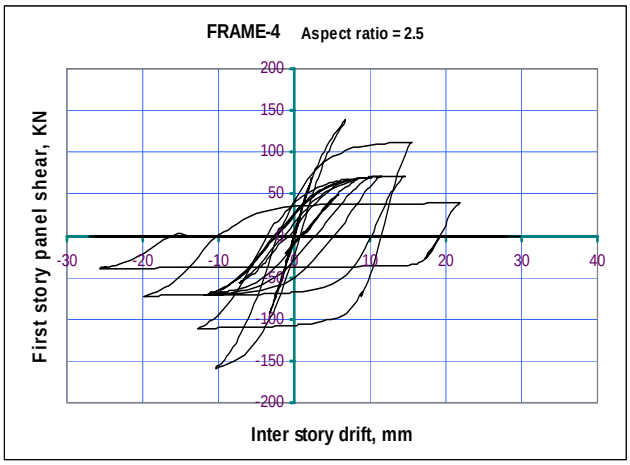

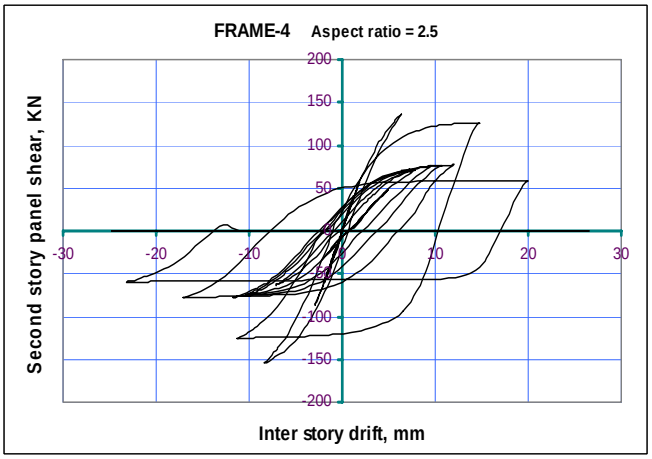

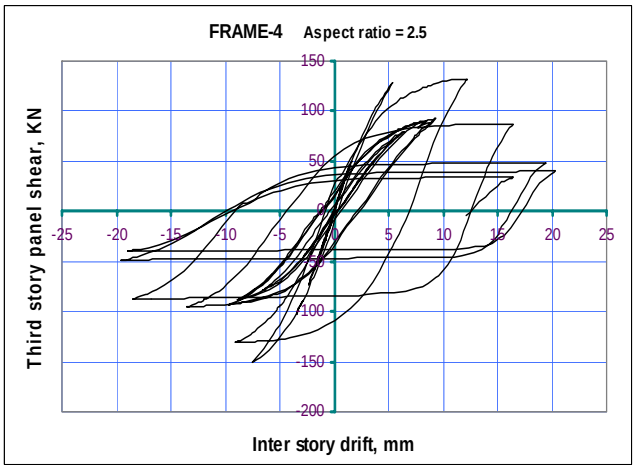

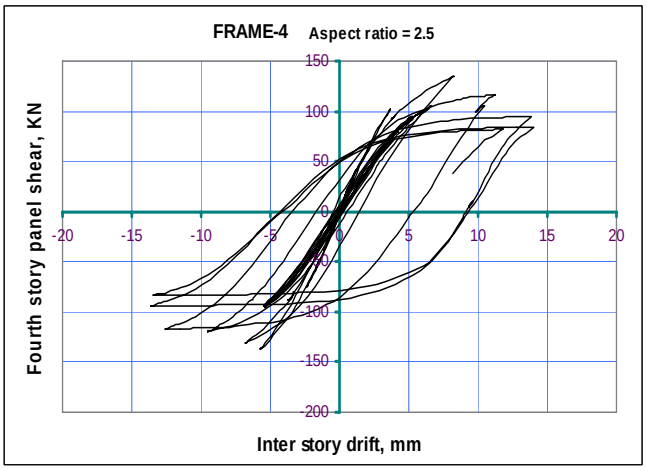

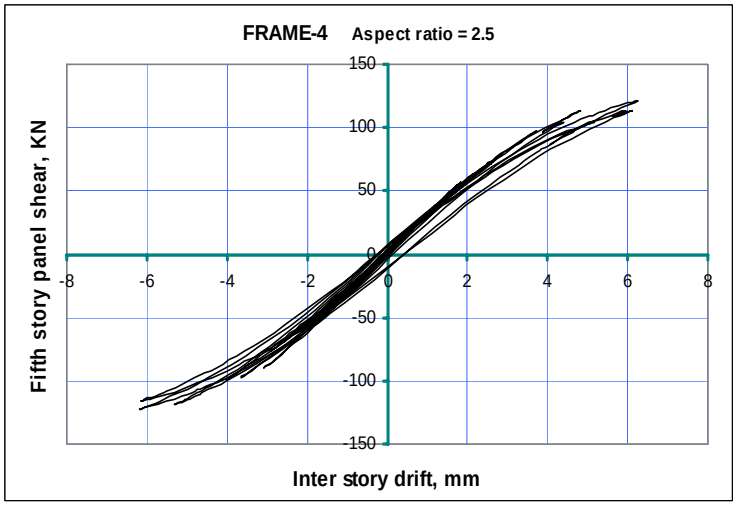

Fig. B.12 Infill shear vs. inter-story drift at different story levels – FRAME-4 with aspect ratio = 2.5

APPENDIX-C Tabulated Calculations

Table C-1 Lumped mass at floor level of each story

Mass calculations in Tons													
						Mass of column				Mass of wall			
Heigh, m	Lateral length, m	Infilled Bay length, m	Number of Columns	Noumber of infilled bays	Length of bare bay, m	Floor	Roof	Mass of beam	Mass of slab	Floor	Roof	Floor Mass	Roof Mass
3	5	3	2	1	6	2.45	1.22	3.61	5.82	1.82	0.91	**13.70**	**11.56**
3	5	3.5	2	1	6	2.45	1.22	3.76	6.90	2.17	1.08	**15.28**	**12.97**
3	5	4	2	1	6	2.45	1.22	3.91	7.98	2.52	1.26	**16.86**	**14.37**
3	5	4.5	2	1	6	2.45	1.22	4.07	9.06	2.87	1.43	**18.44**	**15.78**
3	5	5	2	1	6	2.45	1.22	4.22	10.13	3.22	1.61	**20.02**	**17.19**
3	5	5.5	2	1	6	2.45	1.22	4.37	11.21	3.57	1.78	**21.60**	**18.59**
3	5	6	2	1	6	2.45	1.22	4.53	12.29	3.92	1.96	**23.18**	**20.00**
3	5	6.5	2	1	6	2.45	1.22	4.68	13.37	4.27	2.13	**24.76**	**21.40**
3	5	7	2	1	6	2.45	1.22	4.83	14.44	4.62	2.31	**26.34**	**22.81**
3	5	7.5	2	1	6	2.45	1.22	4.98	15.52	4.97	2.48	**27.92**	**24.21**
3	5	8	2	1	6	2.45	1.22	5.14	16.60	5.32	2.66	**29.50**	**25.62**
3	5	8.5	2	1	6	2.45	1.22	5.29	17.68	5.67	2.83	**31.08**	**27.03**
3	5	9	2	1	6	2.45	1.22	5.44	18.76	6.02	3.01	**32.66**	**28.43**
3	5	3	3	1	6	3.67	1.83	6.73	18.11	1.82	0.91	**30.33**	**27.58**
3	5	3.5	3	1	6	3.67	1.83	6.88	19.19	2.17	1.08	**31.91**	**28.99**
3	5	4	3	1	6	3.67	1.83	7.03	20.27	2.52	1.26	**33.49**	**30.39**
3	5	4.5	3	1	6	3.67	1.83	7.19	21.34	2.87	1.43	**35.07**	**31.80**
3	5	5	3	1	6	3.67	1.83	7.34	22.42	3.22	1.61	**36.65**	**33.21**
3	5	5.5	3	1	6	3.67	1.83	7.49	23.50	3.57	1.78	**38.23**	**34.61**
3	5	6	3	1	6	3.67	1.83	7.65	24.58	3.92	1.96	**39.81**	**36.02**
3	5	6.5	3	1	6	3.67	1.83	7.80	25.66	4.27	2.13	**41.39**	**37.42**

3	5	7	3	1	6	3.67	1.83	7.95	26.73	4.62	2.31	**42.97**	**38.83**
3	5	7.5	3	1	6	3.67	1.83	8.10	27.81	4.97	2.48	**44.55**	**40.23**
3	5	8	3	1	6	3.67	1.83	8.26	28.89	5.32	2.66	**46.13**	**41.64**
3	5	8.5	3	1	6	3.67	1.83	8.41	29.97	5.67	2.83	**47.71**	**43.05**
3	5	9	3	1	6	3.67	1.83	8.56	31.05	6.02	3.01	**49.30**	**44.45**
3	5	3	4	1	6	4.89	2.45	9.85	30.40	1.82	0.91	**46.96**	**43.60**
3	5	3.5	4	1	6	4.89	2.45	10.00	31.48	2.17	1.08	**48.54**	**45.01**
3	5	4	4	1	6	4.89	2.45	10.15	32.56	2.52	1.26	**50.12**	**46.41**
3	5	4.5	4	1	6	4.89	2.45	10.31	33.63	2.87	1.43	**51.70**	**47.82**
3	5	5	4	1	6	4.89	2.45	10.46	34.71	3.22	1.61	**53.28**	**49.23**
3	5	5.5	4	1	6	4.89	2.45	10.61	35.79	3.57	1.78	**54.86**	**50.63**
3	5	6	4	1	6	4.89	2.45	10.76	36.87	3.92	1.96	**56.44**	**52.04**
3	5	6.5	4	1	6	4.89	2.45	10.92	37.94	4.27	2.13	**58.02**	**53.44**
3	5	7	4	1	6	4.89	2.45	11.07	39.02	4.62	2.31	**59.60**	**54.85**
3	5	7.5	4	1	6	4.89	2.45	11.22	40.10	4.97	2.48	**61.18**	**56.25**
3	5	8	4	1	6	4.89	2.45	11.38	41.18	5.32	2.66	**62.77**	**57.66**
3	5	8.5	4	1	6	4.89	2.45	11.53	42.26	5.67	2.83	**64.35**	**59.07**
3	5	9	4	1	6	4.89	2.45	11.68	43.33	6.02	3.01	**65.93**	**60.47**
3	5	3	5	1	6	6.12	3.06	12.97	42.69	1.82	0.91	**63.59**	**59.62**
3	5	3.5	5	1	6	6.12	3.06	13.12	43.77	2.17	1.08	**65.17**	**61.03**
3	5	4	5	1	6	6.12	3.06	13.27	44.84	2.52	1.26	**66.75**	**62.43**
3	5	4.5	5	1	6	6.12	3.06	13.43	45.92	2.87	1.43	**68.33**	**63.84**
3	5	5	5	1	6	6.12	3.06	13.58	47.00	3.22	1.61	**69.91**	**65.25**
3	5	5.5	5	1	6	6.12	3.06	13.73	48.08	3.57	1.78	**71.49**	**66.65**
3	5	6	5	1	6	6.12	3.06	13.88	49.16	3.92	1.96	**73.07**	**68.06**
3	5	6.5	5	1	6	6.12	3.06	14.04	50.23	4.27	2.13	**74.65**	**69.46**
3	5	7	5	1	6	6.12	3.06	14.19	51.31	4.62	2.31	**76.24**	**70.87**
3	5	7.5	5	1	6	6.12	3.06	14.34	52.39	4.97	2.48	**77.82**	**72.27**
3	5	8	5	1	6	6.12	3.06	14.50	53.47	5.32	2.66	**79.40**	**73.68**
3	5	8.5	5	1	6	6.12	3.06	14.65	54.55	5.67	2.83	**80.98**	**75.09**
3	5	9	5	1	6	6.12	3.06	14.80	55.62	6.02	3.01	**82.56**	**76.49**

Table C-2 Stiffness calculation for masonry infill

Stiffness calculations in KN/m

Masonry unit strength, f'_{cb} in Mpa	Mortar streng th, f'_j in Mpa	Prism strengt h, f'_p in Mpa	Coeff icient of fricti on, μ	Cohesi ve capacit y of mortar, τ_o in Mpa	Modulus of elasticity of masonry , E_m in MPa	Modulus of elasticity concrete, E_c in Mpa	Story heigh t in cm	Bay width in cm	Diagon al inclinat ion, θ in deg.	Constant λ	Sliding shear failure, KN	Compres sion failure, KN	Maximu m shear - V_m in KN	Maxim um displac ement - U_m in mm	Initial stiffness - K_o in KN/m	Shear at yield -V_y in KN	Displa cemen tat yield - U_y in mm
7.5	5	4.37	0.5	0.17	3300	24000	300	300	0.79	0.00929	109.04	158.32	109.04	9.74	22401.14	107.94	4.82
7.5	5	4.37	0.5	0.17	3300	24000	300	350	0.70	0.00925	111.95	189.06	111.95	9.12	24540.67	110.82	4.52
7.5	5	4.37	0.5	0.17	3300	24000	300	400	0.63	0.00917	118.16	220.36	118.16	8.94	26418.43	116.96	4.43
7.5	5	4.37	0.5	0.17	3300	24000	300	450	0.57	0.00906	125.89	252.18	125.89	9.01	27939.79	124.62	4.46
7.5	5	4.37	0.5	0.17	3300	24000	300	500	0.51	0.00893	134.46	284.47	134.46	9.23	29135.97	133.10	4.57
7.5	5	4.37	0.5	0.17	3300	24000	300	550	0.47	0.00881	143.53	317.20	143.53	9.55	30065.44	142.08	4.73
7.5	5	4.37	0.5	0.17	3300	24000	300	600	0.43	0.00868	152.93	350.31	152.93	9.94	30785.02	151.38	4.92
7.5	5	4.37	0.5	0.17	3300	24000	300	650	0.40	0.00856	162.55	383.78	162.55	10.37	31342.14	160.91	5.13
7.5	5	4.37	0.5	0.17	3300	24000	300	700	0.38	0.00844	172.34	417.57	172.34	10.85	31774.16	170.60	5.37
7.5	5	4.37	0.5	0.17	3300	24000	300	750	0.35	0.00832	182.25	451.66	182.25	11.35	32109.85	180.41	5.62
7.5	5	4.37	0.5	0.17	3300	24000	300	800	0.33	0.00822	192.25	486.04	192.25	11.88	32371.10	190.31	5.88
7.5	5	4.37	0.5	0.17	3300	24000	300	850	0.31	0.00811	202.32	520.67	202.32	12.42	32574.55	200.28	6.15
7.5	5	4.37	0.5	0.17	3300	24000	300	900	0.29	0.00801	212.45	555.54	212.45	12.98	32732.89	210.30	6.42